UNIVERSITÉ DU QUÉBEC À MONTRÉAL

INSTITUT DE PHYSIQUE DU GLOBE DE PARIS

QUANTIFICATION ET TRAÇAGE GÉOCHIMIQUE DES EXPORTS FLUVIAUX : EXEMPLES
DE BASSINS HYDROGRAPHIQUES DU CANADA

THÈSE

PRÉSENTÉE EN COTUTELLE

COMME EXIGENCE PARTIELLE

DU DOCTORAT EN SCIENCES DE LA TERRE, SPÉCIALISATION GÉOCHIMIE

PAR

ÉRIC ROSA

AVRIL 2011

UNIVERSITÉ DU QUÉBEC À MONTRÉAL
Service des bibliothèques

Avertissement

AVANT-PROPOS

La présente étude a été réalisée dans le cadre d'un contrat de cotutelle de thèse entre l'Université du Québec à Montréal et l'Institut de Physique du Globe de Paris.

Le corps de la thèse se compose de quatre articles scientifiques rédigés en langue anglaise qui seront soumis pour publication. La balance de la thèse est rédigée en langue française, conformément aux exigences des universités d'attache.

Le corps de cette thèse est constitué de travaux issus de collaborations entre chercheurs agissant à titre de co-auteurs, ce qui exige une justification de l'implication du candidat à l'obtention du doctorat. Pour la totalité de la présente thèse, le candidat a agi à titre de premier auteur. L'étudiant a été en charge de la gestion des échantillonnages, des analyses en laboratoire, de l'interprétation des résultats et des calculs subséquents. Les échantillons du fleuve Saint-Laurent récupérés avant 2005 ont été analysés par les membres du laboratoire d'isotopes stables au GEOTOP (ISG) avant l'initiation de cette thèse. La nomination des co-auteurs a respecté les règles en vigueur à ce sujet à l'Université du Québec à Montréal.

REMERCIEMENTS

TABLE DES MATIÈRES

LISTE DES FIGURES

LISTE DES TABLEAUX

LISTE DES ANNEXES

Les annexes sont présentées en format numérique (.jpg) avec le CD-ROM qui accompagne la présente thèse. Ces annexes sont des cartes géologiques (lithologie et dépôts meubles) des basins versants étudiés.

Annexe A : Couvert végétal au niveau de la région d'étude

Annexe B : Distribution des tourbières au niveau de la région d'étude

Annexe C : Géologie (lithologie et couverture de dépôts meubles) des bassins hydrographiques à l'étude.

(C1) Koksoak
(C2) Great Whale
(C3) La Grande
(C4) Pontax
(C5_6) Nemiscau_Rupert
(C7) Broadback
(C8) Bell
(C9) Harricana
(C10) Nelson
(C11) Ashuapmushuan
(C12) Outaouais
(C13) Gatineau
(C14) Du Lièvre
(C15) Du Nord
(C16) St-Laurent

RÉSUMÉ

La prévisibilité des changements dans la qualité et la quantité des ressources hydriques renouvelables repose sur une étude quantitative des mécanismes qui contrôlent ces paramètres. En lien avec cette problématique, la présente étude privilégie une approche fondée sur le monitoring géochimique des exports fluviaux dissous (δ^2H-δ^{18}O, cations majeurs, carbone organique dissous (COD), Nd, Sr, ^{87}Sr/^{86}Sr, U, (^{234}U/^{238}U)). L'étude a pour objectif (i) de tracer le cycle de l'eau et (ii) de documenter les taux d'altération chimique des roches au sein bassins hydrographiques des baies d'Hudson, de James et d'Ungava (HJUB) ainsi que du fleuve Saint-Laurent. La région d'étude couvre plus de $2,8 \times 10^6$ km^2 sur 15 degrés de latitude. Les rivières Koksoak, Great Whale, La Grande et des Outaouais et les fleuves Nelson et Saint-Laurent ont fait l'objet d'un suivi temporel alors que dix autres rivières de la région ont été échantillonnées ponctuellement (durant la fonte des neiges et l'étiage estival) afin de fournir des informations complémentaires.

Les teneurs en ^{2}H-^{18}O des rivières étudiées présentent des variations saisonnières systématiques dont l'amplitude atteint 1 à 5‰ (δ^{18}O). L'appauvrissement en isotopes lourds marquant la fonte des neiges constitue le trait caractéristique des profils isotopiques saisonniers. Lors de la période libre de glace, des enrichissements graduels en isotopes lourds sont observés en réponse à l'évaporation. La rivière La Grande est une exception à cette règle en raison de l'effet tampon causé par les réservoirs hydroélectriques qui la ponctuent. Lorsque rapportées dans un graphique δ^2H vs δ^{18}O, les rivières définissent des droites évaporatoires situées sous la droite des eaux météoriques et ayant une pente plus faible que cette dernière. À partir de bilans de masses isotopiques, il a été estimé que 10% de l'eau atteignant le bassin de la rivière des Outaouais est évaporée avant de rejoindre l'exutoire de cette dernière dans le fleuve Saint-Laurent. De façon similaire, on estime à 5-15% les taux d'évaporation dans les bassins hydrographiques du nord-est du Canada. Les rivières drainant les bassins hydrographiques contigus du nord-est du Canada définissent un gradient isotopique latitudinal (δ^{18}O$_{(‰ \text{ vs VSMOW})}$ = -0.36*Latitude+4.4‰) parallèle à celui rapporté pour les précipitations au niveau de la même région. Cette observation tend à indiquer que le gradient isotopique hérité des précipitations est conservé dans les rivières, malgré les processus subséquents à la recharge des bassins.

Au sein des bassins de l'HJUB, les taux d'altération des roches ont été étudiés à partir des exports fluviaux dissous. Les rivières du bouclier présentent des concentrations en cations majeurs variant entre 62 et 360 µM, des teneurs en néodyme ([Nd]) allant de 0.57 à 4.72 nM et des teneurs en COD variant entre 241 et 1777 µM. En comparaison, le fleuve Nelson présente des concentrations en cations majeurs plus élevées (1200-2276 µM), des [Nd] plus faibles (0.14-0.45 nM) et des [COD] intermédiaires (753-928 µM). Au sein des rivières Koksoak, Great Whale et Nelson, les concentrations en cations dissous (Na-K-Mg-Ca-Sr) présentent des variations saisonnières qui transcrivent l'effet des conditions hydro-climatiques. Comme pour les teneurs en ^{2}H-^{18}O, la dilution causée par la fonte des neiges constitue le trait caractéristique des chroniques saisonnières. Les rivières étudiées exportent vers l'HJUB un flux cationique dissout (Na-K-Mg-Ca-Sr) de 8×10^6 tonnes*an^{-1}. Au sein des bassins hydrographiques, les taux d'altération chimique (cationique) des roches varient entre 1.0 et 5.6 tonnes*km^{-2}*an^{-1}. Le contrôle lithologique est proéminent, tel que suggéré par la relation établie entre l'abondance de roches volcaniques et sédimentaires (V+S%) dans les bassins et les taux d'altération cationiques des roches (ACR): ACR=0.8*(V+S%)+0.9. Les flux de Nd sont découplés des taux d'altération des roches mais corrélés aux flux de COD (r^2=0.95). Ces derniers diminuent vers le nord et semblent tributaires des conditions hydro-climatiques. Les exports fluviaux d'uranium ont été étudiés afin de fournir des précisions sur les processus d'altération des roches. Les rivières drainant le Bouclier canadien et la Plate-Forme Intérieure présentent des signatures [U] vs (^{234}U/^{238}U) distinctes. Dans le fleuve Nelson (Plate-Forme Intérieure) les [U] varient entre 1.05 et 2.45 nM et les déséquilibres (^{234}U/^{238}U) atteignent 1.21 à 1.25. Les [U] sont plus faibles au sein des du Bouclier canadien (0.04 - 1.24 nM) alors que les déséquilibres (^{234}U/^{238}U) sont plus variables (1.11 - 1.99). Dans l'ensemble, les rivières étudiées exportent 3.4×10^5 moles*an^{-1} d'uranium vers l'HJUB, avec un ratio (^{234}U/^{238}U) moyen de 1.27. Les flux d'U sont découplés des taux d'altération des roches et l'accumulation d'uranium au sein de dépôts organiques semble intervenir sur les budgets à l'échelle des bassins. Les signatures (^{234}U/^{238}U) distinctes des rivières étudiées pourraient offrir la possibilité de tracer les exports fluviaux dissous au sein du domaine océanique de l'HJUB.

ABSTRACT

The predictability of changes in the quality and quantity of renewable water resources relies on a quantitative study of the mechanisms that control these parameters. In connection with this problem, this study favors an approach based on the geochemical monitoring of dissolved riverine exports (δ^2H-δ^{18}O, major cations, dissolved organic carbon (DOC), [Nd], [Sr], ^{87}Sr/^{86}Sr, [U], (^{234}U/^{238}U)). The study aims at (i) tracing the water cycle and at (ii) quantifying rock chemical weathering rates in major river basins in central and eastern Canada. The study area covers more than 2.8 x10^6 km^2 over 15 degrees of latitude and encompasses the major basins of Hudson Bay, James and Ungava (HJUB) as well as the St. Lawrence River. The Koksoak, Great Whale, La Grande, Nelson, Ottawa and St. Lawrence rivers were monitored in time whereas ten other rivers flowing within the same region were sampled during spring snowmelt and summer baseflow, providing complementary data.

The studied rivers present systematic seasonal δ^{18}O-δ^2H patterns with amplitudes reaching 1 to 5 ‰ (δ^{18}O). Heavy-isotope depletions mark the snowmelt event and gradual heavy-isotope enrichments occur in response to evaporation during the ice-off season. The La Grande River constitutes an exception due to the buffering effect of hydroelectric reservoirs that smooth out the temporal isotopic fluctuations. When reported in a δ^2H vs δ^{18}O chart, the studied rivers define Local Evaporation Lines (LEL) extending below the Meteoric Water Line (MWL). Isotopic mass balance calculations suggest that approximately 10% of the total inflow to the Ottawa River Basin is lost through evaporation before reaching its outlet in the St. Lawrence River. The rivers draining contiguous basins of Northeastern Canada define a River Water Line (RWL) arising from imbricate Local Evaporation Lines (LEL). A method using the distance between the RWL and the MWL is proposed for estimating the average evaporation over inflow ratio (5 to 15%) at the scale of the study area. These rivers also define a latitudinal isotopic gradient (δ^{18}O (‰ vs. VSMOW) = -0.36 * Latitude +4.4 ‰) that is parallel to that reported for precipitation over the same region. This observation suggests that the isotopic gradient inherited rainfall is preserved in rivers, despite the subsequent hydrological processes occurring within the basins.

Landscape chemical denudation rates were addressed based on the dissolved chemistry of rivers flowing into the HJUB. The rivers of the Canadian Shield depict major cation concentrations ranging between 62 and 360 µM, neodymium concentrations ([Nd]) of 0.57 to 4.72 nM and variable dissolved organic carbon concentrations ([DOC]) (241 – 1777 µM). In comparison, the Nelson River (Interior Platform) shows higher major cation concentrations (1200 – 2276 µM), lower [Nd] (0.14 to 0.45 nM) and intermediate [DOC] (753 – 928 µM). Within the HJUB basins, the dissolved cation concentrations (Na-K-Mg-Ca-Sr) show seasonal variations that transcribe the effect of hydro-climatic conditions. As for δ^2H-δ^{18}O patterns, the dilution caused by snowmelt constitutes the main feature of the seasonal patterns. Altogether, the studied rivers export 8x10^6 tons*yr^{-1} of dissolved major cations and 50 tons*yr^{-1} of dissolved Nd towards the HJUB. Basin scale total rock cationic denudation rates (TRCDR) range from 1.0 to 5.3 tons*yr^{-1}*km^2 and are essentially controlled by lithology, as illustrated by the relationship established between rock denudation rates and the proportion of sedimentary and volcanic rocks (%S+V) within the basins: TRCDR=0.08(%S+V)+0.9. Contrastingly, dissolved Nd exports are decoupled from rock weathering rates and seem to be strongly dependent upon organic matter cycling, as illustrated by the tight coupling between Nd and DOC fluxes. These fluxes decrease northwards, likely in response to the hydro-climatic gradient. Riverine dissolved U contents were studied in order to provide further information regarding weathering sources and processes in the HJUB region. The rivers draining the Canadian Shield vs. that draining the Interior Platform depict distinct [U] vs. (^{234}U/^{238}U) clusters. In the Nelson River (draining the Interior Sedimentary Platform), U-concentrations are highest (1.05 - 2.45 nM) whereas (^{234}U/^{238}U) show little variability (1.21 – 1.25). U concentrations are comparatively lower in the rivers of the Canadian Shield (0.04 – 1.24 nM) whereas (^{234}U/^{238}U) span from 1.11 to 1.99. Altogether, the studied rivers export 3,4x10^5 moles.yr^{-1} of U towards the HJUB, with an amount-weighted average (^{234}U/^{238}U) of 1.27. At the scale of the study area, U and major cations exports are decoupled, suggesting that rock weathering processes do not solely control U budgets. First-order calculations reveal that U accumulation in peatlands could significantly impact basin-scale U budgets. The distinct [U] vs (^{234}U/^{238}U) clusters defined by the monitored rivers of the HJUB region (Koksoak, Great Whale, La Grande and Nelson) should allow tracing the source of dissolved U in the nearby oceanic domain.

1. INTRODUCTION GÉNÉRALE

1.1. Mise en contexte

D'un point de vue scientifique, la présente étude s'insère dans le cadre des démarches visant à améliorer la compréhension de deux processus qui dictent l'évolution de la surface terrestre : le cycle de l'eau et l'altération chimique. D'un point de vue pratique, elle s'insère dans le cadre des démarches visant à améliorer la prévisibilité des changements dans la qualité et la quantité des ressources hydriques renouvelables, en lien avec les changements climatiques et les pressions anthropiques sur ces ressources. De tels enjeux sont jugés comme fondamentaux par l'Organisation Scientifique et Culturelle des Nations Unies (UNESCO, 2009).

C'est notamment dans ce contexte que s'insère l'approche fondée sur l'étude des grandes rivières (Meybeck et Ragu, 1995; Gaillardet et al., 1999), ces dernières transportant une signature géochimique héritée de processus s'opérant à l'échelle des bassins qu'elles drainent. Ainsi, l'établissement de bilans géochimiques réalisés à partir des flux d'ions majeurs, de matière organique, d'éléments traces et d'isotopes exportés par les rivières permet une étude quantitative des grands cycles géologiques, climatiques, hydrologiques et biologiques.

La présente étude privilégie une telle approche et vise à évaluer comment se transcrivent les incidences du climat et de l'environnement géologique sur le cycle de l'eau et sur l'altération chimique au sein des bassins hydrographiques des Baies d'Hudson, James et d'Ungava (HJUB) et du Saint-Laurent. Deux grands thèmes y sont abordés (sections 1.2 et 1.3):

1- La problématique de l'étude du cycle de l'eau par une approche géochimique
2- La problématique de l'altération chimique au sein des bassins hydrographiques

1.2. Problématique de l'étude du cycle de l'eau par une approche géochimique

Dans un contexte où les changements climatiques et les pressions anthropiques risquent d'avoir un impact sur les ressources hydriques renouvelables à l'échelle planétaire, quels sont les apports de la géochimie à la compréhension du cycle de l'eau?

La géochimie des isotopes stables constitue une piste de réponse à cette question. De fait, il est reconnu que les contenus en isotopes stables (^{2}H-^{18}O) des eaux naturelles décrivent des variations spatiotemporelles répondant à des processus de fractionnement isotopique qui sont en grande partie liés aux conditions hydro-climatiques. Entre autres, l'évaporation et la diffusion en phase vapeur au-dessus des océans (Craig et Gordon, 1965), la condensation au sein des masses atmosphériques (Craig, 1961) et l'évaporation au niveau des eaux continentales (Gonfiantini, 1986; Gibson et al., 1993; 2001; 2002; Gat, 1996; Gibson et Edwards, 2002) engendrent des fractionnements des isotopes de la molécule d'eau. Ainsi, les eaux naturelles acquièrent une signature isotopique permettant de tracer le cycle de l'eau.

Notamment, une documentation du cycle de l'eau a été établie grâce au programme « *Global Network for Isotopes in Precipitation* » (GNIP), une entreprise chapeautée par l'Agence Internationale d'Énergie Atomique (IAEA) et l'Organisation Météorologique Mondiale (WMO). Depuis le lancement du programme GNIP en 1961, une littérature scientifique s'est développée autour du thème de l'étude de la composition isotopique des précipitations à l'échelle du globe (Craig, 1961; Dansgaard, 1964; Merlivat and Jouzel, 1979; Rozanski et al., 1993; Fritz et al., 1987; Araguàs Araguàs et al., 2000; Bowen and Wilkinson, 2002; Bowen and Revenaugh, 2003; Birks et al., 2004). C'est en complémentarité et dans la continuité du programme GNIP que se situe le « *Global Network for Isotopes in Rivers* » (GNIR) (Gibson et al., 2002; Vitvar et al., 2007), un programme parrainé par L'IAEA. Par ce projet, l'IAEA vise notamment à documenter les impacts des changements climatiques et des pressions anthropiques sur l'hydrologie des rivières.

Un avantage de l'approche fondée sur l'étude des rivières découle du fait que ces dernières intègrent de l'information sur les processus hydrologiques s'opérant à l'échelle des bassins, tamponnant ainsi les variations ponctuelles pouvant résulter d'effets topographiques et hydro-climatiques locaux. Or, si Kendall et Coplen (2001) ont établi que les rivières préservent une archive de la signature isotopique des précipitations qui alimentent leur bassin, décrypter l'influence des processus hydrologiques

subséquents aux précipitations sur la composition isotopique des rivières s'avère complexe. Notamment, les incidences superposées des processus de recharge (Fritz et al., 1987; Clark et Fritz, 1987), d'évaporation (Gonfiantini, 1986; Gibson et al., 1993; 2001; 2002; 2008; Gat, 1996; Telmer et Veizer, 1997; Gibson and Edwards, 2002; Yi et al., 2008), de formation de glace (Gibson et Prowse, 2002), de fonte des neiges (Laudon et al., 2002) et de mélange (Yang et al., 1996; Myre, 2007; Yi et al., 2010) ayant lieu au sein des bassins hydrographiques doivent être prise en compte, en plus des perturbations anthropiques affectant les cours d'eaux (ouvrages de régulation de débits, réservoirs hydroélectriques, réseaux de pompage et d'irrigation).

Ainsi, les rivières transportent un signal isotopique complexe, et malgré l'ampleur des efforts accordés à leur étude (voir les ouvrages de synthèse proposés par Mook, 2000; Gibson et al., 2005), nombre de questions méritent toujours d'être abordées. Dans le cadre de la présente étude, trois principales questions ont été traitées:

1- Les variations en ^{2}H-^{18}O telles que mesurées à l'exutoire des grandes rivières transcrivent-elles les effets des variations hydro-climatiques saisonnières dans les bassins hydrographiques?

2- Les rivières conservent-elles un signal isotopique permettant de retracer la composition isotopique moyenne de la recharge et des précipitations à l'échelle des bassins?

3- Les teneurs en ^{2}H-^{18}O telles que mesurées à l'exutoire des grandes rivières, comparées à celles des précipitations, peuvent-elles êtres transcrites en grands bilans hydrologiques?

1.3. Problématique de l'altération chimique

En raison de leur instabilité thermodynamique aux conditions de pression et température rencontrées à la surface de la Terre, la plupart des minéraux constituant les formations géologiques s'altèrent chimiquement de façon spontanée et irréversible en interagissant avec l'eau issue des précipitations. Dès 1845, Ebelmen décrivait l'altération chimique comme une réaction de neutralisation consommant des protons, transformant les minéraux primaires en phases secondaires et libérant des ions.

En ce qui concerne l'altération des silicates (1) et des carbonates (2), deux principaux modes d'altération chimique seront considérés, l'un consommant des protons issus de l'acide carbonique (a), l'autre consommant des protons issus de l'acide sulfurique (b):

$$CaSiO_3 + 2H_2CO_3 + H_2O \rightarrow Ca^{2+} + 2HCO_3^- + H_4SiO_4 \qquad (1a)$$

$$CaCO_3 + H_2CO_3 = Ca^{2+} + 2HCO_3^- \qquad (2a)$$

$$CaSiO_3 + H_2SO_4 + H_2O \rightarrow Ca^{2+} + SO_4^{2-} + H_4SiO_4 \qquad (1b)$$

$$2CaCO_3 + H_2SO_4 \rightarrow 2Ca^{2+} + SO_4^{2-} + 2HCO_3^- \qquad (2b)$$
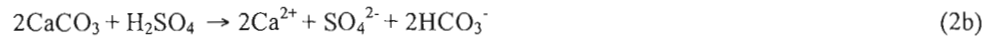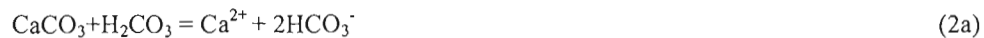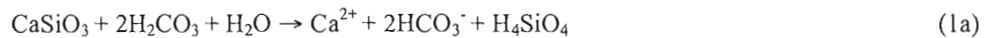
Ainsi, on s'aperçoit que dans le cas où les protons sont dérivés de l'acide carbonique, l'altération des silicates (Ca-Mg) (1a) suivie de la précipitation de calcite dans les océans (inverse de la réaction 2a) agit comme un mécanisme de consommation de CO_2. Suivant une telle logique, Walker et al (1981) établissent formellement l'hypothèse selon laquelle à l'échelle des temps géologiques, la concentration du CO_2 atmosphérique est régulée par un mécanisme de boucle de rétroaction négative, alors que le taux d'altération des silicates dépend de la température, qui elle même est fonction du CO_2 atmosphérique participant à l'effet de serre. D'un autre côté, Raymo (1988) propose qu'à l'échelle globale, les taux de soulèvement tectoniques (plutôt que la température) dictent les taux d'altération chimique. Bien que ces deux hypothèses ne soient pas mutuellement exclusives, elles soulèvent des questions en ce qui a trait aux mécanismes qui contrôlent l'altération chimique, et c'est dans ce contexte que se situe l'étude des grands cycles géochimiques continentaux: comment peut-on évaluer quantitativement l'influence des mécanismes qui dictent la dynamique des taux d'altération chimique contemporains?

L'établissement de bilans de masse à partir des flux dissous exportés par les grandes rivières constitue une piste de solution à cette question. Notamment, les incidences de la lithologie, de la topographie, des taux de soulèvement tectonique, des taux d'érosion physique, de la température, du taux de ruissellement et du couplage avec le cycle de la matière organique sur l'intensité des flux dissous exportés par les rivières ont été illustrés (eg.: Garrels et Mackenzie, 1971; Meybeck, 1987; Edmond et al., 1996; Huh et al., 1998; 1999; Gaillardet et al., 1995; 1999; Galy et France-Lanord, 1999; Millot et al., 2002; 2003; Dupré et al., 2003; France-Lanord et al., 2003; Viers et al., 2007). Avec l'amélioration des méthodes permettant d'évaluer les contributions relatives de différentes lithologies aux flux exportés par les rivières (Garrels et Mackenzie, 1971; Négrel et al., 1993; Gaillardet et al., 1997; Bricker et al., 2003) et de documenter les réactions d'altération (Galy et France-Lanord, 1999; Spence et Telmer, 2006, Calmels et al., 2007; Lerman et al., 2007), il devient possible de mieux contraindre les effets des influences environnementales sur les taux d'altération de certains types de roches. On retiendra, par exemple, l'établissement de règles quantitatives liant les taux d'altération chimique à la température et au taux de ruissellement (White et Blum, 1995; Dessert et al., 2003). Ainsi, avec une documentation croissante de la composition des grandes rivières (ex.: voir la compilation GEMS/GLORI, Meybeck et Ragu, 1995), l'établissement de budgets d'altération chimique (et de consommation de CO_2) à l'échelle planétaire semble à portée de main (Gaillardet et al., 1999; Viers et al., 2003). Or, malgré l'ampleur des développements scientifiques et techniques récents, certaines incertitudes persistent. Notamment, les variations saisonnières dans les flux exportés par les rivières sont encore souvent mal contraintes, un paramètre qui semble pourtant critique, notamment pour les régions à saisonnalité proéminente (ex.: voir Tipper et al., 2006). De plus, les études fondées sur la comparaison de bassins contrastés reposent souvent sur des données récupérées sous des conditions et des échelles de temps différentes, compliquant les comparaisons directes. Ainsi, deux sous-questions seront abordées dans la présente étude :

1- Peut-on évaluer les incidences des conditions hydro-climatiques sur les taux d'altération chimique à partir d'un monitoring saisonnier des flux dissous (ions majeurs, carbone organique et éléments traces) mesurés à l'exutoire de grandes rivières?

2- Peut-on, en comparant l'intensité des flux dissous exportés par des rivières drainant des bassins contigus, établir l'importance relative des paramètres qui dictent les taux d'altération chimique?

1.4. L'utilisation des déséquilibres (^{234}U/^{238}U) comme outil d'étude de l'altération chimique

Dans un contexte où l'on cherche à tracer les flux géochimiques exportés par les rivières, comment identifier des traceurs géochimiques sensibles aux processus d'altération?

L'étude des déséquilibres isotopiques de l'uranium (^{234}U/^{238}U) mesurés en phase dissoute semble constituer une piste de réponse. Notamment, la mobilité préférentielle de l'isotope fils (^{234}U) lors des interactions eau-roche a été mise en évidence. Cette observation est couramment attribuée à l'effet de recul (Tcherdyntsev, 1955), un processus associé à la désintégration de ^{238}U par l'émission d'une particule alpha, produisant des intermédiaires (^{234}Th-^{234}Pa) qui se désintègrent rapidement en ^{234}U. Or, la désintégration alpha de ^{238}U résulte en un transfert d'énergie à l'atome fils, un processus pouvant engendrer des dommages dans les structures cristallines. En conséquence, l'isotope ^{234}U, qui risque de se trouver au sein de sites cristallins endommagés, a tendance à être lessivé préférentiellement (par rapport à l'isotope père, ^{238}U) lors des interactions eau-roche. Ce processus semble influencer grandement les rapports d'activité (^{234}U/^{238}U) tels que mesurés dans les eaux de surface, qui présentent généralement un excès en ^{234}U par rapport à l'équilibre séculaire (ex.: voir Osmond et Ivanovich, 1992). Toujours en lien avec l'effet de recul, (Kigoshi, 1971) propose même que sur une échelle de temps suffisamment longue, l'éjection directe de ^{234}Th des surfaces minérales pourrait expliquer les excès de ^{234}U mesurés dans les eaux naturelles, notamment dans les eaux souterraines (ex.: voir Osmond et Cowart, 1992; Sun et Semkow, 1998).

Ainsi, l'amplitude des déséquilibres (^{234}U/^{238}U) mesurés dans les eaux naturelles est susceptible de dépendre de la nature des minéraux soumis aux interactions eau-roche, des taux de dissolution de ces minéraux, de la disponibilité de surfaces minérales fraiches et de la durée des interactions eau-roche. L'uranium transporté en phase dissoute dans le réseau hydrographique pourrait donc constituer un traceur isotopique permettant de documenter la dynamique d'altération des roches.

Dans les systèmes fluviaux, les isotopes de l'U ont notamment été utilisés pour documenter les sources d'altération chimique et quantifier les temps de transfert des particules (Vigier et al., 2001; Dosseto et al., 2006 a, b, c, Chabaux et al., 2006; Granet et al., 2007; Chabaux et al., 2008). Or, si le contrôle qu'impose la lithologie sur les déséquilibres (^{234}U/^{238}U) des eaux de surface semble important dans certains contextes (Sarin et al., 1990; Pande et al., 1994; Vigier et al., 2005), d'autres paramètres d'influence ont également été identifiés. Entre autres, les taux d'altération physique et la production de surfaces minérales fraiches (Kronfeld et Vogel, 1991; Robinson et al., 2004), le rôle de la phase colloïdale (Porcelli et al., 1997; Andersson et al., 1998; Riotte et al., 2003) et les mélanges entre les

eaux souterraines et les eaux de surface (Riotte et Chabaux, 1999; Riotte et al., 2003; Durand et al., 2005) semblent influer sur les déséquilibres (^{234}U/^{238}U) mesurés dans les rivières. Ainsi, les processus régulant les déséquilibres (^{234}U/^{238}U) méritent d'être étudiés d'avantage afin de mieux contraindre leurs incidences.

De surcroît, en vue des incertitudes portant sur l'évaluation du temps de séjour océanique de l'uranium (3.2 - 5.6 x10^5 yrs) (Dunk et al., 2002), il semble qu'une quantification plus précise des flux exportés par les rivières soit nécessaire. En outre, peu d'études ont abordé la question des variations saisonnières dans les flux et les déséquilibres isotopiques de l'uranium dans les rivières (Grzymko et al., 2007; Ryu et al., 2009).

La présente étude abordera la question suivante en ce qui a trait à l'utilisation de l'uranium à titre de traceur géochimique :

1- Quels sont les paramètres environnementaux qui dictent l'intensité et le déséquilibre isotopique (^{234}U/^{238}U) des flux d'uranium exportés par les rivières de l'HJUB?

2. OBJECTIFS

L'objectif général de la présente étude est d'évaluer les incidences de l'environnement géologique et du climat sur le cycle de l'eau et l'altération chimique au sein des grands bassins hydrographiques du nord-est du Canada. En lien avec les problématiques soulevées, les objectifs spécifiques sont :

1- De documenter le cycle de l'eau et d'établir des bilans hydriques à partir des chroniques isotopiques (^{2}H-^{18}O) des rivières,

2- D'évaluer les taux et les paramètres de contrôle de l'altération chimique dans les bassins hydrographiques de la région de l'HJUB,

3- D'évaluer le potentiel d'utilisation des déséquilibres (^{234}U/^{238}U) à titre de traceur des processus d'altération chimique et des exports fluviaux dissous dans les bassins hydrographiques de la région de l'HJUB.

3. APPROCHE PROPOSÉE

En lien avec cette problématique et afin de répondre aux objectifs proposés, la présente étude privilégie une approche fondée sur le monitoring géochimique des exports fluviaux dissous (δ^2H-δ^{18}O, cations majeurs, carbone organique dissous (COD), Nd, Sr, ^{87}Sr/^{86}Sr, U, (^{234}U/^{238}U)). La démarche repose essentiellement sur l'évaluation des variations temporelles et spatiales de la géochimie des rivières:

1- L'échelle temporelle :

    a. Par la documentation de la variabilité saisonnière dans les concentrations, compositions isotopiques et flux exportés par les rivières étudiées.

    b. Par la documentation de la variabilité interannuelle de la composition isotopique de la molécule d'eau (au niveau du bassin hydrographique du fleuve Saint-Laurent).

2- L'échelle spatiale :

    a. Par la comparaison de rivières drainant des bassins contigus sur plus de 15 degrés de latitude.

    b. Par l'évaluation de l'évolution géochimique de l'eau au long de certaines rivières.

4. PLAN

Dans un premier lieu, le site d'étude et les méthodes seront brièvement décrits. Chacun des chapitres constituant le cœur de la thèse comportera également un survol de ces aspects.

Les deux premiers chapitres du corps de cette thèse portent sur l'étude des chroniques isotopiques (^{2}H-^{18}O) réalisées sur les rivières de la région d'étude. Dans ces chapitres, les incidences du climat, des régimes de précipitations et de l'évaporation sur le cycle hydrologique dans les bassins sont étudiées par la documentation des isotopes stables de la molécule d'eau (^{2}H-^{18}O) au sein des rivières. La cyclicité saisonnière des signaux (δ^2H-δ^{18}O) y est abordée afin de documenter la dynamique hydrologique des bassins. Des méthodes permettant d'estimer la composition isotopique de la recharge, des mélanges de sources ainsi que les taux d'évaporation dans les bassins sont abordées. Cette première étape s'avèrera nécessaire à l'interprétation de la saisonnalité mesurée dans les flux géochimiques exportés par les rivières (ci-dessous).

Dans un premier lieu (Chapitre 1), la problématique de l'étude du cycle hydrologique des rivières est abordée à partir de séries temporelles (^{2}H-^{18}O) longues de 12 ans réalisées aux stations d'échantillonnage du Fleuve Saint-Laurent et de la rivière des Outaouais, le bassin hydrographique méridional de la région d'étude. Le cycle hydrologique des rivières est d'abord mis en évidence et discuté en fonction de la saisonnalité proéminente de la région. Ensuite, des bilans de masse isotopiques sont proposés afin de quantifier les processus de mélanges de tributaires et d'évaporation au sein des bassins. Finalement, la variabilité interannuelle des teneurs en ^{2}H-^{18}O est discutée et mise en lien avec les processus environnementaux pouvant l'expliquer.

Suivant une approche méthodologique similaire, le Chapitre 2 porte sur les chroniques ^{2}H-^{18}O mesurées au sein des bassins hydrographiques contigus du nord-est du Canada. La région d'étude permet d'échantillonner un profil latitudinal de plus de 12 degrés. L'étude vise à évaluer si le gradient isotopique des précipitations est conservé par les rivières. Les variations isotopiques saisonnières de la rivière La Grande (rivière harnachée) y sont également comparées à celles de son analogue naturel le plus proche, la Grande Rivière de la Baleine, avec pour objectif de documenter les impacts des

installations hydroélectriques sur le cycle hydrologique des rivières. Finalement, une méthode d'évaluation de l'évaporation moyenne sur la zone d'étude est proposée.

Ces deux premiers chapitres permettent de définir ce que représente le signal géochimique d'un échantillon récupéré en un temps donné dans une rivière. Si la question peut sembler triviale à première vue, le déphasage et l'atténuation des séries temporelles (^{2}H-^{18}O) mesurées dans les rivières par rapport à la saisonnalité des conditions hydro-climatiques justifie la démarche. Il s'agit d'une étape fondamentale puisque subséquemment, des aliquotes de ces échantillons serviront à établir l'intensité des flux dissouts exportés par ces rivières.

Les deux chapitres suivants portent sur la documentation des processus d'altération chimique des roches au sein des bassins hydrographiques. L'approche repose sur une quantification des exports fluviaux dissous.

Le troisième chapitre porte sur les problématiques liées à l'étude de l'altération chimique, en lien avec la saisonnalité des flux exportés par les rivières. L'intensité de l'altération chimique dans les grands bassins de la région de la baie de James, de la Baie d'Hudson et de la Baie d'Ungava (HJUB) est calculée à partir des flux dissouts (ions majeurs, carbone organique et lanthanides) exportés par les rivières. La relation entre l'abondance des roches volcaniques et sédimentaires et les taux d'altération y est quantifiée, de même que le lien entre les flux de lanthanides et de matière organique dissoute.

Le quatrième chapitre explore les possibilités d'utilisation des déséquilibres (^{234}U/^{238}U) en phase dissoute à titre de géochimique des exports fluviaux. La relation entre les concentrations d'uranium dissout, les déséquilibres (^{234}U/^{238}U) et les sources lithologiques y est illustrée. Le rôle de l'accumulation d'uranium dans les tourbières et sols organiques et de son impact sur l'intensité des flux exportés par les rivières y est abordé.

Finalement, en conclusion générale, un survol des retombées de cette thèse est présenté, en lien avec les recommandations scientifiques qui en émergent.

5. RÉGION D'ÉTUDE

La région d'étude est décrite au début de chacun des chapitres constituant le cœur de cette thèse, en fonction des objectifs spécifiques de chacun de ces chapitres. Un sommaire est rapporté ci-dessous.

5.1. Cadre géographique et physiographique

Les bassins hydrographiques étudiés dans le cadre de cette thèse couvrent environ 2.8×10^6 km^2 sur plus de 15 degrés de latitude (Fig. 1, Tableau 1) et alimentent les baies d'Hudson, James et d'Ungava (HJUB) et l'Atlantique Nord (Bassin du fleuve Saint-Laurent). Les rivières échantillonnées transportent près de 50% des flux d'eau douce atteignant l'HJUB et l'essentiel des flux atteignant l'exutoire de l'estuaire fluvial du Saint-Laurent. La superficie des bassins hydrographiques, leurs taux de ruissellement et les débits des rivières qui les drainent sont rapportés au Tableau 1.

L'intensité du ruissellement est faible au sein du bassin du fleuve Nelson en comparaison aux autres bassins hydrographiques étudiés (Tableau 1), traduisant essentiellement un climat plus aride au niveau des prairies canadiennes en comparaison à la région du Bouclier Canadien située à l'est de la Baie d'Hudson. Le lecteur est référé à la carte MCR 4145 (1991, Atlas National du Canada, Énergie, Mines et Ressources Canada) pour une illustration des régimes de précipitation au sein de la région d'étude. La région est caractérisée par une saisonnalité proéminente, tel qu'illustré par les écarts mesurés au niveau des températures moyennes mensuelles (Tableau 2). Un important gradient climatique latitudinal y est également enregistré, les températures moyennes annuelles s'échelonnant entre -6°C à Kuujjuaq (Bassin de la rivière Koksoak) et à 6°C à Montréal (Bassin du fleuve Saint-Laurent) (Tableau 2). Ainsi, le couvert végétal décrit une transition entre la forêt mixte au sud de la région d'étude à la toundra plus au nord (voir carte numérique, annexe A) alors que les tourbières sont abondantes sur toute la région d'étude (voir carte numérique, annexe B). Le relief y est relativement peu accidenté, à l'exception des altitudes maximales atteignant environ 3000 m à l'extrême ouest du bassin du Fleuve Nelson, au piedmont des Rocheuses Canadiennes. Au sein des autres bassins, les altitudes maximales atteignent environ 700 m (carte MCR 4097, 1991, Atlas National du Canada, Énergie, Mines et Ressources Canada).

Figure 1. Région d'étude.
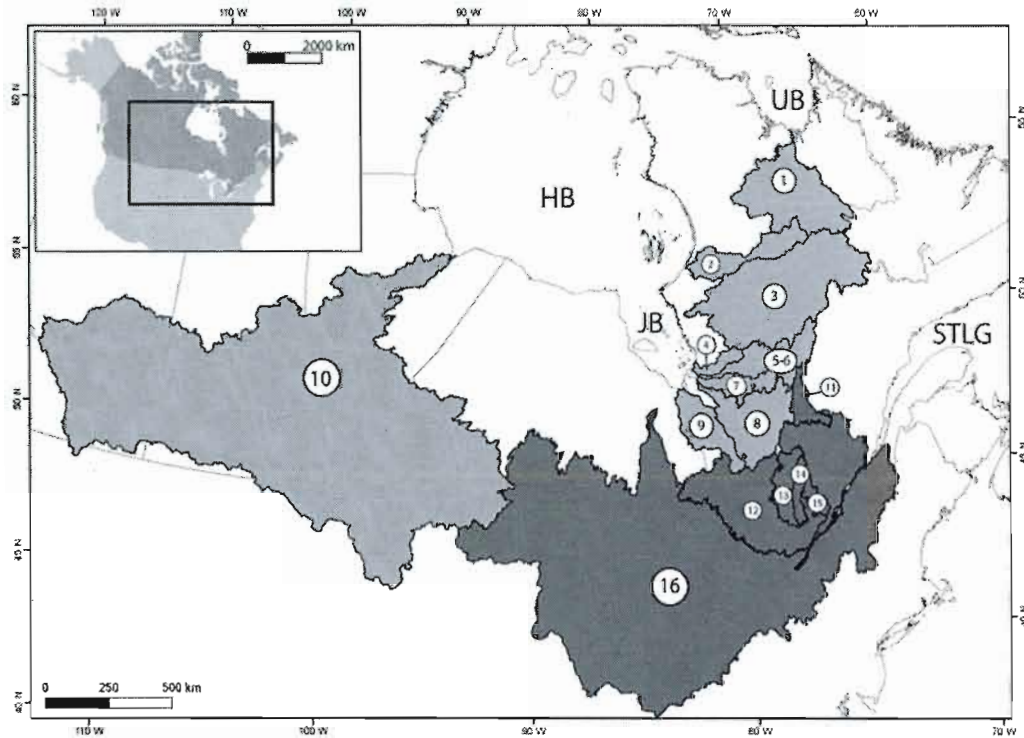
Les bassins hydrographiques étudiés sont représentés par des numéros et leur description est présentée au tableau 1.

Tableau 1. Caractéristiques des bassins hydrographiques étudiés.

Bassin	Q (m³/s)	A (Km²)	Ruissellement (mm/an)	Province Géologique	R. Int. (%)	R. Mét. (%)	R. Séd. (%)	R. Volc. (%)
(1) Koksoak[1]	1600	94311	535	S,C	68	1	20	10
(2) Great Whale[1]	676	42700	499	S	99	0	0	1
(3) La Grande[3]	3808	177678	676	S	69	26	2	3
(4) Pontax[1]	111	6020	579	S	57	38	1	5
(5) Nemiscau[3]	53	3015	549	S	ND	ND	ND	ND
(6) Rupert[4]	848	40900	654	S	51	28	17	4
(7) Broadback[3]	367	17100	677	S	60	25	1	14
(8) Bell[1]	497	22200	706	S	50	19	0	31
(9) Harricana[1]	70	3680	604	S	23	23	3	50
(10) Nelson[2]	4024	1100000	115	PI, PBH, C, S, CO	9	0	90	1
(11) Ashuapmushuan[1]	290	15300	599	S	5	94	1	0
(12) Outaouais[3]	1750	149000	370	G, PSTL	14	61	19	5
(13) Gatineau[1]	144	6840	665	G	10	88	2	0
(14) Du Lièvre[1]	100	4530	699	G	4	86	10	
(15) Du Nord[1]	33	1170	883	G	ND	ND	ND	ND
(16) St-Laurent[3]	10500	1153000	287	G, A, PSTL	25	31	39	5

Les numéros de basins (#) correspondent à ceux illustrés à la fig. 1. Le couvert lithologique est évalué à partir de la carte 1860A de la Commission Géologique du Canada (Wheeler et al., 1996). Les provinces géologiques sont : Supérieur (S), Churchill (C), Plate-forme Intérieure (PI), Plate-forme de la Baie d'Hudson (PBH), Cordillère de l'Ouest (CO), Plate-forme du Saint-Laurent (PSTL), Appalaches (A). Les débits et surfaces de bassins sont tirés de: [1]Ministère du développement durable, de l'environnement et des parcs (MDDEP), [2]Water Survey of Canada, [3]Hydro-Quebec (communication personnelle). Les débits et superficies de bassins correspondent aux secteurs localisés en amont des sites d'échantillonnage.

Tableau 2. Données climatiques au sein de la région d'étude.

Station	Bassin hydrographique	Lat. / Long.	Température moyenne annuelle (min. mensuel; max. mensuel) (°C)	Pluie (mm)	Neige (cm)
Kuujjuaq	(1) Koksoak	58,10° / 68,42°	-6 (-24 ; 12)	277	257
Kuujjuarapik	(2) Great Whale	55,28° / 77.75°	-4 (-23 ; 11)	415	241
Radisson	(3) La Grande	58,63° / 77,70°	-3 (-23 ; 14)	437	267
Matagami	(8) Bell	49,77° / 77,82°	-1 (-20 ; 16)	618	314
Amos	(9) Harricana	48,57° / 78,13°	1 (-17 ; 17)	671	248
Winnipeg	(10) Nelson	49,92° / 97,23°	3 (-18 ; 20)	416	111
Mont Laurier	(14) Du Lièvre	46,57° / 73,55°	3 (-14 ; 18)	791	224
Montréal	(16) Saint-Laurent	45,52° / 73,42°	6 (-10 ; 21)	820	221

Les données sont tirées des archives nationales d'information et de données climatologiques, Normales climatiques au Canada 1971-2000, Environnement Canada. Les minimum et maximum des températures moyennes mensuelles sont rapportés entre parenthèse à la colonne quatre, à côté des températures moyennes annuelles.

5.2. Environnement géologique

Des cartes géologiques été produites pour chacun des bassins versants à l'étude (Annexes numériques C1 à C16). Les âges et types de roches drainées ainsi que la couverture de dépôts meubles au sein des bassins étudiés y sont illustrés. La quantification de la couverture des principales formations géologiques (roches sédimentaires, volcaniques, métamorphiques, et intrusives) drainées par les bassins hydrographiques est rapportée au Tableau 1. Les cartes géologiques et les calculs ont été produits à partir des cartes 1860A (Wheeler et al., 1996) et 1880A (Fulton, 1995) de la Commission géologique du Canada et de la délimitation des bassins hydrographiques du *Water Survey of Canada* (*National Scale Frameworks Hydrology Data, NRCan, 2008*). La délimitation du bassin de la rivière La Grande a été fournie par Hydro-Québec.

Le cadre géologique est décrit au début des chapitres 3 et 4, en fonction des objectifs qui y sont abordés. Pour une description de la géologie générale de la région d'étude, le lecteur est référé aux travaux de synthèse de Hocq (1994), Stott (1993), Card et Poulsen (1998) et Davidson (1998) et aux cartes 1860A (Wheeler et al., 1996) et 1880A (Fulton, 1995) de la commission géologique du Canada. Les travaux de Shaw et al (1967; 1986), décrivent la composition chimique des roches au sein de la région d'étude.

5.3. Justification du choix de la région d'étude

Tel que mentionné précédemment, l'objectif général de cette thèse est d'évaluer les contrôles environnementaux sur le cycle de l'eau et l'altération chimique, en favorisant une approche géochimique. Les contrastes géologiques, hydrologiques et climatiques entre les bassins étudiés sont propices à l'atteinte de cet objectif. D'une part, la diversité de la mosaïque géologique couverte par les bassins permettra d'étudier le contrôle géologique sur la qualité de l'eau des rivières. D'autre part, la saisonnalité proéminente ainsi que l'importance du gradient climatique mesuré sur les 15 degrés de latitude que couvre la région d'étude seront propices à l'évaluation des incidences du climat sur l'intensité des flux dissous exportés par les rivières. Ce point s'avère important, notamment au sein d'une région où l'hydrologie des rivières pourraient s'avérer sensible aux impacts des changements climatiques (Déry et al., 2004; 2005; 2009; Boyer et al., 2010). Ces aspects, entres autres, justifient le choix de la région d'étude.

6. MÉTHODES

6.1. Sites d'échantillonnage

Les sites d'échantillonnages ont été sélectionnés en fonction de leur accessibilité et de la présence d'infrastructures d'échantillonnage préexistantes. Leur localisation géographique et leurs particularités sont rapportées au Tableau 3. Les sites d'échantillonnage des rivières Koksoak, Great Whale et La Grande ont été sélectionnés et échantillonnés en collaboration avec Environnement Canada et constituent maintenant le réseau de monitoring des rivières du nord du Québec de cet organisme.

Lors de la sélection des lieux d'échantillonnage, les sites situés en aval de rapides ou de barrages hydroélectriques ont été privilégiés car ils offrent la possibilité de tirer avantage de l'homogénéisation de la phase dissoute des rivières. Dans les cas où ce critère ne pouvait être satisfait, des échantillons de surface ont été récupérés au centre des rivières, en utilisant une bouteille à messager ou un contenant de LDPE fixé à une perche ou une corde (selon la turbulence et la profondeur du cours d'eau au niveau du site d'échantillonnage).

Tableau 3. Description des sites d'échantillonnage.

Bassin	Lat/long	Particularités du site d'échantillonnage	Prélèvement	Collaborateurs
(1) Koksoak	58,029 / 68,475	Localisé en aval de la jonction des rivières Caniapiscau et des Mélèzes, régime non turbulent	Centre de la rivière, 30 cm sous la surface, bouteille LDPE fixée à une tige d'échantillonnage.	Micheal Kwan, *Makivik Research Corporation*
(2) Great Whale	55,279 / 77,650	Localisé en aval de rapides, environ 7km en amont de Kuujjuarapik	Centre de la rivière, 30 cm sous la surface, bouteille LDPE fixée à une tige d'échantillonnage	Claude Tremblay, Centre d'études Nordiques de l'Université Laval
(3) La Grande	53,781 / 77,530	Prise d'eau du barrage LG-2, à l'intérieur de la centrale, en amont des turbines.	Directement à partir d'un robinet d'échantillonnage au sein du Barrage LG-2	Jean-Louis Fréchette, Environnement Illimité, Alain Tremblay, Hydro-Québec
(4) Pontax	51,733 / 77,383	Au niveau de faibles rapides	À partir de la berge, bouteille LDPE fixée à une perche	
(5) Nemiscau	51,688 / 75,825	Régime non turbulent	Centre de la rivière, à partir d'un pont, en utilisant bouteille LDPE fixée à une corde	
(6) Rupert	51,353 / 77,423	En aval de rapides	À partir de la berge, bouteille LDPE fixée à une perche	
(7) Broadback	51,185 / 77,465	En aval de rapides	À partir de la berge, bouteille LDPE fixée à une perche	
(8) Bell	49,769 / 77,627	Régime non turbulent	Centre de la rivière, à partir d'un pont, en utilisant une bouteille à messager	
(9) Harricana	48,790 / 78,013	En aval de rapides	Centre de la rivière, à partir d'un pont, en utilisant une bouteille LDPE fixée à une corde	
(10) Nelson	56,685 / 93,790	En aval d'un barrage hydroélectrique	Centre de la rivière, 30 cm sous la surface, bouteille LDPE fixée à une tige d'échantillonnage	Terry Dick, *University of Manitoba*
(11) Ashuapmushuan	48,658 / 72,445	Régime non turbulent	Centre de la rivière, à partir d'un pont, en utilisant une bouteille à messager	
(12) Outaouais	45,567 / 74,384	En aval d'un barrage hydroélectrique	Centre de la rivière, à partir du tablier du barrage hydroélectrique de Carillon, en utilisant une bouteille à messager	
(13) Gatineau	46,620 / 75,916	En aval de rapides	À partir de la berge, bouteille LDPE fixée à une perche	
(14) Du Lièvre	46,549 / 75,514	Régime non turbulent	Centre de la rivière, à partir d'un pont, en utilisant une bouteille à messager	
(15) Du Nord	45,780 / 74,005	Au niveau de faibles rapides	À partir de la berge, bouteille LDPE fixée à une perche	
(16) St-Laurent	46,809 / 71,190	À l'exutoire de l'estuaire fluvial, au niveau de battement des marées	Usine de pompage de Lévis (voir Hélie et al., 2002; 2005)	

6.2. Filtration et stockage

Lorsque les conditions de terrains le permettaient, la conductivité, le pH et l'alcalinité ont été mesurés au moment de l'échantillonnage. Dans les cas où les conditions météorologiques compliquaient les mesures (notamment lorsque la température de l'air était significativement sous 0°C), les échantillons ont été transportés au laboratoire et les mesures ont été faites à l'intérieur d'un délai d'une journée. Les procédures de prélèvement et de préservation sont rapportées dans le Tableau 4.

Tableau 4. Sommaire des méthodes de prélèvement.

Paramètre	Filtration	Préservation	Bouteilles de stockage	Nettoyage des bouteilles
Cations majeurs (Na, Mg, K, Ca), Sr et lanthanides	0.22 µm, membrane PES, seringue, sur le site	pH=2 (HNO_3 distillé), 4°C	HDPE 30 ml	3 x Milli-Q, trempage HNO_3 5%, 1 x Milli-Q, 3 rinçages avec l'eau d'échantillonnage
Uranium	0.45 µm, membrane nylon, erlenmeyer et pompe manuelle, délai < 20h suivant l'échantillonnage, l'échantillon étant conservé dans une glacière, à 4°C et à l'obscurité	pH=2 (HNO_3 distillé), 4°C	HDPE 1 l	3 x Milli-Q, trempage HNO_3 5%, 1 x Milli-Q, 3 rinçages avec l'eau d'échantillonnage
Anions (Cl, SO_4, H_4SiO_4)	0.22 µm, membrane PES, seringue, sur le site	Congélation	HDPE 30 ml	3 x Milli-Q, trempage Milli-Q, 3 rinçages avec l'eau d'échantillonnage
Carbone organique dissout	0.30 µm, filtre EPM-2000, erlenmeyer et pompe manuelle, délai < 24h suivant l'échantillonnage, l'échantillon étant conservé dans une glacière, à 4°C et à l'obscurité	4°C	Verre ambré avec bouchon conique, 125 ml	Trempage + rinçage Milli-Q, chauffage à 500°C, 3 rinçages avec l'eau d'échantillonnage
Isotopes de la molécule d'eau (^{2}H-^{18}O)			HDPE 30 ml	3 rinçages avec l'eau d'échantillonnage

6.3. Méthodes analytiques

Les méthodes analytiques utilisées dans le cadre de la présente étude sont discutées dans les chapitres constituant le corps de cette thèse. Un sommaire des méthodes est présenté dans le Tableau 5.

Tableau 5. Sommaire des méthodes analytiques.

Paramètre	Volume requis	Séparation chimique	Standards de validation	analyse	Reproductibilité externe (2σ)	Blancs procéduraux [Blanc total] / [échantillon le moins concentré]
[Ca-Mg-Na-K]	5 ml	N.A.	SLRS-4	Chromatographie ionique (Dionex DX-120) (IPGP)	< 5%	< 5%
[Sr] et [lanthanides]	5-15 ml	N.A.	SLRS4	ICP-MS (X7 Series, ThermoElectron) (IPGP)	Nd < 5% Sr < 10%	< 0,1%
$^{87}Sr/^{86}Sr$	5-15 ml	Selon Meynadier et al.,(2007)	NIST ($^{87}Sr/^{86}Sr = 0.71027 \pm 0.00006$, n=30)	MC-ICP-MS (Neptume™) (IPGP)	< 10%	< 0,1%
[U] – ($^{234}U/^{238}U$)	1000 ml	Modifié de Gariépy et al., 1994. Double-spike ^{233}U-^{236}U.	HU-1 ($^{234}U/^{238}U = 1.003 \pm 0.006$, n=16)	TIMS (dilution isotopique) (VG-Sector) (GEOTOP)	($^{234}U/^{238}U$) ≈ 1% [U] < 1%	< 0,1%
[NO$_3$-SO$_4$-Cl]	10 ml	N.A.	Standards internes	Chromatographie ionique (Dionex DX-120) (IPGP)	< 5%	< 5%
[COD]	125 ml	N.A.	Standards internes K-H-pht	*Wet oxidation (Shimadzu™ TOC-5000A)* (GEOTOP)	< 5%	< 0,5%
δ^2H-$\delta^{18}O$	30 ml	N.A.	Voir chap. 1	Voir chap. 1	Voir chap. 1	Voir chap. 1

CHAPITRE 1 : Controls on the stable Isotope Composition of the St. Lawrence River

Rosa Eric[1,2],
Hillaire-Marcel Claude[1],
Hélie Jean-François[1],
Myre Alexandre[1]

[1]*GEOTOP - Université du Québec à Montréal (UQAM), C.P. 8888 Succursale Centre-ville, Montreal, Quebec, Canada H3C 3P8.*

[2]*Equipe de Géochimie et Cosmochimie, Institut de Physique du Globe de Paris, Univ. Paris 7.*

Controls on the Isotopic Composition of the St. Lawrence River

ABSTRACT

Linkages between riverine $\delta^{18}O$-δ^2H and hydro-climatic factors have been investigated based on isotopic time series recorded in the St. Lawrence River. Three stations were monitored from 1997 to 2008. They include the St Lawrence River main channel, south of Montreal Island, the outlet of the St. Lawrence River fluvial estuary and its main tributary, the Ottawa River. All monitoring sites depict systematic seasonal isotopic cycles characterized by heavy isotopes depletions during the snowmelt period and gradual heavy isotope enrichments throughout the ice-off season. Isotopic mass balance calculations suggest that ~10% of the total inflow to the Ottawa River basin is lost through evaporation before reaching the river outlet. In its southern channel, the seasonal isotopic pattern of the St. Lawrence River is strongly dependent upon evaporation and thermal stratification processes occurring within the Great Lakes, the latter constituting its head. At the outlet of its fluvial estuary, the seasonal isotopic pattern of the St. Lawrence River mainly responds to mixing between three components: waters from the Great Lakes, the Ottawa River and small tributaries. Isotopic mass balances allow partitioning streamflow components at this site. Over the sampling period, the range of 12-months running average $\delta^{18}O$ variations reached approximately 0.4‰ and 0.8‰ in the St. Lawrence River southern channel and in the Ottawa River, respectively. The δ^2H_{xs} fluctuations roughly mirrored the $\delta^{18}O$ variations at both sites. Such variations are interpreted as alternating periods of enhanced and reduced evaporation rates.

1. INTRODUCTION

Since the creation of the Global Network for Isotopes in Precipitation (GNIP, 1961-present), an extensive number of researches have focused on atmospheric waters isotopic properties (Craig, 1961; Dansgaard, 1964; Merlivat and Jouzel, 1979; Rozanski et al., 1993; Araguàs Araguàs et al., 2000; Bowen and Wilkinson, 2002; Bowen and Revenaugh, 2003). More recently, the International Atomic Energy Agency (IAEA) launched the Global Network for Isotopes in Rivers (GNIR) (Gibson et al., 2002; Vitvar et al., 2007), an undertake aimed at complementing the GNIP network.

An advantage of the GNIR approach is that rivers carry an integrated signal of hydrological processes operating at the basin scale. However, if Kendall and Coplen (2001) have highlighted that the isotopic signal of precipitation can be preserved in rivers, deciphering the incidence of post-rainfall processes on surface waters isotopic contents remains a challenge. Among others, the superimposed incidences of recharge (Fritz et al., 1987; Clark and Fritz, 1987), evaporation (Gonfiantini, 1986; Gibson et al., 1993; 2001; 2002a; 2002b; Gat, 1996; Telmer and Veizer, 2000; Gibson and Edwards, 2002), ice formation (Gibson and Prowse, 1999; 2002), snowmelt (Laudon et al., 2002) and mixing processes (Yang et al., 1996; Yi et al., 2010) need to be accounted for when studying the ^{2}H-^{18}O systematic of rivers. Yet, only few studies have addressed the ^{2}H-^{18}O temporal variability in large rivers, although constraining this parameter seems much needed for better documenting the post-rainfall processes influencing riverine isotopic systematics.

In this study, we focus on the seasonality and inter-annual (1997-2008) variability of ^{2}H-^{18}O contents in the St. Lawrence River System. We aim at documenting the environmental controls on the river's isotopic compositions. Basin recharge isotopic contents, evaporation and tributary mixing processes are addressed on the basis of isotopic time series. This complements previous studies documenting the geochemistry of the St. Lawrence River System (Gat et al., 1994; Yang et al., 1996; Telmer and Veizer, 1997; 2000; Huddart et al., 1999; Hélie et al., 2002; Rondeau et al., 2005; Hélie and Hillaire-Marcel, 2006).

2. STUDY AREA

The St Lawrence River system drains a 1.61×10^6 km^2 Eastern Canadian catchment dominated by mixed and boreal forest (Fig. 1). The catchment ranks 13th worldwide in terms of drainage area (St. Lawrence Center, 1996) and 16th in terms of total discharge. The river flows into the northern Atlantic Ocean with an average discharge of ~12 000 m^3/s. The basin undergoes a prominent seasonality. In Ottawa, located near the center of the basin (Fig. 1), average air temperatures range between -10.5°C in January and 21°C in July (*Environment Canada, Climatic Archive Database*). Average precipitation reaches ~800 to 1200 mm/yr over the basin (*Energy, Mines and Resources Canada, MCR 4145*). Between the Great Lakes and the outlet of its fluvial estuary (in proximity of Lévis, Fig. 1), the St. Lawrence River flows over the St. Lawrence Platform, which consists of Paleozoic sedimentary rocks. The river drains waters from the Grenvillian and Appalachian orogens that are located on its northern and southern flanks, respectively. Maximum elevations within the basin reach 700-1000 meters.

One notable feature of the St. Lawrence River system is the presence of the Great Lakes at its head (Fig. 1; Table 1). The riverine portion of the St Lawrence River takes its source below these interconnected lakes, at the outlet of Lake Ontario (the lowermost of the five Great Lakes). The water flowing from Lake Ontario accounts for approximately 90% of discharge in the St. Lawrence River south channel on a yearly basis (average discharge of 8100 m^3/s), located on the south shore of the Montreal Island (Fig. 1). The main north-shore tributary of the St. Lawrence River is the Ottawa River (Fig. 1). The latter drains a 149 000 km^2 watershed (Telmer and Veizer, 2000) and presents an average discharge of approximately 1900 m^3/s. These two water masses (inputs from the Great Lakes and the Ottawa River) do not mix completely within the St. Lawrence River before reaching the outlet of the fluvial estuary (near Lévis, Fig. 1) where tidal mixing homogenizes the water masses (Frenette *et al.*, 1989; St Lawrence Centre, 1996, Hélie et al., 2002; Hélie et Hillaire-Marcel, 2006).

At Lévis, 550 km below Lake Ontario's outlet (Lévis, Fig. 1), the river draws water from 1 153 000 km^2 (>70%) of the total watershed area. Discharge rates are highest during the spring snowmelt event, and lowest during early fall and midwinter, with an average of approximately 12 000 m^3/s. At Lévis, the two main water sources contributing to discharge are the Great Lakes and The Ottawa River. The Ottawa River can contribute to as much as 50% of the total water discharge during spring snowmelt. Conversely, during summer baseflow, the contributions from tributaries are reduced to a minimum, and as much as 80% of the total flow measured at Lévis can originate from the Great Lakes. However, this pattern is not completely natural, and human impacts on discharge rates need to be considered.

Notably, the Saunders – Moses power dam significantly damps the hydrograph below the outlet of Lake Ontario. Similarly, hydroelectric installations influence the Ottawa River, although the latter still presents a seasonal cycle characterized by highest discharge rates during the snowmelt period.

More information on water quantity and quality in the St. Lawrence River system can be found in the state of the environment report on the St. Lawrence River (St. Lawrence Center, 1996).

3. METHODOLOGY

3.1. Sampling sites

The choice and characteristics of the three sampling stations exploited in this study are discussed in Hélie et al (2002) and Hélie and Hillaire-Marcel (2006) and briefly summarized below.

The first station (Montreal sampling station) is located at a pumping facility of the city of Montreal (Fig. 1) (Charles-J.-des-Baillets pumping station) where the water is collected in the central part of the St. Lawrence River South Channel. The water collected at this station mainly represents the outflow from Lake Ontario (St Lawrence Centre, 1996; Hélie et al., 2002) and the data from this site are used to constrain inputs from the Great Lakes into the St Lawrence River. The influence of tributaries located downstream from Lake Ontario's outlet is small. A comparison of discharge rates measured at the outlet of Lake Ontario with discharge rates measured in the St. Lawrence River South Channel at Montreal (sampling station) reveals that on average, approximately 90% of the total flow measured at Montreal originates from Lake Ontario (based on data from the *Water Survey of Canada, Archived Hydrometric Data*). Total discharge at the Montreal sampling station averaged approximately 8100 m^3/s during the sampling period (*Water Survey of Canada, Archived Hydrometric Data*).

The second sampling station is located on the St Lawrence River at Lévis (Fig. 1). This station is used to record the signal at the outlet of the St. Lawrence River fluvial estuary. At this site, tidal mixing creates a well-mixed fluvial cross section. Water samples were systematically collected 2 hours before low tide to ensure that they would not be mixed with brackish waters from the estuary. Daily average discharge rates were approximately 12 000 m^3/s during the sampling period (St Lawrence Centre, unpublished data).

The third sampling station is located on the Ottawa River at the Carillon hydroelectric dam (Fig. 1), a facility operated by Hydro-Québec. It allows collecting waters from the Ottawa River in proximity of its confluence with the St. Lawrence River. Discharge rates compiled from Hydro-Quebec data yielded an average daily discharge rate of approximately 1 900 m^3/s over the study period.

3.2. Sampling frequency

Samples were collected on a bi-monthly to monthly basis between 1997 and 2008, inclusively. Sampling frequency was intensified (weekly) during the snowmelt period in order to capture the isotopic composition of water at peak discharge.

3.3. Samples Preparation and Analysis

Samples were stored in 30 ml high-density polyethylene bottles (HDPE) until analysis. All sampling bottles were rinsed three times with sampling water before being filled.

For oxygen and hydrogen isotopic analyses, 200 μl of water were transferred into septum vials and equilibrated in a heated rack with a known volume of CO_2 and H_2 respectively. The equilibrated gas was then analyzed by dual inlet mass spectrometry on a Micromass Isoprime isotope ratio mass spectrometer at the Stable Isotopes laboratory of the GEOTOP research center (*Université du Québec à Montréal*). In all cases, the isotopic compositions of samples are corrected using two internal reference waters ($\delta^{18}O$ = -6.71±0.05‰ ; -20.31±0.05‰ and $\delta^{2}H$ = -51±1.5‰ ; -155±0.05‰) calibrated on the VSMOW-SLAP scale (Coplen, 1996). Internal water standards are run between each series of 10 samples in order to check for instrumental stability. All measurements are duplicated and the analytical uncertainty is $\leq$ 2‰ on $\delta^{2}H$ and $\leq$ 0.1‰ on $\delta^{18}O$ at the 1σ level. Values are reported in permil units (‰) against the Vienna Standard Mean Ocean Water standard (VSMOW):

$$\delta_{(sample)} = \left[\frac{\left(\frac{^{18}O}{^{16}O}\right)_{(sample)}}{\left(\frac{^{18}O}{^{16}O}\right)_{(VSMOW)}} - 1 \right] * 1000$$

4. RESULTS

Yearly and monthly statistics are summarized in Tables 2, 3 and 4. Over the 12-years monitoring period, the Ottawa River (Carillon sampling station) presented $\delta^{18}O$ (δ^2H) values ranging between -12.0‰ (-85‰) and -9.4‰ (-70‰), yielding an amount-weighted average of -10.8‰ (-79‰) (Table 2). In the southern channel of the St. Lawrence River (Montreal sampling station), $\delta^{18}O$ (δ^2H) values ranged between -8.5‰ (-64‰) and -6.1‰ (-48‰) with an amount-weighted average of -7.0‰ (-53‰) (Table 3). Intermediate values between that of Carillon and Montreal were generally recorded at the outlet of the St. Lawrence River fluvial section (Lévis sampling station) where $\delta^{18}O$ (δ^2H) values ranged between -12.3‰ (-88‰) and -7.0‰ (-53‰) for an amount-weighted average of -8.7‰ (-64‰) (Table 4). At Lévis, the variability of $\delta^{18}O$ values (SD($\delta^{18}O$) = 1‰) is approximately twice that recorded at the Carillon (SD($\delta^{18}O$) = 0.5‰) and Montreal (SD($\delta^{18}O$) = 0.4‰) stations.

The entire dataset of $\delta^{18}O$-δ^2H values recorded at the three monitoring stations are reported in Fig. 2. Roughly parallel isotopic cycles were recorded at the three stations: heavy isotope depletions are recorded in response to spring snowmelt (month of April), gradual heavy isotope enrichments occur throughout the ice-off period (until September-October) and intermediate values are recorded during the ice-on period. The δ^2H vs $\delta^{18}O$ regressions evaluated at the monitoring stations are reported in (Fig. 3) where the Eastern Canadian Interior Meteoric Water Line ECI-MWL ($\delta^2H=7.6\delta^{18}O+6.5$, Fritz et al., 1987) is also shown. Overall, the data plot below the MWL and align along slopes lower than that of the MWL (Fig. 3).

5. DISCUSSION

5.1. Controls on the isotopic composition of the Ottawa River

The Ottawa River presents a clear seasonal isotopic cycle (Fig. 2; Fig. 4) that is lagged and damped with respect to that observed in precipitation (Fig. 5). This is due to water transit time, mixing and evaporation within the basin. Marked heavy isotope depletions are recorded during the snowmelt period (month of May-June), in response to the supply of heavy-isotope depleted meltwaters. This marked snowmelt period is followed by gradual heavy isotope enrichments during the ice-off season (May to October) in response to evaporation and a return to average isotopic compositions over the ice-on season, when the proportion of hydrological inputs to the river from groundwaters and large lakes are at maximum. These seasonal fluctuations accounted for $\delta^{18}O$ variations of ~2.6‰ over the monitoring period (1997-2008). Telmer and Veizer (2000) discussed the temporal isotopic trends observed in the Ottawa River Basin based on data collected in 1993-1994. Regarding the documentation of seasonality, the data collected during the present study (1997-2008) are in good agreements with the conclusions of these authors.

5.1.1. Evaporation within the Ottawa River Basin

Isotopic mass balance calculations can be used for documenting evaporation processes in various settings (eg.: Craig and Gordon, 1965; Gonfiantini, 1986; Gibson, 1993; Telmer and Veizer 2000; Gibson and Edwards, 2002; Gibson et al., 2008 and references therein). Telmer and Veizer (2000) proposed an estimate of the average evaporation over inflow ratio within the Ottawa River basin based on isotopic data. Here, we use a similar approach but provide new estimates of key model parameters.

We estimate the long-term average Evaporation over Inflow ratio (E/I) for the entire basin drained by the Ottawa River. We follow a calculation method based on a steady state isotopic mass balance:

$$I_C = Q_C + E_C \qquad \text{(Eq. 1)}$$

$$I_C \delta_I = Q_C \delta_Q + E_C \delta_E \qquad \text{(Eq. 2)}$$

$$x = \frac{\delta_I - \delta_Q}{\delta_E - \delta_Q} \qquad \text{(Eq. 3)}$$

$$\delta_E = \frac{\alpha * \delta_L - h\delta_A - \varepsilon}{1 - h + \varepsilon_K}$$

(Eq. 4)

where I_C, Q_C and E_C are the catchment inflow, surface outflow and evaporation losses, respectively, with corresponding δ values δ_I, δ_Q and δ_E. δ_E is evaluated using the formulation of Craig and Gordon (1965), with $\alpha* = \alpha_{(V/L)} = 1/\alpha_{(L/V)}$ evaluated from Horita and Wesolowski (1994):

$$1000\ln\alpha_V^L(^{18}O) = -7.685 + 6.7123\left(\frac{10^3}{T}\right) - 1.6664\left(\frac{10^6}{T^2}\right) + 0.3504\left(\frac{10^9}{T^3}\right)$$

$$1000\ln\alpha_V^L(^2H) = 1158.8\left(\frac{T^3}{10^9}\right) - 1620.1\left(\frac{T^2}{10^6}\right) + 794.84\left(\frac{T}{10^3}\right) - 161.04 + 2.0002\left(\frac{10^9}{T^3}\right)$$

where T is in Kelvin. All terms in equation 4 are in decimal notations (not in permil notation). The ε term in Eq. 4 represents a small positive quantity and is evaluated as $1/\alpha* - 1$. δ_A is the isotopic composition of the atmosphere. Finally, ε_K is the kinetic enrichment factor (Gonfiantini (1986)):

$\varepsilon_K(^{18}O) = 14.2(1-h)$

$\varepsilon_K(^2H) = 12.5(1-h)$

where h is the air relative humidity (between 0 and 1). Note that Eq. 3 can be solved independently for δ^2H and $\delta^{18}O$.

Under the conditions encountered here, the validity of an evaporation / inflow ratio on the basis of eq. 3 relies on some parameter estimations and key assumptions (model parameters are summarized in Table 6):

1- The δ^2H-$\delta^{18}O$ composition of the Ottawa River falls on a Local Evaporation Line (LEL) (e.g. see Gibson et al., 2008 and references therein). This first assumption is consistent with the distribution of data in δ^2H vs $\delta^{18}O$ plots (Fig.3), where the Ottawa River samples fall below the MWL and align on a slope that is lower than that of the MWL. We attribute this pattern to

heavy isotope enrichment in the residual water in response to evaporation during the ice-off season.

2- The regression line constructed using monthly average δ^2H and $\delta^{18}O$ values can be extrapolated to its intercept with the MWL, providing a realistic estimate of the average isotopic composition of recharge (δ_I) within the basin (Fig. 6): $\delta^{18}O_I = -12.4‰$; $\delta^2H_I = -87‰$. The δ_I value obtained from this intercept calculation seems realistic in view of the long-term average isotopic composition of precipitation measured at the Ottawa and Ste. Agathe CNIP stations (Table 5).

3- For satisfying the calculations requirements, we must assume that the isotopic composition of water measured at Carillon is equal to the bulk average isotopic composition of water within the basin. We assume that using the amount weighted average isotopic composition of the Ottawa River over the monitoring period (1997-2008) ($\delta^{18}O_Q = -10.8‰$; $\delta^2H_Q = -79‰$) constitutes a reasonable estimate.

4- Mean air relative humidity (h) is assumed to be 75%, consistent with local climatic conditions (eg.: see Environment Canada, Climatic archive database). Similarly, the average air temperature during the ice-off season is assumed to be approximately 10 °C.

5- Finally, the isotopic composition of atmospheric moisture (δ_A) is fitted for satisfying consistency with the LEL slope (see Gibson et al., 2008). Using this method, we evaluate a δ_A of ($\delta^{18}O_A = -24.0‰$; $\delta^2H_A = -176‰$). Assuming an equilibrium temperature of 10°C during the ice-off period, it would mean that this atmospheric vapor is in equilibrium with liquid precipitation having an average isotopic composition of ($\delta^{18}O_P = -13.6‰$; $\delta^2H_P = -97‰$), consistent with the δ18O-δ2H relationship of the Eastern Canadian Meteoric Water line as evaluated by Fritz et al. (1987).

Based on the calculated and/or estimated values for each parameter (Table 6), we estimate an average E/I ratio of ~10% for the entire Ottawa River Basin. This ~10% value must represent an upper limit to the real basin-scale E/I ratio, as part of the recharge may reach the deep groundwater reservoir and remain isolated from the river network. The E/I value calculated here is similar to that estimated by Telmer and Veizer (2000) (8%) although some key parameters (especially the δ_A term) and the calculation methodology used here differed from that of Telmer and Veizer (2000). In addition, our data provides a longer temporal coverage, improving the evaluation of an average LEL for the Ottawa River. Therefore, we consider that the data and calculations presented here provide a useful complement to their calculations.

5.2. Controls on the isotopic composition of the St. Lawrence River South Channel

As reported in section 2, the contribution from Lake Ontario accounts for ~90% of the total flow measured at the Montreal Sampling station on a yearly basis. Therefore, processes occurring within the Great Lakes most likely impart the prominent control on the isotopic composition of water sampled at the Montreal station.

The Great Lakes are dimictic lakes. They are thermally stratified during the summer and nearly homogeneous or weakly stratified during the winter (Boyce et al., 1989). Under such conditions, we propose that the isotopic cycle recorded in the St. Lawrence River Southern Channel can be divided in ice-off, ice-on and transition periods (Fig. 7; Fig. 8). The ice-off period (Fig. 7-a; Fig. 8) lasts from the establishment of thermal stratification in Lake Ontario in spring or early summer until the beginning of freezing in late fall. During this time period, the water flowing from Lake Ontario is likely to mainly originate from its epilimnion, with reduced influence from the hypolimnion due to thermal stratification (Fig. 7-a). As evaporation goes on through the ice-off season (until October / November), Lake Ontario's epilimnion undergoes gradual heavy isotope enrichment (Fig. 8; Fig. 9). High evaporation rates over the Great Lakes persist until late fall, when surface water temperatures exceed that of the air. This explains the lag observed between maximum heavy-isotope enrichments recorded at Montreal and the maximum recorded in air temperature and precipitation heavy isotope contents within the basin (Fig. 8).

During the transition period occurring between the ice-off season and the establishment of the ice-on period (Fig. 7-b, 8), surface water cooling and wind-driven mixing induces a partial vertical mixing within the lake. Under these conditions, the water sampled in the St. Lawrence River South Channel evolves towards an isotopic composition that is closer to the bulk average isotopic composition of Lake Ontario (Fig. 9).

Following this transition period is the ice-on period (Fig 7-c), when Lake Ontario becomes nearly homogeneous (Boyce et al., 1989) or weakly stratified (IFYGL, 1981). During this time period, the isotopic composition of water sampled at Montreal shows gradual heavy-isotope depletion, until the end of the ice-on period (Fig. 8).

Following the ice-on period, ice and snow melting induces a rapid depletion in heavy isotopes in the lake surface waters, resulting in a marked decrease in heavy isotope contents at Montreal (Fig. 7-d;

Fig. 8; Fig. 9). The influence of tributaries located downstream of Lake Ontario is likely to be highest during this time period.

The convective overturning caused by the warming of surface waters follows this process (Fig. 7-e) and therefore, we propose that shortly after snowmelt, the bulk average isotopic composition of Lake Ontario can be sampled in the St. Lawrence River south channel at Montreal (Fig. 8; Fig. 9).

5.2.1. Evaporation within the Great Lakes Basin (St. Lawrence River South Channel)

Although isotopic mass balance calculations have been used for documenting evaporation processes in the Ottawa River basin (section 5.1.1), we argue that for the St. Lawrence River south channel, solving equation 3 on the basis of the data available here would be unrealistic. First, the isotopic composition measured in the St. Lawrence south channel must carry an isotopic signal inherited from multi-stage evaporation processes occurring within the five interconnected Great Lakes that constitute the head of the riverine system, as suggested by surveys conducted on these lakes (Dr. Thomas Edwards, personal communication). In addition, considering the different water residence times within each of the Great Lakes (Table 1), the thermal stratification and mixing processes within the lakes and the contribution of water evaporated from the lakes to the regional atmospheric moisture, we argue that more data is still needed for estimating the key parameters required to solve eq. 3. We therefore stress the need for an exhaustive isotopic survey of the Great Lakes for solving these multi-stage evaporation processes. Such an endeavor seems much needed, as it would allow complementing physically based evaporation estimates for the Great Lakes (e.g. see Aubert and Richards, 1981).

5.3. Controls on the isotopic composition of the St. Lawrence River Fluvial Estuary

In this section, we evaluate the potential of using the isotopic composition of water at the outlet of the St. Lawrence River fluvial estuary for partitioning streamflow components. The graphs and calculations presented below are based on monthly average isotopic and discharge values. This has the advantage of reducing the variability induced by the transfer time of waters from the various sources before reaching the fluvial estuary. The calculations therefore represent multi-year monthly averages rather than instantaneous values.

As stated in section 2, two main water sources feed the St. Lawrence River fluvial estuary: the Great Lakes and the Ottawa River, together accounting for approximately 75-90% of the total discharge measured at Lévis (based on monthly average discharge rates). These two water sources are characterized by contrasting isotopic compositions, the Ottawa River showing a marked heavy-isotope depletion with respect to the water sampled in the St. Lawrence South Channel (Fig. 2; Fig. 3). Therefore, the isotopic composition of water at the outlet of the St. Lawrence River, which is intermediate between the above components, is strongly dependent upon mixing proportions between inputs from the Great Lakes and the Ottawa River. This is illustrated by the inverse correlation observed between the isotopic composition of water at Lévis and the ratio of discharge recorded at Carillon over that recorded at Montreal ($Q_{(CAR)}/Q_{(MTL)}$) (Fig. 10-a). An increased contribution from the Ottawa River, which is depleted in heavy isotopes with respect to the water sampled in the St. Lawrence South Channel at Montreal, results in a lower $\delta^{18}O$ at Lévis, and vice-versa. Yet, it is also clear from Fig. 10-b that the contributions from unsampled tributaries located between Montreal and Lévis are not negligible. This is illustrated by the fact that all points fall below the 1:1 equiline when the $\delta^{18}O$ values measured at Lévis are plotted against the amount weighted $\delta^{18}O$ value of the St. Lawrence South Channel and Ottawa rivers taken together $[\delta_{(OTT+MTL)} = [Q_{(CAR)}*\delta_{(CAR)}+Q_{(MTL)}*\delta_{(MTL)}] / Q_{(CAR+MTL)}]$ (Fig. 10-b).

The influence of these unsampled tributaries on discharge rates and on the isotopic composition of water at the outlet of the St. Lawrence River fluvial estuary can be expressed in terms of discharge and isotopic residuals:

$$Q_{(Residual)} = Q_{(LEV)} - Q_{(OTT+MTL)} \qquad\qquad (Eq.\ 4)$$

$$\delta_{(Residual)} = \delta_{(L\acute{E}V)} - \delta_{(OTT+MTL)} \qquad\qquad (Eq.~5)$$

It is clear from Figs. 11-12 that the mean monthly isotopic ($\delta^{18}O$) and discharge residuals show opposite patterns. The greatest isotopic residuals ($\sim$ -1.5‰) are recorded during the spring snowmelt period, whereas the smallest ($\sim$ -0.30‰) are recorded in September, consistent with contributions from unsampled tributaries that are at maximum during snowmelt and at minimum during summer baseflow. The interest of the regressions presented in Figures 10 to 12 is that it reveals that streamflow components at the outlet of the St. Lawrence River fluvial estuary can be partitioned based on the isotopic composition of water. For instance, for given monthly average $\delta^{18}O$ values measured at Carillon, Montreal and Lévis, one can estimate the relative contributions from the Ottawa and St. Lawrence River south channel to the total flow at the outlet of the fluvial estuary (Fig. 10-a) and an isotopic residual (Fig. 10-b). From this isotopic residual, one can estimate the relative contribution from unsampled tributaries to the total flow at Lévis (Fig. 12). The interest of such isotopic mass balances is that the total discharge at Lévis cannot be measured directly due to tidal effects. Due to this complication, Environment Canada provides estimates of discharge rates at Lévis based on a summation of flow in the Ottawa River, in the St. Lawrence River south channel and in the smaller tributaries located between the Montreal Island and Lévis. In this context, isotopic mass balances could stand as a reliable method for validating discharge rates estimated from physical measurements.

In addition, based on discharge and isotopic residuals, the bulk average isotopic compositions of unsampled tributaries can be evaluated. The $\delta^{18}O$ values of this component range between approximately -15.4‰ in April and -9.7‰ in September. Applying similar calculations using δ^2H values allows the calculation of the following bulk average δ^2H vs $\delta^{18}O$ regression for the unsampled tributaries: $\delta^2H \approx 6.3\delta^{18}O-9$, $r^2=0.97$.

5.4. Inter-Annual Variability and isotopic trends

The 12-month running average $\delta^{18}O$ and ^2H excess ($^2H_{xs}=\delta^2H-8\delta^{18}O$) calculated in the St. Lawrence and Ottawa rivers are reported in Fig. 13 Over the study period, some months were not sampled due to field and/or logistics constraints. The missing monthly values were interpolated from the time series. Although not statistically irreproachable, we argue that this is the most robust way to account for missing data within the time series. We have chosen to use 12 months for the running averages in order to account for one complete hydrological year at each value. Averages are weighted according to monthly discharge rates. Below, we focus on the potential hydro-climatic processes that could explain the recorded $\delta^{18}O$ and ^2Hxs variations. Only the Carillon and Montreal sampling stations are considered, since the isotopic variations recorded at Lévis have been shown to mainly respond to mixing processes involving these two components (section 5.3).

Over the sampling period, the range of 12-months average $\delta^{18}O$ variations reached approximately 0.4‰ and 0.8‰ at Montreal and Carillon, respectively (Fig. 13). The standard deviations on 12-month average $\delta^{18}O$ distributions reach 0.1‰ at Montreal and 0.2‰ at Carillon. The $^2H_{xs}$ fluctuations roughly mirror the $\delta^{18}O$ variations at both sites (Fig. 13). Such patterns were not observed at the Ottawa CNIP station over the same period (Birks et al.,CNIP data), suggesting that changes in precipitation isotopic contents are unlikely to explain the trends recorded in the St. Lawrence and Ottawa Rivers. Alternating periods of enhanced (highlighted in lighter grey, Fig. 13) and reduced (highlighted in darker grey, Fig. 13) evaporation rates therefore stand as a realistic hypothesis for explaining the data. These short-term (i.e. 1-3 years) isotopic variations could not be reconciled with major climatic indexes (AO, NAO, ENSO) and are neither directly linked to yearly average temperatures, nor to snow or rain amounts as recorded at the meteorological stations within the basin. We attribute this to the buffering effect imposed by the large water volume within the basins that induce some inertia with respect to the more dynamic atmosphere. In addition to short-term variations, unsteady decreases in $\delta^{18}O$ ($\sim$ -0.1 to -0.4‰) (Fig. 13) accompany general increasing trends in $^2H_{xs}$ ($\sim$ 1-1.5‰) at both sites over the 12-years monitoring period. The regression lines reported in Fig. 13 highlight these trends. Here again, this does not seem to be linked to changes in precipitation isotopic contents. A general decrease in evaporation rates over the monitored period therefore stands as a plausible explanation. Nevertheless, one should bear in mind that the $\delta^{18}O$ and $^2H_{xs}$ trends recorded over the study period remain of relatively small magnitude with respect to the amplitude of temporal variations recorded for both parameters (eg.: see Tables 2-3). Notably, an intensified sampling program (i.e. based on daily to weekly samplings) could help reducing the variability associated with 12-month average calculations.

In addition, the question remains open concerning the meaning of the trends as they might simply result from short-term variations that are in fact superimposed over longer-term (i.e. decadal or perhaps longer) trends or they might truly reflect modifications in the water cycle (gradual decrease in evaporation rates) at the scale of the St. Lawrence river basin. We see this open question as a strong argument in favor of maintaining the long-term monitoring of riverine and precipitation isotopic contents. This seems much needed for better understanding basin hydrology vs climate long-term relationships. Notably, endeavors such as the GNIR program (Gibson et al., 2002; Vitvar et al., 2007) seem especially fit for solving such questions.

6. CONCLUSION

In this study, we focused on the seasonality and inter-annual (1997-2008) variability of δ^2H-$\delta^{18}O$ in the St. Lawrence and Ottawa rivers in an attempt to evaluate the linkages between riverine isotopic composition and hydro-climatic conditions. The isotopic signal recorded in the Ottawa River allowed a first order estimate of the evaporation / inflow (E/I) ratio within the basins it drains. The calculations revealed that ~10% of the total inflow to the Ottawa River Basin is lost through evaporation before reaching the river outlet. Within the St. Lawrence south channel, the recorded seasonal isotopic fluctuations are attributed to variations in Lake Ontario's thermal stratification. At the outlet of the fluvial estuary, isotopic variations essentially respond to tributary mixing processes and streamflow components can be partitioned on the basis of isotopic analyses. Yearly running averages calculated from the 12-years dataset at the Carillon (Ottawa River) and Montreal (St. Lawrence River South Channel) sampling stations tend to indicate alternating periods of enhanced and reduced evaporation rates. Gradual decrease in $\delta^{18}O$ (-0.1 to -0.4‰) and increase in $^2H_{xs}$ are superimposed upon these short-term (1-3 yrs) variations at both stations. This could indicate a general decrease in evaporation rates, but the question remains open concerning the meaning of the te,mporal trends, as they might simply result from short-term variations that are in fact superimposed upon longer-term (i.e. decadal or longer) trends or they might truly reflect modifications in the water cycle at the scale of the St. Lawrence river basin. We see this raised and unanswered question as a strong argument in favor of the long-term monitoring of riverine and precipitation isotopic contents. This seems much needed for better understanding basin hydrology vs climatic synoptic long-term relationships, an issue that is critical for evaluating the sustainability of surface water resources.

Table 1. Great Lakes physical characteristics.

Lake	Area[1]	Datum[1]	Volume[1]	Mean depth[2]	Hydraulic residence time[3]
	km^2	m	km^3	m	Year
Superior	82100	182.88	12110	148	190
Michigan	57800	175.81	4920	85	100
Huron	59600	175.81	3540	59	20
St. Clair	1114	174.25	6	5	<1
Erie	25700	173.31	484	19	3
Ontario	18960	74.01	1640	86	8

Hydrologic and physical characteristics of the Great Lakes. Data are from [1] IFYGL (1981), [2] by dividing of lake volume by lake surface area and [3] Quinn (1992).

CARILLON

Table 2a. Summary of yearly results: Carillon sampling station.

	n	DW AVG $\delta^{18}O$	A AVG $\delta^{18}O$	MED $\delta^{18}O$	MIN $\delta^{18}O$	MAX $\delta^{18}O$	SD $\delta^{18}O$	DW AVG δ^2H	A AVG δ^2H	MED δ^2H	MIN δ^2H	MAX δ^2H	SD δ^2H
1997	6	-11.4	-11.3	-11.2	-12.0	-10.7	0.5	-83	-83	-83	-85	-80	2
1998	16	-10.6	-10.5	-10.3	-11.5	-9.6	0.6	-79	-78	-77	-84	-76	3
1999	14	-10.5	-10.5	-10.5	-11.3	-9.4	0.5	-78	-77	-78	-83	-72	4
2000	8	-10.4	-10.4	-10.2	-11.0	-10.0	0.4	-77	-77	-76	-81	-73	3
2001	13	-10.6	-10.5	-10.5	-11.5	-9.5	0.5	-78	-78	-77	-84	-74	3
2002	16	-10.5	-10.4	-10.3	-11.1	-10.1	0.3	-77	-77	-77	-79	-72	2
2003	19	-11.0	-10.9	-10.8	-12.0	-10.2	0.5	-80	-80	-80	-85	-77	2
2004	26	-11.0	-10.9	-11.1	-11.3	-10.2	0.4	-81	-80	-80	-83	-76	2
2005	28	-11.0	-10.8	-10.8	-11.6	-9.8	0.6	-80	-79	-79	-84	-74	3
2006	25	-10.8	-10.7	-10.8	-11.3	-9.8	0.4	-79	-79	-79	-82	-73	2
2007	23	-10.8	-10.5	-10.7	-11.2	-9.7	0.5	-79	-77	-78	-82	-70	4
2008	25	-10.9	-10.8	-10.8	-11.6	-10.3	0.4	-80	-79	-79	-84	-77	2

n=number of samples, DW AVG= discharge weighted average, A AVG=Amount weighted average, MED=median value, SD=Standard deviation. All data are expressed in ‰ vs VSMOW on the VSMOW-SLAP scale.

Table 2b. Summary of monthly results: Carillon sampling station.

	n	A AVG $\delta^{18}O$	MED $\delta^{18}O$	MIN $\delta^{18}O$	MAX $\delta^{18}O$	SD $\delta^{18}O$	A AVG δ^2H	MED δ^2H	MIN δ^2H	MAX δ^2H	SD δ^2H
January	15	-10.6	-10.6	-11.1	-10.2	0.3	-78	-78	-81	-72	2
February	15	-10.7	-10.8	-11.2	-10.1	0.3	-79	-79	-82	-76	2
March	20	-10.9	-10.9	-11.5	-10.2	0.3	-80	-79	-85	-77	2
April	32	-11.2	-11.2	-12.0	-10.2	0.3	-81	-81	-85	-77	2
May	24	-11.2	-11.2	-11.6	-10.7	0.3	-81	-82	-84	-78	2
June	19	-11.0	-11.0	-12.0	-10.4	0.4	-80	-80	-85	-75	3
July	20	-10.6	-10.6	-11.3	-10.1	0.3	-79	-78	-84	-75	2
August	14	-10.4	-10.3	-11.1	-9.8	0.4	-77	-77	-82	-73	3
September	15	-10.2	-10.2	-10.7	-9.8	0.3	-76	-76	-80	-72	2
October	17	-10.1	-10.0	-10.9	-9.4	0.4	-76	-76	-80	-70	2
November	19	-10.2	-10.3	-10.7	-9.5	0.3	-76	-76	-79	-73	2
December	9	-10.3	-10.3	-10.9	-10.1	0.3	-76	-76	-80	-73	2

n=number of samples, A AVG=Amount weighted average, MED=median value, SD=Standard deviation. All data are expressed in ‰ vs VSMOW on the VSMOW-SLAP scale.

MONTREAL

Table 3a. Summary of yearly results: Montreal sampling station.

	n	DW AVG $\delta^{18}O$	A AVG $\delta^{18}O$	MED $\delta^{18}O$	MIN $\delta^{18}O$	MAX $\delta^{18}O$	SD $\delta^{18}O$	DW AVG $\delta^{2}H$	A AVG $\delta^{2}H$	MED $\delta^{2}H$	MIN $\delta^{2}H$	MAX $\delta^{2}H$	SD $\delta^{2}H$
1997	5	-6.8	-6.8	-6.8	-7.0	-6.6	0.1	-52	-52	-51	-55	-51	2
1998	21	-7.0	-6.9	-6.9	-7.7	-6.3	0.4	-52	-52	-51	-58	-49	2
1999	23	-7.0	-6.9	-6.8	-8.3	-6.4	0.4	-52	-52	-52	-58	-49	2
2000	15	-7.3	-7.3	-7.3	-8.1	-6.7	0.4	-54	-54	-54	-60	-51	3
2001	23	-6.9	-6.8	-6.7	-8.3	-6.1	0.5	-53	-53	-52	-64	-50	4
2002	18	-6.9	-6.8	-6.7	-7.7	-6.3	0.4	-52	-52	-52	-56	-49	3
2003	29	-7.1	-7.1	-7.2	-7.7	-6.3	0.4	-53	-53	-53	-58	-49	3
2004	30	-7.0	-7.0	-6.9	-7.6	-6.4	0.4	-53	-53	-53	-58	-50	3
2005	26	-7.0	-7.0	-6.8	-8.0	-6.1	0.5	-53	-53	-52	-60	-48	3
2006	22	-7.1	-7.0	-7.1	-7.5	-6.5	0.3	-52	-52	-51	-55	-48	2
2007	24	-7.0	-7.0	-7.0	-7.6	-6.5	0.3	-52	-52	-52	-56	-49	3
2008	23	-7.2	-7.1	-7.1	-8.5	-6.5	0.5	-54	-54	-53	-63	-50	3

n=number of samples, DW AVG= discharge weighted average, A AVG=Amount weighted average, MED=median value, SD=Standard deviation. All data are expressed in ‰ vs VSMOW on the VSMOW-SLAP scale.

Table 3b. Summary of monthly results: Montreal sampling station.

	n	A AVG $\delta^{18}O$	MED $\delta^{18}O$	MIN $\delta^{18}O$	MAX $\delta^{18}O$	SD $\delta^{18}O$	A AVG $\delta^{2}H$	MED $\delta^{2}H$	MIN $\delta^{2}H$	MAX $\delta^{2}H$	SD $\delta^{2}H$
January	18	-6.9	-6.8	-7.4	-6.6	0.3	-52	-52	-56	-50	2
February	19	-6.9	-7.0	-7.2	-6.6	0.2	-52	-52	-54	-51	1
March	23	-7.1	-7.1	-7.7	-6.3	0.4	-53	-53	-58	-50	2
April	36	-7.6	-7.5	-8.5	-7.0	0.4	-57	-56	-64	-53	3
May	33	-7.3	-7.4	-7.7	-6.6	0.3	-55	-55	-58	-51	2
June	21	-7.2	-7.1	-7.5	-6.9	0.2	-54	-54	-56	-51	1
July	21	-6.8	-6.9	-7.2	-6.4	0.2	-52	-52	-54	-50	1
August	20	-6.6	-6.7	-7.2	-6.3	0.2	-51	-51	-54	-49	1
September	18	-6.5	-6.5	-6.7	-6.3	0.1	-50	-50	-52	-48	1
October	20	-6.5	-6.5	-6.9	-6.3	0.2	-50	-50	-52	-48	1
November	18	-6.7	-6.7	-7.3	-6.1	0.3	-51	-51	-55	-49	2
December	12	-6.8	-6.8	-7.3	-6.1	0.3	-52	-51	-55	-50	2

n=number of samples, A AVG=Amount weighted average, MED=median value, SD=Standard deviation. All data are expressed in ‰ vs VSMOW on the VSMOW-SLAP scale.

LÉVIS

Table 4a. Summary of yearly results: Lévis sampling station.

	n	DW AVG $\delta^{18}O$	A AVG $\delta^{18}O$	MED $\delta^{18}O$	MIN $\delta^{18}O$	MAX $\delta^{18}O$	SD $\delta^{18}O$	DW AVG $\delta^{2}H$	A AVG $\delta^{2}H$	MED $\delta^{2}H$	MIN $\delta^{2}H$	MAX $\delta^{2}H$	SD $\delta^{2}H$
1997	7	-8.2	-8.1	-7.9	-9.6	-7.5	0.7	-60	-59	-58	-70	-55	5
1998	16	-8.6	-8.2	-7.8	-11.0	-7.1	1.2	-63	-61	-58	-79	-54	7
1999	18	-8.6	-8.5	-8.3	-10.1	-7.0	0.9	-64	-63	-62	-73	-55	5
2000	17	-8.9	-8.8	-8.2	-11.1	-7.4	1.2	-65	-64	-61	-78	-55	7
2001	20	-8.6	-8.4	-8.2	-12.3	-7.1	1.2	-64	-62	-61	-88	-54	8
2002	24	-8.6	-8.5	-8.4	-9.7	-7.0	0.8	-63	-62	-61	-70	-53	5
2003	29	-8.6	-8.5	-7.9	-10.8	-7.0	1.1	-64	-63	-59	-79	-53	7
2004	29	-8.6	-8.5	-8.2	-10.4	-7.2	0.9	-64	-63	-61	-75	-54	6
2005	27	-8.9	-8.6	-8.5	-11.6	-7.0	1.1	-65	-63	-62	-83	-53	7
2006	25	-8.8	-8.7	-8.7	-10.1	-7.2	0.8	-64	-63	-64	-73	-54	5
2007	25	-8.6	-8.4	-8.1	-11.0	-7.1	1.0	-63	-62	-60	-79	-54	6
2008	24	-8.9	-8.6	-8.4	-11.5	-7.6	1.0	-65	-64	-63	-83	-56	7

n=number of samples, DW AVG= discharge weighted average, A AVG=Amount weighted average, MED=median value, SD=Standard deviation. All data are expressed in ‰ vs VSMOW on the VSMOW-SLAP scale.

Table 4b. Summary of monthly results: Lévis sampling station.

	n	A AVG $\delta^{18}O$	MED $\delta^{18}O$	MIN $\delta^{18}O$	MAX $\delta^{18}O$	SD $\delta^{18}O$	A AVG $\delta^{2}H$	MED $\delta^{2}H$	MIN $\delta^{2}H$	MAX $\delta^{2}H$	SD $\delta^{2}H$
January	19	-8.4	-8.4	-9.3	-7.6	0.5	-62	-61	-68	-57	3
February	18	-8.2	-8.2	-9.1	-7.8	0.4	-61	-60	-66	-58	3
March	26	-8.7	-8.4	-11.1	-7.6	0.9	-64	-62	-79	-58	6
April	35	-10.1	-10.1	-12.3	-8.2	0.9	-73	-73	-88	-62	6
May	29	-9.3	-9.3	-10.4	-8.3	0.5	-67	-68	-77	-61	3
June	21	-8.5	-8.6	-9.6	-7.4	0.5	-63	-64	-70	-58	3
July	22	-8.1	-8.0	-8.9	-7.5	0.3	-59	-60	-65	-56	2
August	17	-7.6	-7.5	-8.8	-7.0	0.4	-57	-57	-65	-54	3
September	20	-7.3	-7.3	-7.9	-7.0	0.2	-55	-55	-59	-53	2
October	15	-7.6	-7.5	-8.8	-7.0	0.5	-57	-56	-65	-53	3
November	23	-8.1	-8.1	-9.4	-7.3	0.6	-60	-60	-69	-56	4
December	16	-8.2	-8.1	-9.2	-7.8	0.4	-61	-61	-67	-58	3

n=number of samples, A AVG=Amount weighted average, MED=median value, SD=Standard deviation. All data are expressed in ‰ vs VSMOW on the VSMOW-SLAP scale.

Table 5. Amount weighted average isotopic composition of precipitation at selected CNIP stations.

Site	$\delta^{18}O$	δ^2H	Available data (years)
St. Agathe	-12.6	-88.1	1975-1982
Ottawa	-11.1	-77.0	1973-2007
Egbert	-10.6	-72.4	1993-2002
Simcoe	-9.4	-62.5	1975-1982

Data from Birks et al., 1999-2004, CNIP. All data are expressed in ‰ vs VSMOW on the VSMOW-SLAP scale.

Table 6. Evaluated parameter values: evaporation model (^{18}O ; ^{2}H) for the Ottawa River Basin.

Parameter	Solved for ^{18}O	Solved for ^{2}H
T (°C) (estimated)	10	10
δQ (‰) (measured)	-10.8	-79
δI (‰) (calculated)	-12.35	-87
δA (‰) (calculated)	-24.0	-176
h (estimated)	0.75	0.75
Result: Xc=E/I	0.09	0.10

All data are expressed in ‰ vs VSMOW on the VSMOW-SLAP scale. See text for details on parameters calculations and estimates.

Figure 1. St. Lawrence River drainage basin.
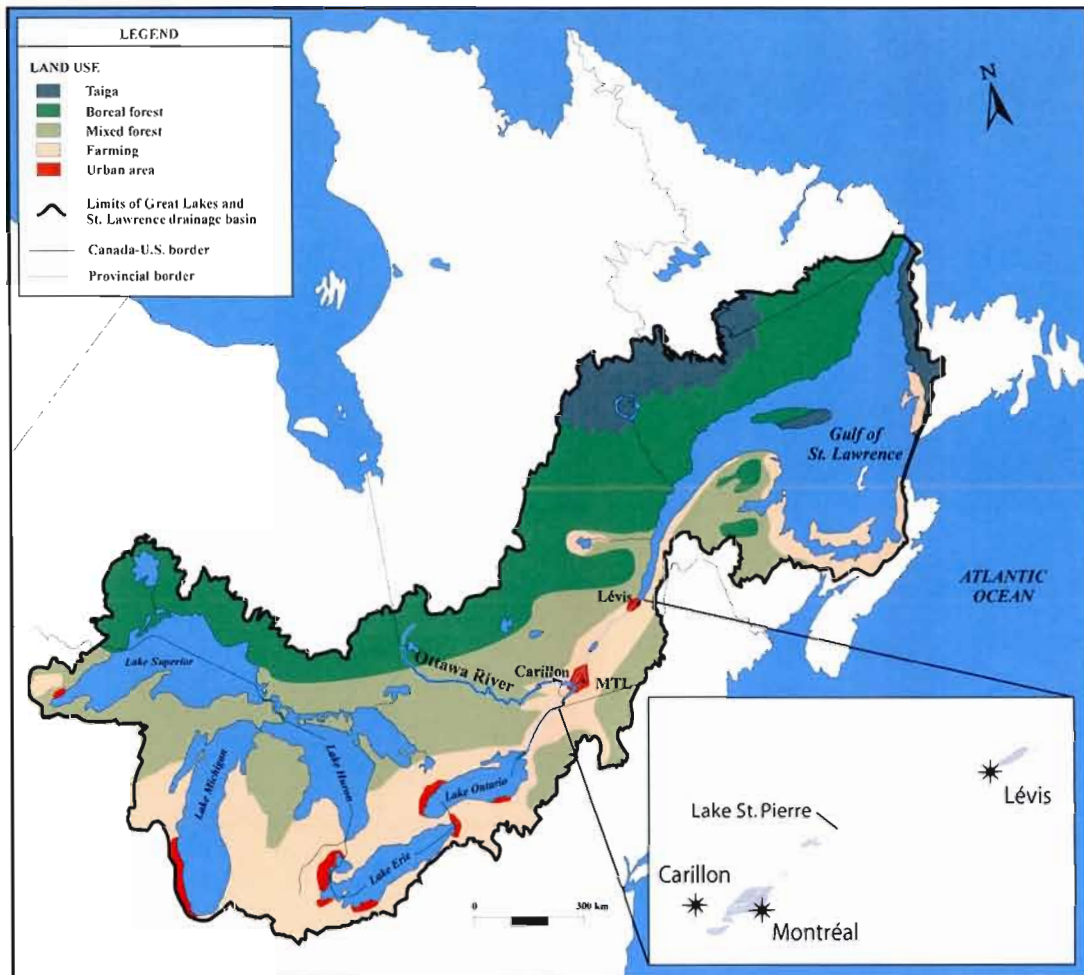
The inlet highlights the location of the three sampling stations.

Figure 2. Isotopic time series of the St. Lawrence and Ottawa Rivers.
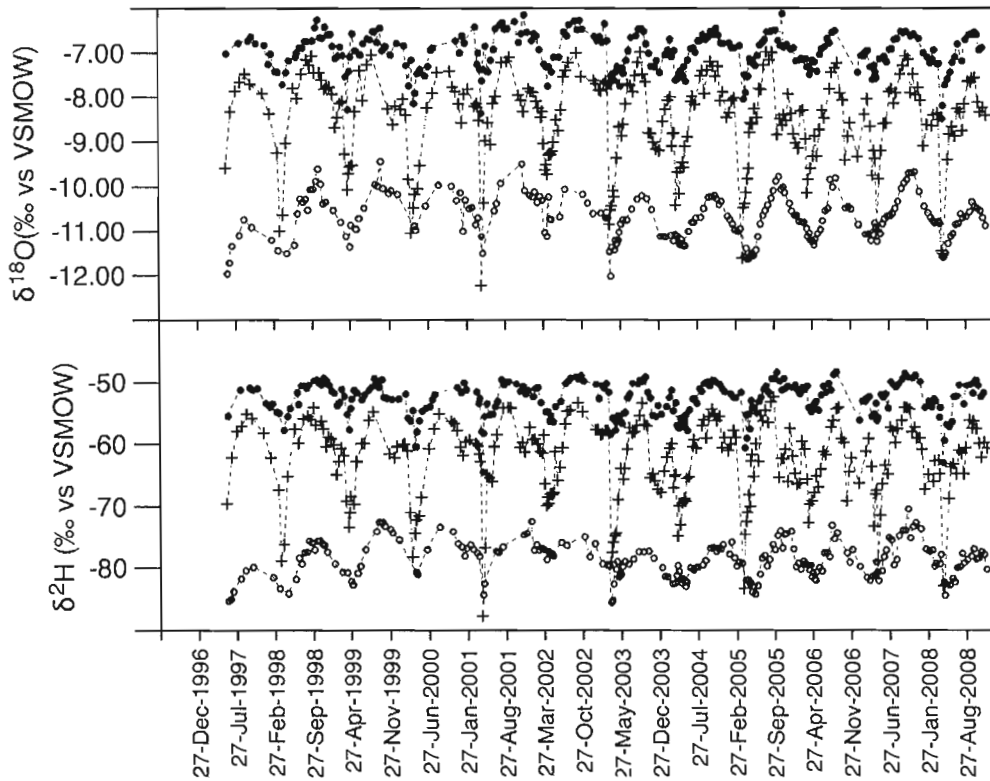
Isotopic time series recorded at the three monitoring sites. Filled circles: Montreal station, + symbol: Lévis station, empty circles: Carillon station. Patterns are roughly parallel at all sites, with highest heavy isotope enrichments recorded at the end of the ice-off season and heavy isotopic depletions during the snowmelt period. The greatest isotopic variability is recorded at the outlet of the St. Lawrence River fluvial section.

Figure 3. $\delta^{18}O$ vs δ^2H correlations.
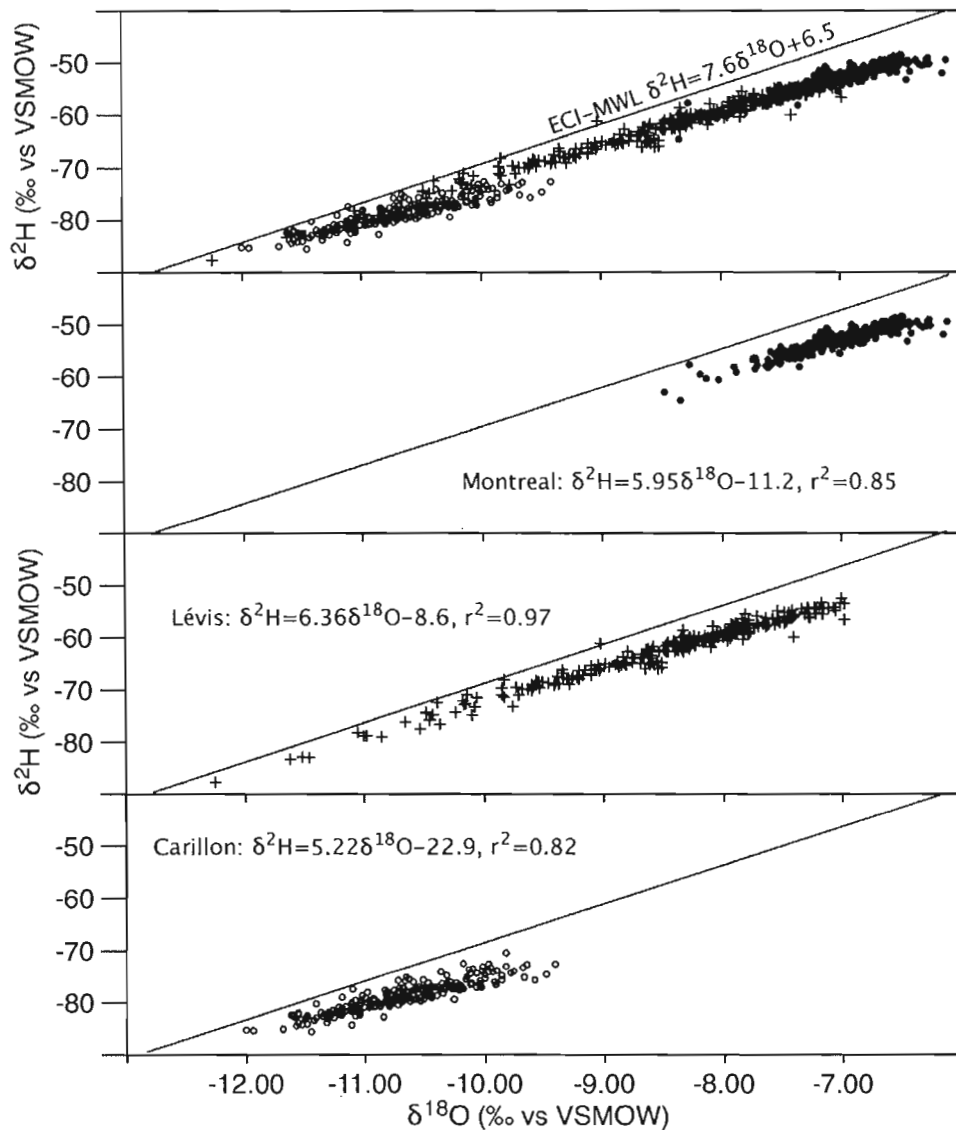
δ^2H vs $\delta^{18}O$ correlations for all data (a) and at the three monitoring stations taken separately: Montreal (b), Lévis (c) and Carillon (d). The EIC-MWL is also reported (Fritz et al., 1987, see text for details). Most of the river data fall below the MWL. The slopes of regressions recorded at the monitoring stations (b through d) are lower than that of the LMWL.

Figure 4. Seasonal isotopic fluctuations in the Ottawa River.
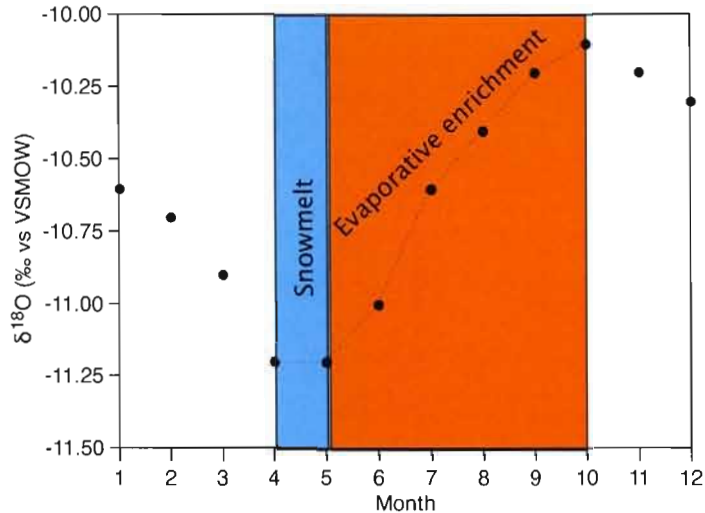
The seasonal isotopic fluctuations measured in the Ottawa River are characterized by a marked decrease in heavy-isotopes marking the contribution from heavy-isotope depleted meltwaters during snowmelt followed by enrichment in heavy-isotopes in response to evaporation during the ice-off season.

Figure 5. Comparison between the Ottawa River and CNIP data
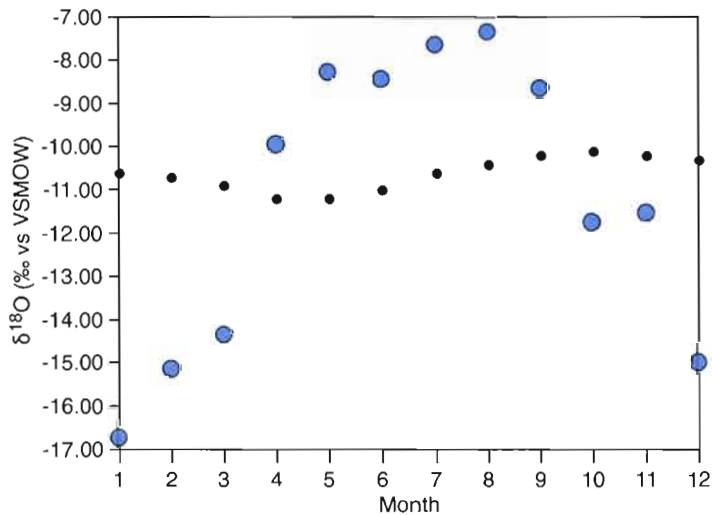
The seasonal isotopic fluctuations measured in the Ottawa River are damped and dephased with respect to the isotopic signal of precipitation at the Ottawa CNIP station. This is attributed to water transit time, mixing and evaporation processes within the basin. See text for details.

Figure 6. Ottawa river isotopic mass balance: evaporation model parameters.
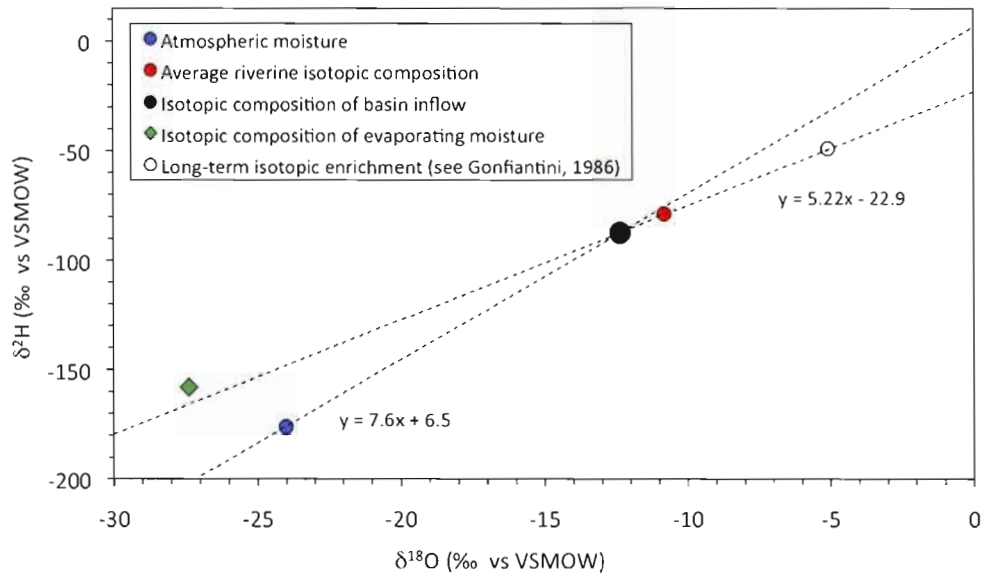
Details of parameters calculations are reported in section 5.1.1.

Figure 7. Lake Ontario – St. Lawrence River conceptual model.
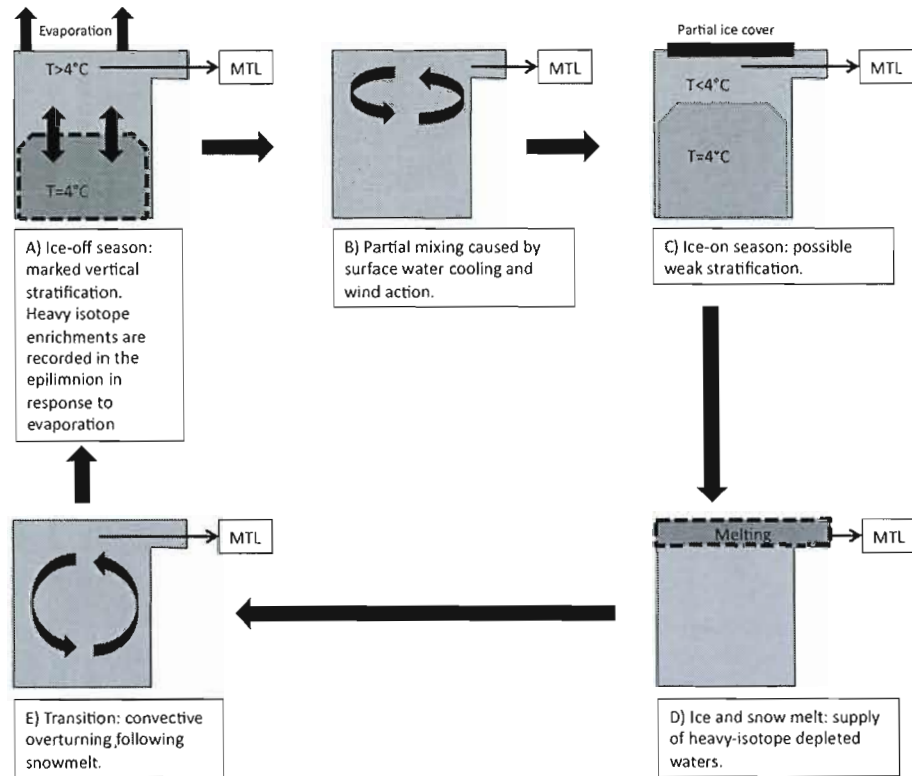
Conceptual model illustrating the physical processes occurring in Lake Ontario and governing the riverine isotopic cycle recorded in the St. Lawrence River south channel.

Figure 8. Seasonal $\delta^{18}O$ cycle recorded at the in the St. Lawrence southern channel.
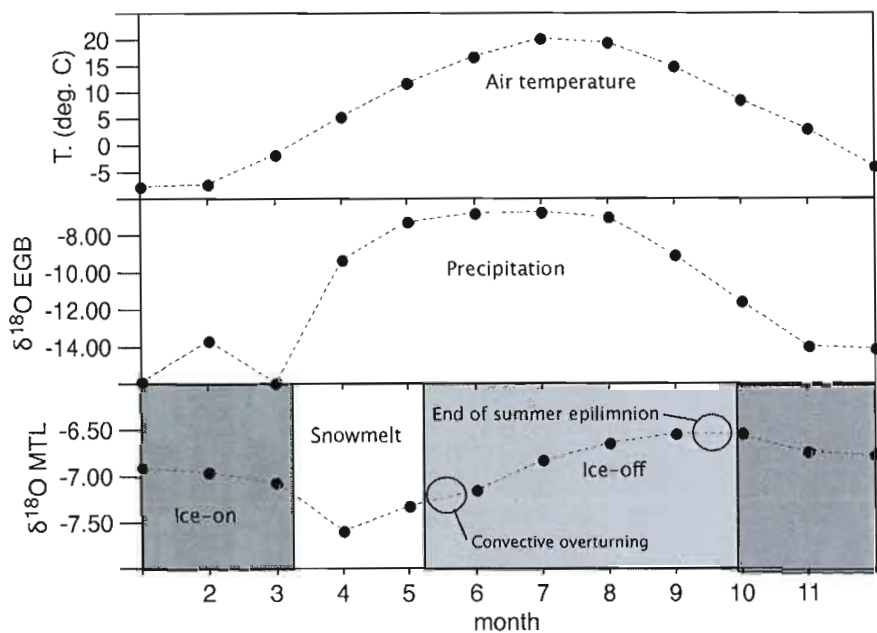
Isotopic composition of precipitation (CNIP data, Birks et al., 2004) and air temperatures (Environment Canada, climatic archive database) at Egbert are also shown. It is proposed that the bulk average isotopic composition of Lake Ontario is measured at Lévis during the convective overturning following snowmelt.

Figure 9. δ^2H-$\delta^{18}O$ correlations in the St. Lawrence southern channel.
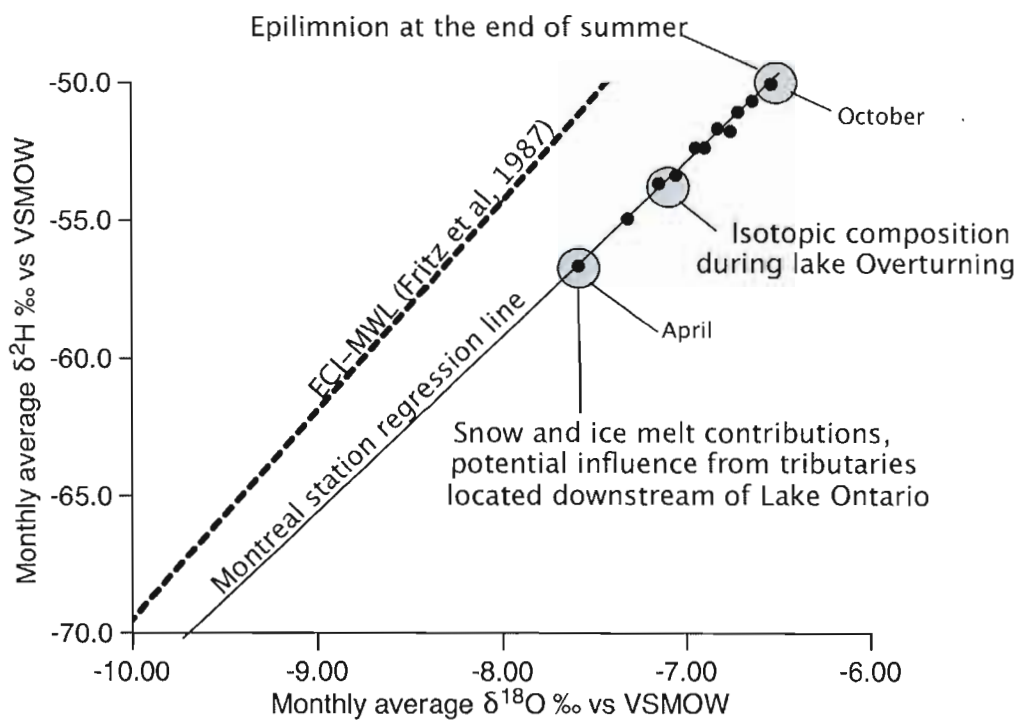
Monthly average δ^2H-$\delta^{18}O$ correlations at Montreal. Data show the gradual enrichment between spring snowmelt (April) and the end of the ice-off season (October).

Figure 10. The influence of tributary mixing on the isotopic signal recorded at Lévis.
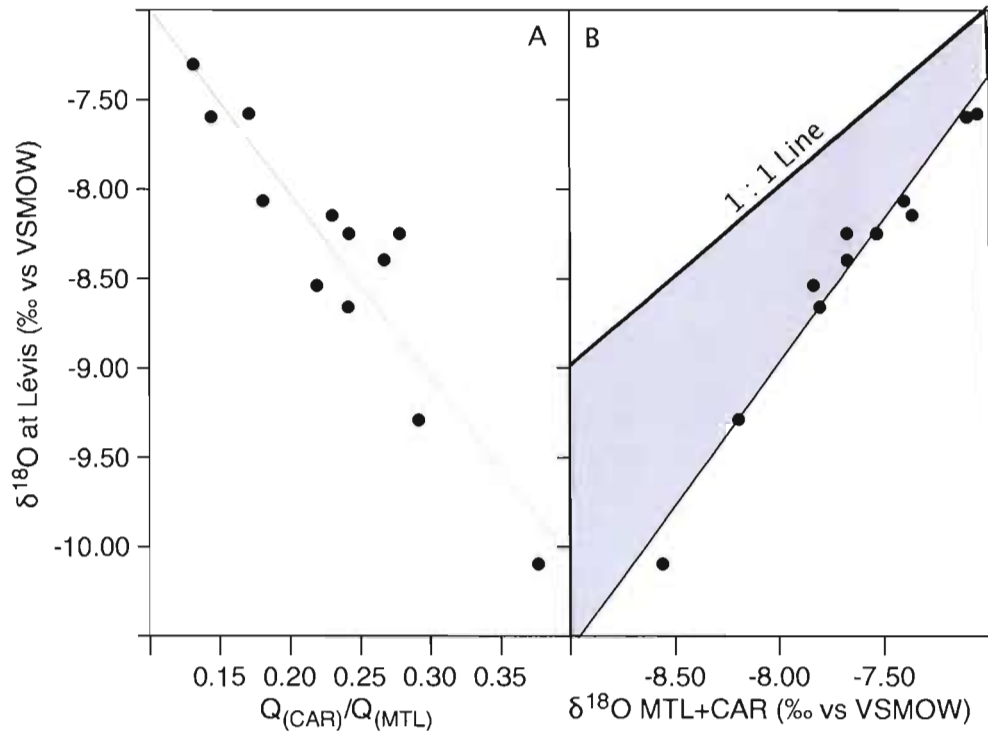
The inverse correlation observed between the ratio of discharge recorded at Carillon over that recorded at Montreal ($Q_{(CAR)}/Q_{(MTL)}$) and the isotopic composition of water at Lévis tends to validate the hypothesis that tributary mixing is a key parameter in regulating the isotopic composition of water at this site (A). The contributions from unsampled tributaries located between Montreal and Lévis explain the $\delta^{18}O$ depletion recorded at Lévis with respect to the amount weighted $\delta^{18}O$ value of the Montreal and Carillon signals taken together (B). The width of the shaded area illustrates that the influence of unsampled tributaries is at maximum during spring snowmelt (minimum $\delta^{18}O$ values). (based on monthly average values, see text for details).

Figure 11. Isotopic and discharge residuals.
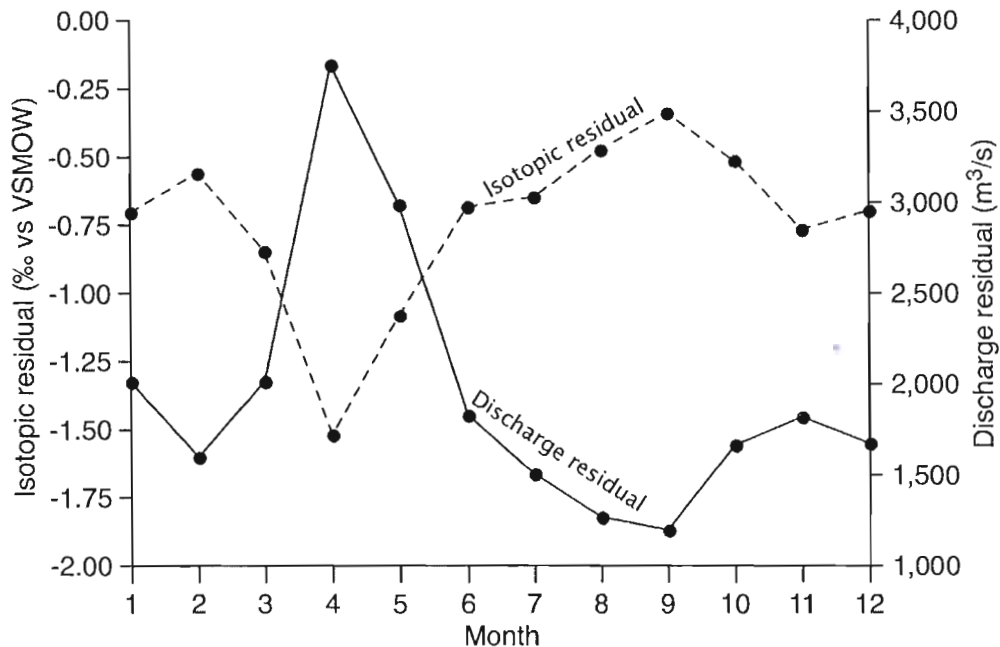
The amplitude of isotopic residuals calculated at Lévis are at maximum during the month of April (spring snowmelt) and at minimum during the month of September, consistent with the calculated discharge residuals. This pattern is consistent with increased contribution from unsampled tributaries during the snowmelt period.

Figure 12. Relationship between isotopic and discharge residuals.
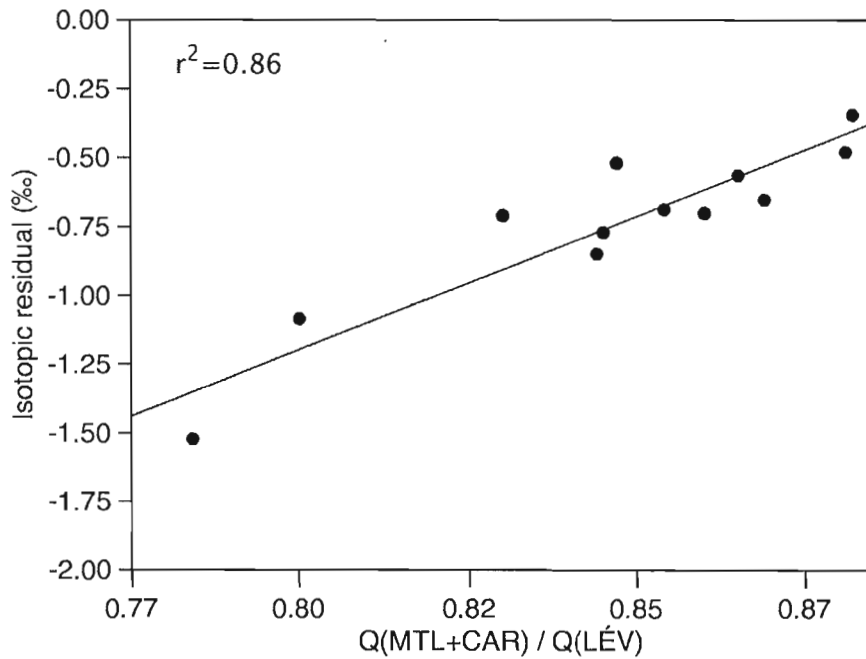
The high correlation coefficient (r^2=0.86) of the regression between absolute isotopic and discharge residuals suggests that the partitioning of streamflow components at the Outlet of the St. Lawrence fluvial estuary can be reliably performed on the basis of an isotopic mass balance.

Figure 13. 12-months $\delta^{18}O$ and $^2H_{xs}$ running averages time series.
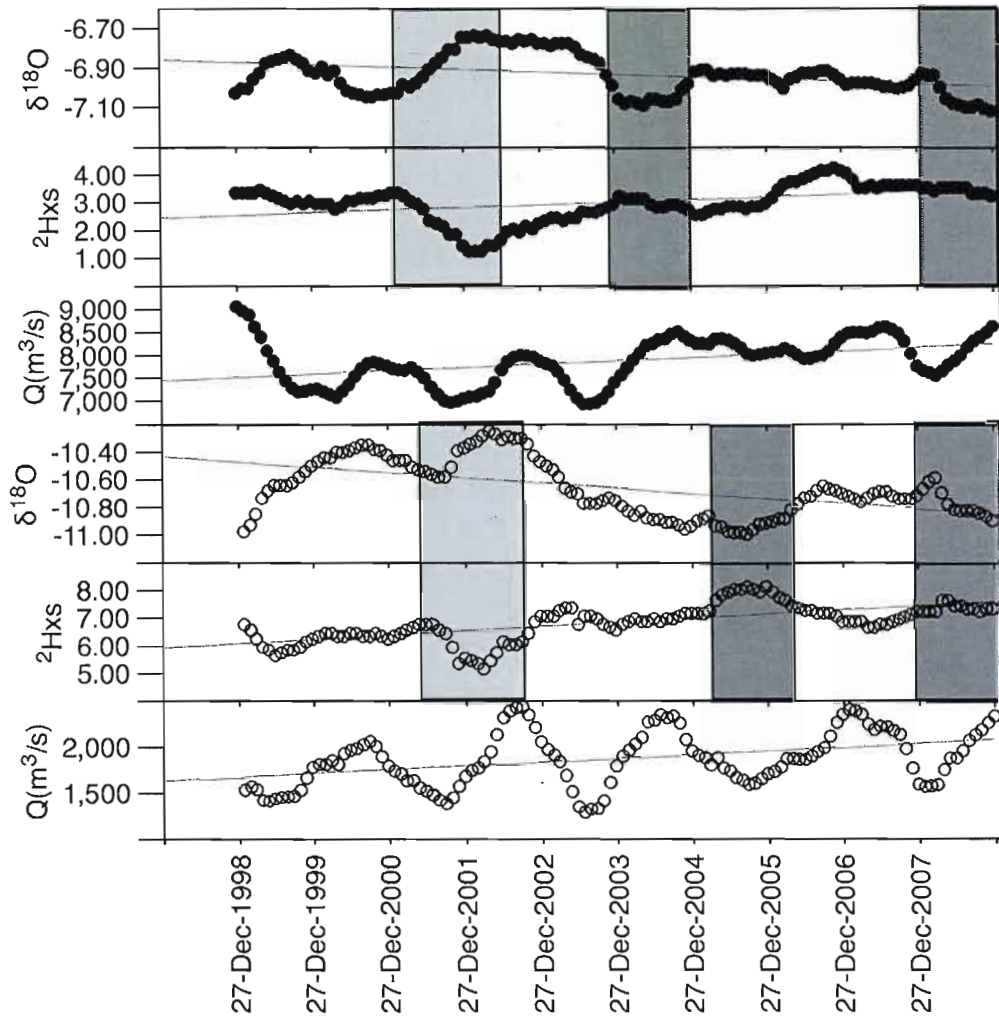
Delta values are reported in ‰ units vs VSMOW. Filled circles=Montreal, empty circles=Carillon. Short-term (i.e. 1-3 years) $^2H_{XS}$ variations roughly mirror the $\delta^{18}O$ variations. This is interpreted as the result of alternating periods of increased (pale grey) and reduced (dark grey) evaporation rates. Superimposed to these short-term variations are slight and unsteady $^2H_{XS}$ increasing trends (black lines) that accompagny the $\delta^{18}O$ gradual depletions recorded over the 12-years monitoring period. These trends tend to indicate overall decreases in evaporation/inflow ratios over the study period.

REFERENCES

Araguas-Araguas L., Froehlich K., Rozanski K. (2000). Deuterium and oxygen-18 isotope composition of precipitation and atmospheric moisture. *Hydrological Processes* **16**: 1341 – 1355.

Birks S.J., Edwards T.W.D., Gibson J.J., Drimmie R.J., Michel F.A. (2004). Canadian Network for isotopes in precipitation. http://www.science.uwaterloo.ca/~twdedwar/cnip/cniphome.html.

Bowen G.J., Wilkinson B. (2002). Spatial distribution of $\delta^{18}O$ in meteoric precipitation. *Geology* **30**, no4: 315-318.

Bowen G.J., Revenaugh J. (2003). Interpolating the isotopic composition of modern meteoric precipitation. *Water Resources Research* **39**, no 10: 1299. doi:10.1029/2003WR002086.

Boyce F.M., Donelan M.A., Hamblin P.F., Murthy C.R., Simons T.J. (1989). Thermal Structure and Circulation in the Great Lakes. *Aymosphere-Ocean* **27** (4): 607-642. doi: 0705-5900/89/0000-0607$01.25/0

Boyer C., Chaumont D., Chartier I., Roy A.G. (2010). Impact of climate change on the hydrology of St. Lawrence tributaries. *Journal of Hydrology* **384**: 65–83. doi:10.1016/j.jhydrol.2010.01.011.

Clark I.D., Fritz P. (1997). Environmental Isotopes in Hydrogeology . CRC Press.

Coplen, T.B. (1996). New guidelines for reporting stable hydrogen, carbon, and oxygen isotope-ratio data. *Geochimica et Cosmochimica Acta* **60** : 3359 - 3360.

Craig H. (1961). Isotopic variations in meteoric waters. *Science* **133**: 1702 – 1703.

Craig H., Gordon L.I. (1965). Deuterium and oxygen-18 variations in the ocean and marine atmosphere. In Tongiorgi E (ed.). *Stable Isotopes in Oceanographic Studies and Paleotemperatures*, Pisa: Cons. Naz. Rich. Lab. Geol. Nucl.: 9 – 130.

Dansgaard W. (1964). Stable isotopes in precipitation. *Tellus* **16**: 436 – 468.

Energy, mines and resources Canada. 1991. Canada Precipitation. The Atlas of Canada, 5th Edition, MCR 4145.

Environment Canada, climatic archive database: http://climate.weatheroffice.gc.ca/climateData

Frenette M., Barbeau C., Verrette J.L. (1989). *Aspects quantitatifs, dynamiques et qualitatifs des sédiments du Saint-Laurent, Projet de mise en valeur du Saint-Laurent*. Hydrotech Inc., Consultants for Environment Canada and the Government of Quebec.

Fritz P., Drimmie R.J., Frape S.K., O'Shea K. (1987). The isotopic composition of precipitation and groundwater in Canada. In *Isotope techniques in water resources developments, IAEA Symposium 299*, March, Vienna; 539 – 550.

Gat J.R., Bowser C.J., Kendall C. (1994). The contribution of evaporation from the Great Lakes to the continental atmosphere: estimate based on stable isotope data. *Geophysical Research Letters* **21**: 557 – 560.

Gat J.R. (1996). Oxygen and hydrogen isotopes in the hydrological cycle. *Annual Review of Earth and Planetary Science* **24**: 225 – 262.

Gibson J.J., Edwards T.W.D., Bursey G.G., Prowse T.D. (1993). Estimating evaporation using stable isotopes: quantitative results and sensitivity analysis for two catchments in northern Canada. *Nordic Hydrology* **24**: 79 – 94.

Gibson J.J., Prowse T.D. (1999). Isotopic characteristics of ice cover in a large northern river basin. *Hydrological Processes* **13**: 2537 – 2548.

Gibson J.J. (2001). Forest – tundra water balance signals traced by isotopic enrichment in lakes. *Journal of Hydrology* **251**: 1 – 13.

Gibson J.J. (2002a). Short-term evaporation and water budget comparisons in shallow arctic lakes using non-steady isotope mass balance *Journal of Hydrology* **264**: 247 – 266.

Gibson J.J. (2002b). A new conceptual model for predicting isotope enrichment of lakes in seasonal climates. *International Geosphere Biosphere Programme IGBP PAGES News* **10**: 10 – 11.

Gibson J.J., Aggarwal P., Hogan J., Kendall C., Martinelli L.A., Stichler W., Rank D., Goni I., Choudhry M., Gat J., Bhattacharya S., Sugimoto A., Fekete B., Pietroniro A., Maurer T., Panarello H., Stone D., Seyler P., Maurice-Bourgoin L., Herczeg A. (2002). Isotope studies in large river basins: a new global research focus. *EOS* **83**(52): 613 – 617.

Gibson J.J., Edwards T.W.D. (2002). Regional surface water balance and evaporation – transpiration partitioning from a stable isotope survey of lakes in northern Canada. *Global Biogeochemical Cycles*. DOI: 10 Đ1029/2001GB001839.

Gibson J.J., Prowse T.D. (2002). Stable isotopes in river ice: identifying primary over-winter streamflow signals and their hydrological significance. *Hydrological Processes* **16**: 873 – 890.

Gibson J.J., Birks S.J. and Edwards T.W.D. (2008). Global prediction of δ_A and δ^2H-$\delta^{18}O$ evaporation slopes for lakes and soil water accounting for seasonality. *Global Biogeochemical Cycles* **22**, GB2031, doi:10.1029/2007GB002997.

Gonfiantini R. (1986). Environmental isotopes in lake studies. In *Handbook of Environmental Isotope Geochemistry* , volume 3, Fritz P, Fontes JCh (eds). Elsevier: New York; 113 – 168.

Hélie J.F., Hillaire-Marcel C., Rondeau B. (2002). Seasonal changes in the sources and fluxes of dissolved inorganic carbon through the St. Lawrence River – isotopic and chemical constraints. *Chemical Geology* **186**: 117 – 138.

Hélie J.F., Hillaire-Marcel C. (2006). Sources of particulate and dissolved organic carbon in the St. Laurence River : isotopic approach. *Hydrological Processes* **20** : 1945 – 1959.

Huddart P.A., Longstaffe F.J., Crowe A.S. (1999). δD and $\delta^{18}O$ evidence for inputs to groundwater at a wetland coastal boundary in the southern Great Lakes region of Canada. *Journal of Hydrology* **214**: 18 – 31.

IFYGL-the International Field Year for the Great Lakes. (1981). Aubert E. and Richards T.L., eds, Great Lakes Environmental Research Laboratory.

Kendall C., Coplen T.B. (2001). Distribution of oxygen-18 and deuterium in river waters across the United States. *Hydrological Processes* **15**: 1363-1393.

Laudon H., Hemon H.F., Krouse H.R., Bishop K.H. (2002). Oxygen 18 fractionation during snowmelt: implications for spring flood hydrograph separation. *Water Resources Research* **38**: 1258. DOI: 10 Ð1029/2002WR001510.

Merlivat L., Jouzel J. (1979). Global climatic interpretation of the deuterium – oxygen 18 relationship for precipitation. *Journal of Geophysical Research* **84**: 5029 – 5033.

Quinn F.H. (1992). Hydraulic residence times for the Laurentian Great Lakes. *Journal of Great Lakes Research* **18**: 22-28.

Rondeau B., Cossa D., Gagnon P., Pham T.T., Surette C. (2005). Hydrological and biogeochemical dynamics of the minor and trace elements in the St. Lawrence River. *Applied Geochemistry* **20** (7) : 1391-1408.

Rozanski K., Araguàs-Araguàs L., Gonfiantini R. (1993). Isotopic patterns in global precipitation. In *Continental Isotopic Indicators of Climate*, Swart PK, McKenzie JA, Lohmann KC (eds). American Geophysical Union: Washington; 1 – 36.

St. Lawrence Centre. (1996). State of the Environment Report on the St. Lawrence River, The St. Lawrence Ecosystem, Vol. 1. Eds MultiMondes, Montreal.

Telmer K.H., Veizer J. (1999). Carbon fluxes, pCO_2 and substrate weathering in a large northern river basin, Canada: carbon isotope perspective. *Chemical Geology* **159**: 61 – 86.

Telmer K., Veizer J. (2000). Isotopic constraints on the transpiration, evaporation, energy and NPP budgets of a large boreal watershed: Ottawa River Basin, Canada. *Global Biogeochemical Cycles* **14**: 149 – 165.

Vitvar P.K., Aggarwal P.K., Herczeg A.L. (2007). Global network is launched to monitor isotopes in rivers. *EOS Transactions*, AGU 88 no 33: 325-326.

Water Survey of Canada, Archived Hydrometric Data Online, http://www.wsc.ec.gc.ca/hydat.

Yang C., Telmer K., Veizer J. (1996). Chemical dynamics of the "St. Lawrence" riverine system: δDH_2O, $\delta^{18}OH_2O$, $\delta^{13}C$-DIC, $\delta^{34}S$-sulfates, and dissolved $^{87}Sr/^{86}Sr$. *Geochimica et Cosmochimica Acta* **60**: 851 – 866.

Yi Y., Gibson J.J., Hélie J.F., Dick T.A. (2010). Synoptic and time-series isotope surveys of the Mackenzie River from Great Slave Lake to the Arctic Ocean, 2003 to 2006. *Journal of Hydrology* **383**: 223-232. doi:10.1016/j.jhydrol.2009.12.038.

CHAPITRE 2: Riverine δ^2H-δ^{18}O as an integrator of basin-scale hydrological processes: new insights from rivers of Northeastern Canada

Rosa Eric[1,2],
Hillaire-Marcel Claude[1],
Hélie Jean-François[1],
Gaillardet J.[2]

[1]*GEOTOP - Université du Québec à Montréal (UQAM), C.P. 8888 Succursale Centre-ville, Montreal, Quebec, Canada H3C 3P8.*

[2]*Equipe de Géochimie et Cosmochimie, Institut de Physique du Globe de Paris, Univ. Paris 7.*

Riverine δ^2H-δ^{18}O as an integrator of basin-scale hydrological processes: new insights from rivers of northeastern Canada

ABSTRACT

This study documents basin-scale recharge and evaporation processes based on river water samples. It focuses on the evaluation of δ^2H-δ^{18}O spatiotemporal variability among basins spanning over more than 12° of latitude in northeastern Canada. The extensively dammed La Grande River and its closest natural analogue, the Great Whale River, were monitored over more than one year in order to document and compare seasonal isotopic variations in both settings. Eleven other rivers with contiguous basins were sampled at least twice (during baseflow and snowmelt) in order to document the riverine latitudinal δ^{18}O-δ^2H gradient. The Great Whale River depicts a clear seasonal isotopic pattern with marked heavy-isotope depletion following snowmelt and gradual heavy-isotope enrichment in response to evaporation during the ice-off season. In the La Grande River, hydrological buffering within hydroelectric reservoirs damps the temporal isotopic fluctuations. Nevertheless the seasonal isotopic variability (<2.5‰ δ^{18}O) remains small with respect to spatial variations recorded among contiguous basins. The rivers depict a clear latitudinal gradient (δ^{18}O=-0.35*Lat+4.4), parallel to that modeled for precipitation. This tends to indicate that although post-rainfall processes influence riverine isotopic contents, rivers generally conserve an archive the isotopic composition of precipitation. The studied rivers define a River Water Line (RWL) arising from imbricate Local Evaporation Lines (LEL) extending below the Meteoric Water Line (MWL). A method using the distance between the RWL and the MWL is proposed for estimating the average evaporation over inflow ratio (E/I $\approx$ 10%) at the scale of the study area.

1. INTRODUCTION

As of today, the most comprehensive isotopic documentation of the water cycle at the global scale arises from the Global Network for Isotopes in Precipitation (GNIP, 1961-today), a program coordinated by the International Atomic Energy Agency (IAEA) and the World Meteorological Organization (WMO). Noteworthy, the isotopic label carried by precipitation allowed defining the Global Meteoric Water Line ($\delta^2H \approx 8\delta^{18}O+10$) (Craig, 1964; Rozanski et al., 1993) and highlighting the processes regulating the systematic δ^2H-$\delta^{18}O$ geographic distribution of precipitation (Craig, 1961; Dansgaard, 1964; Merlivat and Jouzel, 1979; Rozanski et al., 1993; Araguas Araguas et al., 2000; Bowen and Wilkinson, 2002; Bowen and Revenaugh, 2003). More recently, the IAEA launched the Global Network for Isotopes in Rivers (GNIR) (Gibson et al., 2002; Vitvar et al., 2007), a program aimed at documenting the natural and anthropogenic influences on river runoff and standing as a useful complement to GNIP. Kendall and Coplen (2001) highlighted that the isotopic signal carried by rivers can be reconciled with that imparted by precipitation. Although rivers remain indirect proxies of precipitation isotopic contents, they present the advantage of accounting for processes operating at the basin scale, yielding a response that is integrated in both time and space. Therefore, over a given area, the δ^2H-$\delta^{18}O$ geographical distribution of rivers draining contiguous basins allows a coverage that complements that of precipitation sampled at unevenly distributed GNIP stations. In addition, the isotopic label carried by continental surface waters (lakes, pounds, wetlands, rivers, shallow groundwaters) reflects the influence of post-rainfall recharge (Fritz et al., 1987; Clark et Fritz, 1997), evaporation (Gonfiantini, 1986; Gibson et al., 1993; 2001; 2002a; 2002b; Gat et al., 1994; Gat, 1996; Telmer and Veizer, 2000; Gibson and Edwards, 2002), ice formation (Gibson and Prowse, 1999; 2002), snowmelt (Laudon et al., 2002) and mixing processes (Yang et al., 1996; Yi et al., 2010), among others. Because a significant proportion of surface waters ultimately return to the oceans through the river network, documenting riverine ^2H-^{18}O appears to stand as a valuable approach for a quantitative assessment of the above processes. However, although noteworthy developments are observed in the United States (Kendall and Coplen, 2001) and Northwestern Canada (Mackenzie GEWEX study, Gibson et al., 2005; St Amour et al., 2005; Yi et al., 2010), the data remains fragmentary over Northeastern Canada. This adds to the uncertainty associated with the anticipation of short-term modifications in the water cycle, although basins set in this an area are likely to be impacted by ongoing climatic variations (Déry and Wood, 2004; Déry et al., 2005; Boyer et al., 2010) and precise information on factors influencing river runoff seems much needed.

In this study, we aim at documenting basin-scale recharge and evaporation processes on the basis of δ^2H-δ^{18}O riverine and precipitation systematic. The question is addressed through the documentation of δ^2H-δ^{18}O spatiotemporal variability in rivers of Northeastern Canada. In addition, we propose a new method for estimating evaporation / inflow ratios at the sub-continental scale on the basis of combined runoff and precipitation isotopic data.

2. STUDY AREA

The catchments included in this study are illustrated in Fig. 1. Watersheds depicted in light grey are part of the Hudson, James and Ungava Bays (HJUB) catchment, whereas those colored in dark grey are part of the St Lawrence River catchment. Watershed characteristics and sampling sites location are reported in Table 1.

2.1. Hydrology and Climate

The watersheds included in this study cover more than 12° of latitude. Mean annual temperatures range between approximately 6°C at Ottawa (Fig. 1) and -6°C at Kuujjuaq (northern section of the Koksoak River Basin) (Environement Canada, climatic archive database). The seasonality is prominent, for example, at Chapais (located near the center of the study area, Fig. 1), air temperatures range between -19°C in January and 16°C in July (*Environment Canada, Canadian Climate Normals*). Boreal forest dominates in the southern portion of the study area and a gradual transition towards taiga is observed northwards.

The study area constitutes a large mixing zone between three main atmospheric moisture sources (Fig. 1): the arctic stream, the Westerlies and the Tropical Stream originating from the Gulf of Mexico (cf.: Fritz et al., 1987). Runoff rates (calculated as mean annual discharge divided by watershed area) vary from ~370 to ~883 mm/yr in the Ottawa and Du Nord River basins, respectively (Table 1). Natural hydrographs present patterns with increased discharge rates in response to spring snowmelt and small increases during the fall season. However, some of the studied rivers are affected by hydroelectric installations and flow control structures, causing the discharge and isotopic fluctuations to be decoupled from natural hydro-climatic conditions. Notably, on the eastern shore of James Bay, the La Grande River and its main upstream tributary (Laforge River) together host 7 major hydroelectric reservoirs covering a total area of more than 13 000 km². In its lower section, the La Grande River also

receives water from the Boyd-Sakami diversion, supplying waters from southern rivers that were diverted towards the Robert-Bourassa reservoir. At the outlet of the Robert-Bourassa reservoir, in the downstream section of the river (selected as a sampling site), discharge rates are highest during the winter period, when hydroelectricity demand is highest. Throughout the year, the River discharge responds to management strategies by Hydro-Quebec as a function of water supplies and electricity demand. The Great Whale River, which flows parallel to the La Grande River and drains a basin that is contiguous to the northern limit of the La Grande River basin (Fig. 1), remains unaffected by hydroelectric installations. It therefore represents the closest "natural analogue" to the La Grande River. The Koksoak River was also modified due to hydroelectric diversions. In 1985, its upstream section was modified for building the Caniapiscau Reservoir that now constitutes the head of the La Grande – Laforge Rivers. Although the total discharge at the outlet of the Koksoak River has been reduced by approximately 30%, the river discharge still responds to natural hydro-climatic conditions. Finally, the Rupert River was sampled prior to its diversion towards the La Grande hydroelectric complex.

3. METHODOLOGY

3.1. Sampling and analysis

Some of the samples were retrieved during a project aimed at documenting the geochemical signal carried by rivers flowing into the Hudson, James and Ungava Bays (HJUB) (Rosa et al.,in prep., see chapters 3-4). The exact locations and timings of samplings are reported in Table 1 and Appendix 1, respectively.

Samples from the Koksoak and Great Whale Rivers were collected a few kilometers upstream of the rivers mouths, as close as possible to the center of the river main channel. Water samples were collected approximately 30 cm below surface using a polypropylene container attached to a pole. During the ice-free period, samples were retrieved from a small boat. During the winter period, samples were collected from a hole drilled in the ice after removing ice residues using an augured spoon. Samples from the La Grande River were collected at a sampling facility located within the LG2 hydroelectric power plant, directly from an untreated water-supply line ahead of the turbines.

The other rivers were sampled during field expeditions conducted in August 2008 and May 2009. These samples were collected from bridges, riverbanks and at the outlet of hydroelectric reservoirs along the river courses. When samples had to be collected from riverbanks (due to field constraints), sites located downstream of rapids were chosen in order to recover well mixed waters. After collection, all samples were stored in 30 ml high-density polypropylene (HDPE) bottles at 4°C until analysis. For oxygen and hydrogen isotopic analyses, 200 μl of water were transferred into septum vials and equilibrated in a heated rack with a known volume of CO_2 and H_2 respectively. The equilibrated gas was then analyzed by dual inlet mass spectrometry on a Micromass Isoprime isotope ratio mass spectrometer at the Stable Isotopes laboratory of the GEOTOP research center (*Université du Québec à Montréal*). The isotopic compositions of samples are corrected using two internal reference waters ($\delta^{18}O$ = -6.71±0.05‰ ; -20.31±0.05‰ and δ^2H = -51±1.5‰ ; -155±1.5‰) calibrated at the VSMOW-SLAP scale (Coplen, 1996). Internal water standards are run between each series of 10 samples in order to check for instrumental stability. All measurements are duplicated and the analytical uncertainty is ≤ 2‰ on δ^2H and ≤ 0.1‰ on $\delta^{18}O$ at the 1σ level. Values are reported in permil units (‰) against the Vienna Standard Mean Ocean Water standard (VSMOW): $\delta=[(^{18}O/^{16}O)_{sample}/(^{18}O/^{16}O)_{smow} - 1]*1000$.

3.2. Precipitation and Discharge Rates Data

The Regional Meteoric Water Line (RMWL) used in the following discussion is compiled from unweighted isotopic analyses of the three closest stations of the Canadian Network For Isotopes in Precipitation (CNIP) (Birks et al., CNIP database), namely the Ottawa, Sainte-Agathe and Chapais stations (Fig. 1): $\delta^2H=7.7\delta^{18}O+8$. Although the three stations are located in the southern half of the study area, we argue that it provides the most representative available estimate of the MWL in the region of interest.

Daily discharge rates are used to calculate the amount-weighted average isotopic composition of each river. Discharge rates in the La Grande River were provided by Dr. Alain Tremblay (Hydro-Québec) from non-disclosure information of Hydro-Quebec. It corresponds to the total flow measured at the outlet of the Robert-Bourassa hydroelectric reservoir. Discharge rates in the Koksoak and Great Whale Rivers (after July 2008) are based on daily measurements from the *Ministère du Développement durable, de l'environnement et des parcs (MDDEP)*. For the period before July 2008, discharge rates of the Great Whale River are taken from a compilation of the *International Polar Year project* (Dr. Stephen Déry, University of Northern British Columbia). These values are averages since measurements were not performed on a daily basis by the MDDEP during this time period. In the Koksoak and Great Whale rivers, gauging stations are located upstream of the sampling sites and discharge rates have been corrected assuming that discharge along the river course is proportional to the area of the watershed drained. The discharge rates presented for the other rivers (sampled during the August 2008 and May 2009 field expeditions) are those measured at the closest MDDEP gauging stations.

4. RESULTS

Analytical results are presented in Appendix 1 and summarized in Table 2. The average isotopic compositions recorded in the Ottawa and St. Lawrence rivers (Rosa et al.,in prep., see Chapter 1) are also reported for comparison purposes, as these Basins are contiguous to the south of the study area.

Overall, the recorded $\delta^{18}O$ (δ^2H) values range between -17.0‰ (-128‰) and -10.7‰ (-75‰) in the Koksoak and Du Nord rivers, respectively. Similarly, the amount-weighted average $\delta^{18}O$ (δ^2H) range between -16.5‰ (-124‰) and -11.4‰ (-80‰) in the Koksoak and Du Nord rivers, respectively. The heavy-isotope content of river waters decreases northwards. The Great Whale and La Grande Rivers were monitored. In the Great Whale River, $\delta^{18}O$ (δ^2H) values range between -16.0‰ (-121‰) and -13.6‰ (-106‰). The isotopic variability is comparatively low in the La Grande River, where $\delta^{18}O$ (δ^2H) ranges by less than 0.6‰ (4‰).

5. DISCUSSION

5.1. Temporal variability

The isotopic time series recorded in the La Grande and Great Whale Rivers (monitored sites) are illustrated in Fig. 2, allowing the comparison between an impounded river and its closest "natural state analogue". For comparison purposes, the Koksoak River is also illustrated, although this site is less constrained due to a limited number of samples (n=6).

The Great Whale River presents a clear seasonal isotopic cycle (Fig. 2) that is lagged and damped with respect to that observed in precipitation (Fig. 3). Marked heavy isotope depletions are recorded during the snowmelt period (month of May-June), followed by gradual heavy isotope enrichments during the ice-off season (May to October) and a return to average isotopic compositions over the ice-on season. These fluctuations account for $\delta^{18}O$ variations of ~2.5‰. Although less documented, the Koksoak River appears to follow a somewhat similar seasonal isotopic pattern, with the snowmelt event slightly delayed (month of May-June) with respect to the Great Whale River basin. Similar riverine seasonal isotopic patterns have been highlighted for the Ottawa River (Telmer and Veizer, 2000; Rosa et al.,in prep., see Chapter 1). The depletions in heavy isotopes recorded during the spring season mark the supply of heavy-isotopes depleted snows that accumulated within the basins over the ice-on period and that are quickly transferred to the hydrographic network during snowmelt. The subsequent gradual heavy-isotope enrichments observed throughout the ice-off season are attributed to basin-scale evaporation processes. The δ^2H-$\delta^{18}O$ distribution of data (Fig. 4) further supports this interpretation, as δ^2H-$\delta^{18}O$ values plot below the RMWL and define regressions with slopes that are lower than that of the RMWL. Such regressions are interpreted as local evaporation lines (c.f. Gibson et al., 2008 and references therein). Their intercepts with the Local Meteoric Water Line (LMWL) provide estimates of the mean isotopic composition of recharge within the corresponding drainage basin whereas increasing ^2H-^{18}O isotopic enrichments along these LEL reflect increased evaporation effects (eg.: see Telmer and Veizer, 2000; Gibson and Edwards, 2002).

The La Grande River stands as an exception due to its narrow range of temporal isotopic variations ($\delta^{18}O$ variations of less than 0.60‰). Despite the fact that the Great Whale and La Grande basins undergo similar hydro-climatic conditions, $\delta^{18}O$ variations are more than four times smaller in the La Grande River. This is attributed to the buffering effect caused by the hydroelectric reservoirs (n=6) found along the La Grande River and its upstream tributary, the Laforge River. It appears that the

residence time of water within these hydroelectric reservoirs (as much as 6 months, Hayeur, 2001) is long enough for smoothing out the seasonal isotopic variations. If reservoirs are likely to become thermally stratified during the ice-off season, it appears that the signal is homogenized at their outlets as the turbines intake (located within the hypolimnion) create turbulent mixing. In a somewhat similar fashion, Kendall and Coplen (2001) highlighted that among rivers of the USA, those presenting $\delta^{18}O$ ranges of less than 1‰ are often located below dams and lakes. Hydrological buffering by lakes and/or reservoirs rather than basin scale therefore appears to stand as the main factor for smoothing out seasonal isotopic variations in rivers, at least under the hydroclimatic conditions encountered in North America. The case of thermally stratified lakes is a noteworthy exception to this tendency, as exemplified by the Great Lakes - St. Lawrence River example (Rosa et al.,in prep., see Chapter 1).

5.2. Spatial variability

The spatial variability in riverine isotopic contents is addressed through the documentation of in-stream $\delta^{18}O$ patterns in selected rivers and by a comparison of contiguous basins covering more than 12 degrees of latitude.

5.2.1. In stream variations: longitudinal gradients

Sampling transects were carried along the Great Whale (August 2008) and La Grande (August 2008 and May 2009) rivers in order to address the in-stream isotopic variations. As both rivers roughly flow from east to west, these sampling transects allow documenting the longitudinal isotopic gradient between the Hudson / James Bays (HJB) and a distance of approximately 600 km inland.

The heavy isotope contents of both rivers increase from the rivers' heads towards the HJB (Fig. 5), accounting for $\delta^{18}O$ enrichments of ~1.50‰ and ~0.75‰ along the La Grande and Great Whale rivers, respectively. The two main tributaries of the Great Whale River, the Coats and Denys rivers, were also sampled. These two tributaries reach the Great Whale River in proximity of its outlet into Hudson Bay and present enriched $\delta^{18}O$ values with respect to the Great Whale River.

Much of the variability illustrated in Fig. 5 could be due to tributary mixing processes. For instance, the La Grande River receives water from the Boyd-Sakami diversion in its downstream section. Water originating from this diversion is drawn from southern tributaries that are likely to present heavier

isotopic compositions due to their geographical location (see section 5.2.2). In a similar fashion, the two main tributaries feeding the Great Whale River (Coats and Denys rivers) show marked heavy isotope enrichments with respect to the Great Whale River itself (Fig. 5) and are thus likely to induce an isotopic enrichment below their confluence. These two tributaries draw water from smaller sub-basins located in proximity of Hudson Bay. They are thus likely to be influenced by heavy isotope enriched precipitation originating from fresh atmospheric moisture formed over Hudson Bay. Such a process also seems valid for the Great Whale and La Grande river basins taken as a whole, as precipitation is likely to be enriched in heavy isotopes in proximity of the oceanic domain whereas more distant (i.e. inland) locations receive heavy-isotope depleted precipitation due to amount and altitude effects. Finally, the hypothesis of increasing evaporative effects from the rivers' heads towards their downstream section cannot be ruled out. For instance, water sampled in the upstream sections of rivers had little time to undergo evaporation with respect to waters collected downstream. This is especially true for the case of the La Grande River, as samples were all collected at the outlets of interconnected hydroelectric reservoirs, each of the latter acting as a large evaporation surface. A "string-of-lakes" effect could be observed here.

5.2.2. Latitudinal Gradients

Figure 6 presents the amount-weighted $\delta^{18}O$ of rivers reported against latitude. Also included in the calculation of this isotopic gradient are the data from the Ottawa River (year 2008, data from Chapter 1, Rosa et al., in prep.). However, the St. Lawrence River is not included in the calculation of the riverine latitudinal gradient, as evaporation from the Great Lakes creates a heavy isotope enrichment (Chapter 1, Rosa et al., in prep.) that strongly contrasts with that of surrounding rivers. A clear $\delta^{18}O$ latitudinal gradient of $\sim -0.35‰(\delta^{18}O)/$ °latitude is observed. We argue that although 11 of the rivers used to evaluate this latitudinal gradient were only sampled twice, this has a limited effect on the calculated value. First, these less constrained rivers were sampled in August (baseflow) and May (close to snowmelt) and it is therefore reasonable to assume that an important part of the seasonal isotopic variability was captured. In addition, the extremes of the regression (i.e. basins located at maximum and minimum latitudes) correspond to stations where the $\delta^{18}O$ variability is more documented (i.e. Ottawa, La Grande, Great Whale and Koksoak rivers). Nevertheless, in the future, better constraining this latitudinal riverine $\delta^{18}O$ gradient will rely on a better quantification of temporal isotopic variability within each river. Part of the scatter observed in Fig. 6 may also result from the variable latitudinal range covered by the different basins, as depicted by the latitudinal "error bars".

Since the isotopic composition of precipitation evolves with latitude, the latitudinal range of basins may affect the calculated regression. Similarly, longitudinal isotopic effects on precipitation associated to the distance from the HJB (see section 5.2.1) could explain part of the scatter. Nevertheless, such local heterogeneities do not obscure the observed latitudinal gradient and we argue that using sampling site latitude for calculating the riverine isotopic gradient remains the most robust method in the absence of a quantitative assessment of the average geographical position at which recharge occurs within each of the basins.

For comparison purposes, the second order polynomial equation proposed by Bowen and Wilkinson (2002) for describing the relationship between precipitation $\delta^{18}O$ and latitude at the global scale has been averaged to a first order regression. Over the range of latitudes encountered here, this has very little effect on the predicted $\delta^{18}O$ values (see Fig. 6). The calculated atmospheric gradient yields a value of $-0.36‰(\delta^{18}O)/$ °latitude, almost identical to that recorded here among rivers. However, the riverine $\delta^{18}O$ values measured here systematically fall below the atmospheric $\delta^{18}O$ values proposed by Bowen and Wilkinson (2002). Yet, the authors report that their model produces an overestimation of precipitation $\delta^{18}O$ in Canada ($\sim 3‰$ over the study region) and attribute this (in part) to a component of ^{18}O depleted atmospheric moisture originating from the Arctic. Such an interpretation seems consistent with the riverine $\delta^{18}O$ values reported here. In addition, the parallel riverine and atmospheric isotopic gradients tend to support the hypothesis of a relatively constant mixing proportion of the moisture sources over the study region (Fig. 1).

The riverine $\delta^{18}O$ gradient calculated here is also similar to that reported for rivers of Eastern USA ($\sim -0.42‰(\delta^{18}O)/$ °latitude) (Kendall and Coplen, 2001). Such continuity among riverine $\delta^{18}O$ and the similarity between riverine and atmospheric $\delta^{18}O$ latitudinal gradients tend to indicate that rivers strongly conserve the isotopic label imparted by precipitation, as already proposed by Kendall and Coplen (2001). The high correlation of the riverine $\delta^{18}O$-latitude regression also tends to indicate that although post rainfall processes (i.e. recharge, evaporation, snowmelt, mixing) are likely to significantly modify surface water isotopic compositions, these modifications are related to large-scale hydroclimatic processes rather than to small-scale spatial variability.

5.3. Towards a method for evaluating continental scale average evaporation/inflow ratios?

Kendall and Coplen (2001) reported that the USA "river water line" (RWL) as evaluated from unweighted analyses of samples from 48 contiguous states yields a regression ($\delta^2H=8.11\delta^{18}O+8.99$) that is in good agreement with the GMWL as evaluated by the IAEA and the WMO ($\delta^2H=8.17\delta^{18}O+10.35$) (Rozanski et al., 1993). The authors attribute this to the imbricate nature of the river water line (RWL) that consists of several "local river lines" (LRL) presenting slopes that are lower than that of the GMWL and extend below and above it.

The observations made in Northeastern Canada (this study) are consistent with the interpretation of the imbricate nature of the RWL. However, within the study region, the RWL calculated from the amount weighted ($\delta^2H=8.3\delta^{18}O+12.7$) isotopic values falls below the regional MWL ($\delta^2H=7.7\delta^{18}O+8$) (Fig. 7). We attribute this to post-rainfall evaporative effects that result in heavy isotopes enrichments in rivers. Following this interpretation, we propose that a method based on the distance between the LMWL and the RWL could allow a first order estimate of the average E/I ratio over the study area, given an adequate knowledge of isotopic enrichment slopes (See Gibson et al., 2008). Such a method could essentially rely on the use of isotopic mass balance equations derived for calculating E/I ratios of lakes and basins (Craig and Gordon, 1965; Gonfiantini, 1986; Gibson et al., 1993; Gibson and Edwards, 2002 and references therein):

$$I_C = Q_C + E_C \qquad\qquad\qquad\qquad (Eq.\ 1)$$

$$I_C\delta_I = Q_C\delta_Q + E_C\delta_E \qquad\qquad\qquad\qquad (Eq.\ 2)$$

$$\frac{E}{I} = \frac{\left(\delta_I - \delta_Q\right)}{\left(\delta_E - \delta_Q\right)} \qquad\qquad\qquad\qquad (Eq.\ 3)$$

$$\delta_E = \frac{\alpha^*\delta_L - h\delta_A - \varepsilon}{1 - h + \varepsilon_K} \qquad\qquad\qquad\qquad (Eq.\ 4)$$

where I_C, Q_C and E_C are the catchment inflow, surface outflow and evaporation losses, respectively, with corresponding δ values δ_I, δ_Q and δ_E. δ_E is evaluated using the formulation of Craig and Gordon (1965), with $\alpha^* = \alpha_{(V/L)} = 1/\alpha_{(L/V)}$ evaluated from Horita and Wesolowski (1994):

$$1000\ln\alpha_v^L(^{18}O) = -7.685 + 6.7123\left(\frac{10^3}{T}\right) - 1.6664\left(\frac{10^6}{T^2}\right) + 0.3504\left(\frac{10^9}{T^3}\right)$$

$$1000\ln\alpha_v^L(^2H) = 1158.8\left(\frac{T^3}{10^9}\right) - 1620.1\left(\frac{T^2}{10^6}\right) + 794.84\left(\frac{T}{10^3}\right) - 161.04 + 2.0002\left(\frac{10^9}{T^3}\right)$$

where T is in Kelvin. All terms in equation 4 are in decimal notations (not in permil notation). The ε term in Eq. 4 represents a small positive quantity and is evaluated as $1/\alpha^* - 1$. δ_A is the isotopic composition of the atmosphere. Finally, ε_K is the kinetic enrichment factor (Gonfiantini (1986)):

$\varepsilon_K(^{18}O) = 14.2(1-h)$

$\varepsilon_K(^2H) = 12.5(1-h)$

where h is the air relative humidity (between 0 and 1). Note that Eq. 3 can be solved independently for δ^2H and $\delta^{18}O$.

Here, we apply this approach in order to estimate the average E/I ratio of northeastern Canadian basins. Because the RWL arises from imbricate LEL presenting variable slopes and isotopic enrichments, we propose two main scenarios for evaluating the average E/I ratio over the study area. In the first scenario, we assume an average δ^2H-$\delta^{18}O$ enrichment slope of ~5.8, which is that reported for the Great Whale River. The second scenario assumes a lower average δ^2H-$\delta^{18}O$ enrichment slope of ~5.2, which is similar to the 12-years average slope reported for the Ottawa River (Rosa et al., in prep, see Chapter 1). These scenarios are consistent with the predicted LEL slopes as evaluated by Gibson et al. (2008) for this region. Here, we assume h=75% and fit δ_A in order to reproduced the measured evaporative enrichment slopes. For both scenarios, we use a riverine $\delta^{18}O$ of -13.5‰, which is the middle of the range of riverine $\delta^{18}O$ measured within the study area (-10‰ to -17‰). We assume an average ice-off average temperature of 10°C. The E/I ratios calculated from Eq.3 using both scenarios (see table 3) yields a E/I ratio of ~10%, consistent with the range of evaporation rates calculated from lakes located in northwestern Canada, at similar latitudes (Gibson and Edwards, 2002). The roughly parallel behavior of the LMWL and RWL over the range of δ-values reported in Fig. 7 tends to

indicate that comparable evaporative conditions prevail over the study region, despite the importance of the encountered latitudinal gradient. This also tends to indicate that if local heterogeneities (lakes, wetlands, mountainous areas) may induce local modifications in E/I ratios, the studied basins are large enough to buffer such effects. In addition, rivers affected by hydroelectric reservoirs (La Grande and Ottawa Rivers) do not stand out in Fig. 7, suggesting that water losses caused by enhanced evaporation within reservoirs do not significantly affect the basin-scale E/I ratios.

5.3.1. Robustness of calculations

The method described above only allows first order estimates of the average E/I ratio over northeastern Canada. Improving such calculations will rely on better constraining the LEL and amount-weighted average isotopic composition for each basin. For example, the LEL slope evaluated for the Koksoak River (~7.0) is higher than the range considered in the above calculations (using a slope of 7 yields unrealistic results in E/I calculations.). However, the Koksoak River LEL can only be evaluated from a limited number of samples (n=6) and more data will be required to evaluate if it is statistically different from the LEL range used in the above calculation. In addition, a better documentation of the MWL over the study area would allow refining the calculations. This might be critical for basins located at the higher latitudes of the study region where the MWL is only poorly documented due to the sparsity of CNIP/GNIP stations (see Fig. 1).

Despite the actual limits of the E/I calculations as proposed above, we argue that it shows promising results. In view of the basin-scale integrating capacity of rivers, it seems realistic to propose that producing continental and/or global scale maps of runoff $\delta^{18}O$-δ^2H could soon be within reach, as exemplified by the work of Kendall and Coplen (2001) in USA. We argue that simple E/I calculations based on the coupling of GNIR (IAEA Global Network for Isotopes in Rivers) and GNIP (IAEA-WMO Global network for isotopes in precipitation) data with isotopic enrichment slopes predictions (Gibson et al 2008) could provide key insights into the water cycle, notably through the documentation of evaporation processes. Such data seem critical for anticipating changes in continental freshwaters quantity in the context of a changing climate and intensified human pressures on water resources.

6. CONCLUSION

This study aimed at evaluating if rivers carry an isotopic signal that allows deciphering the influence of large-scale (i.e. sub-continental) recharge and evaporation processes. The question was addressed through the documentation of riverine δ^2H-δ^{18}O spatiotemporal variability in contiguous basins of northeastern Canada.

The rivers of northeastern Canada depict systematic isotopic cycles. Marked heavy-isotope depletions are recorded during the snowmelt period whereas heavy-isotope enrichment occurs throughout the ice-off season in response to evaporation. The La Grande River stands as an exception due to its lower range of δ^{18}O-δ^2H temporal variability, an observation attributed to the buffering effect of the large hydroelectric reservoirs found along the river itself and its upstream tributaries. Among the monitored rivers, δ^2H-δ^{18}O values plot below the LMWL and define local evaporation lines with slopes lower than that of the LMWL. Over the study area, rivers draining contiguous basins define a latitudinal gradient of -0.35‰(δ^{18}O)/ °latitude (from 46°N to 58°N), similar to that previously reported for precipitation and for rivers of Eastern USA. Such continuity among riverine δ^{18}O and the strong similarity between riverine and atmospheric δ^{18}O latitudinal gradients support the hypothesis that rivers preserve an archive of the isotopic label imparted by precipitation. The "river water line" calculated from riverine isotopic values falls below the regional MWL. We attribute this to post-rainfall evaporative effects that result in heavy-isotope enrichment in rivers. We propose that the average distance between the MWL and the RWL allows a first-order estimate of the average evaporation over inflow ratios (E/I). Calculations results suggest that average E/I ratios are of the order of 10% over the study area. The roughly parallel behavior of the LMWL and RWL tends to indicate that similar evaporative conditions prevail over the study region, despite the importance of the encountered latitudinal gradient. This also tends to indicate that if local heterogeneities (lakes, wetlands, mountainous areas) may induce local modifications in E/I ratios, the studied basins are large enough to buffer such effects.

Such findings further highlight the usefulness of GNIR as a complement to GNIP. The basin-scale integrating capacity of rivers and their capacity to preserve an archive of the isotopic signal inherited by precipitation seems especially useful, notably in areas where the acquisition of precipitation isotopic data is complicated by the inaccessibility of the territory. In addition, the use of isotopic mass balances coupling GNIR and GNIP data in large-scale hydrological models could provide key insights into the water cycle, notably through better documentation of evaporation processes.

Table 1. Basins characteristics.

River	Discharge (m^3/s)	Basin Area (Km^2)	Runoff (mm/yr)
Koksoak	1600	94311	535
Great Whale	676	42700	499
La Grande	3808	177678	676
Pontax	111	6020	579
Nemiscau	53	3015	549
Rupert	848	40900	654
Broadback	367	17100	677
Bell	497	22200	706
Harricana	70	3680	604
Ashuapmushuan	290	15300	599
Gatineau*	144	6840	665
Du Lièvre*	100	4530	699
Du Nord*	33	1170	883
Ottawa	*1900*	*149000*	*402*
St. Lawrence	*10500*	*1153000*	*287*

* = Sub-basins of the Ottawa River basin. The locations of the sampling sites along these rivers are listed in Table 2. *Data in italics are from Chapter 1.*

Table 2. Summary of results.

Site	Sampling site Lat/long	AWA δ^{18}O	AWA δ^{2}H	δ^{18}O min	δ^{18}O max	δ^{2}H min	δ^{2}H max
Koksoak	58.029 / -68.475	-16.5	-124	-17.0	-15.5	-128	-117
Great Whale	55.279 / -77.650	-14.7	-112	-16.0	-13.6	-121	-106
La Grande	53.781 / -77.530	-13.8	-105	-14.1	-13.5	-107	-103
Pontax	51.733 / -77.383	-14.1	-103	-14.8	-13.0	-107	-96
Nemiscau[1]	51.688 / -75.825	-13.3	-96	-13.7	-12.8	-99	-94
Rupert[1]	51.353 / -77.423	-13.7	-101	-14.0	-13.4	-103	-99
Broadback	51.185 / -77.465	-13.6	-102	-13.9	-13.2	-103	-100
Bell	49.769 / -77.627	-13.1	-98	-14.3	-11.8	-104	-90
Harricana	48.790 / -78.013	-12.9	-94	-13.7	-11.5	-98	-86
Ashuapmushuan	48.658 / -72.445	-13.8	-99	-14.5	-12.6	-105	-91
Ottawa River – Dozois[1]	47.541 / -77.141	-12.6	-89	-13.6	-11.7	-98	-81
Gatineau*	46.620 / -75.916	-12.6	-91	-13.3	-11.3	-96	-83
Du Lièvre*	46.549 / -75.514	-11.8	-87	-12.5	-11.3	-90	-85
Du Nord*	45.780 / -74.005	-11.4	-80	-11.5	-10.7	-82	-75
Ottawa River at Carillon	*45.567 / -74.384*	*-10.8*	*-79*	*-12.0*	*-9.4*	*-85*	*-70*
St. Lawrence River at Montreal	*45.413 / -73.609*	*-7.0*	*-53*	*-8.5*	*-6.1*	*-64*	*-48*
St. Lawrence River at Lévis	*46.807 / -71.189*	*-8.7*	*-64*	*-12.3*	*-7.0*	*-88*	*-52*

AWA stands for amount weighted average.
[1] sites where instantaneous (i.e. daily) discharge rates are unavailable. At these sites, the arithmetic averages are used instead of amount weighted averages.
*= sub-basins of the Ottawa River Basin.
Data in italics are from Chapter 1.

Table 3. Evaporation model parameters and results (E/I).

Parameter	Scenario 1: LEL slope = 5.2		Scenario 1: LEL slope = 5.8	
	Solved for ^{18}O	Solved for ^{2}H	Solved for ^{18}O	Solved for ^{2}H
T (°C) (estimated)	10	10	10	10
δQ (‰) (measured)	-13.5	-100	-13.5	-100
δI (‰) (calculated)	-15.2	-109	-15.5	-111
δA (‰) (calculated)	-26.5	-194	-24.8	-181
h (estimated)	0.75	0.75	0.75	0.75
Result: Xc=E/I	0.10	0.11	0.09	0.10

Figure 1. Study area.
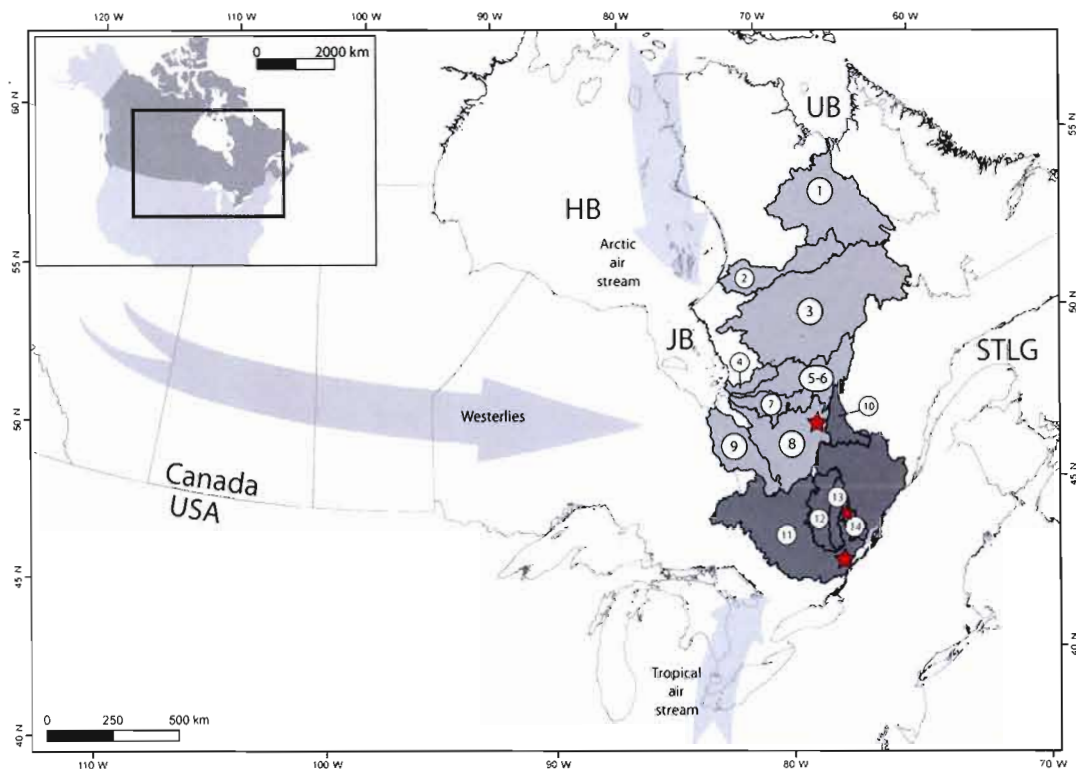
Map of the studied watersheds. Catchments in light grey are part of the HJUB watershed whereas those in dark grey are part of the St. Lawrence watershed. 1-Koksoak, 2-Great Whale, 3-La Grande, 4-Pontax, 5-6-Rupert and Nemiscau, 7-Broadback, 8- Bell (+Nottaway), 9-Harricana, 11-Ottawa, 12- Gatineau, 13- Du Lièvre, 14- Du Nord (+Rouge). The approximate locations of the three closest CNIP stations (from south to north: OTTAWA, Ste-Agathe and Chapais) are depicted by red symbols. The rough patterns of the main air masses mixing over the study area are also illustrated (from Fritz et al., 1987).

Figure 2. $\delta^{18}O$ time series recorded at the monitoring stations.
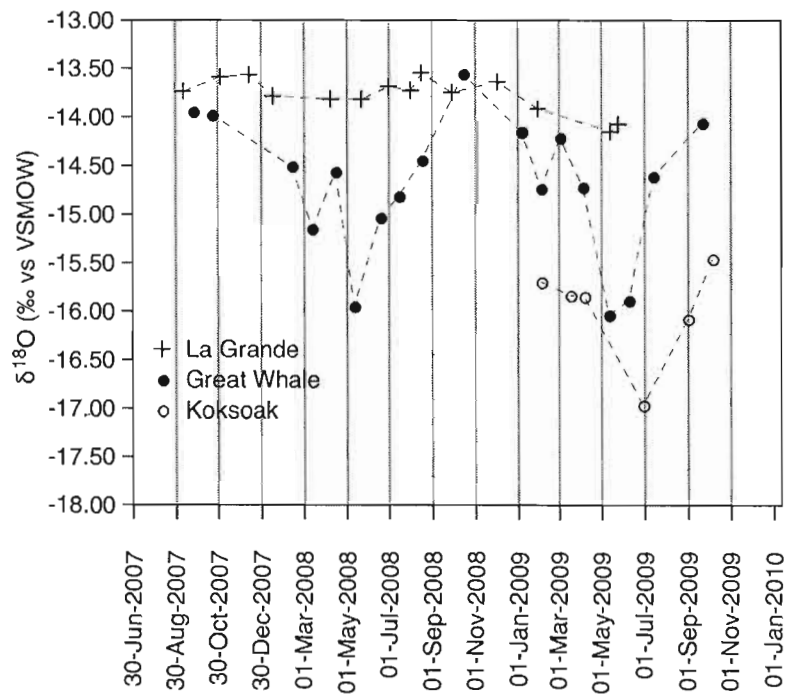
Isotopic time series recorded in the La Grande, Great Whale and Koksoak Rivers. Marked heavy-isotope depletions are observed in the Great Whale and Koksoak Rivers in response to snowmelt (May-June) whereas gradual heavy isotope enrichments occur throughout the ice-off season (June-November). In the La Grande River, seasonal isotopic variations are damped due to the buffering effects of hydroelectric reservoirs.

Figure 3. $\delta^{18}O$ variations at the Chapais CNIP station.
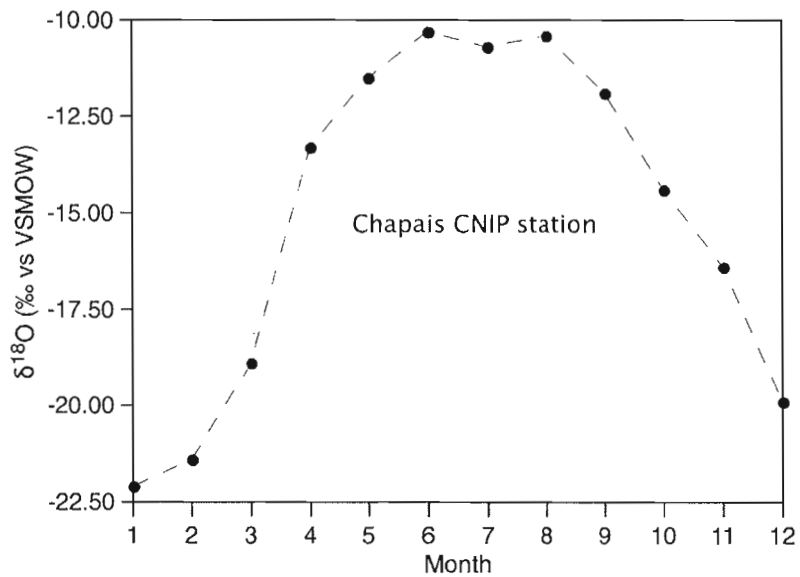
Average monthly $\delta^{18}O$ pattern recorded at the Chapais CNIP station between 1993 and 2003. (Data from Birks et al.,CNIP).

Figure 4. δ^2H-$\delta^{18}O$ regressions at the monitored sites.
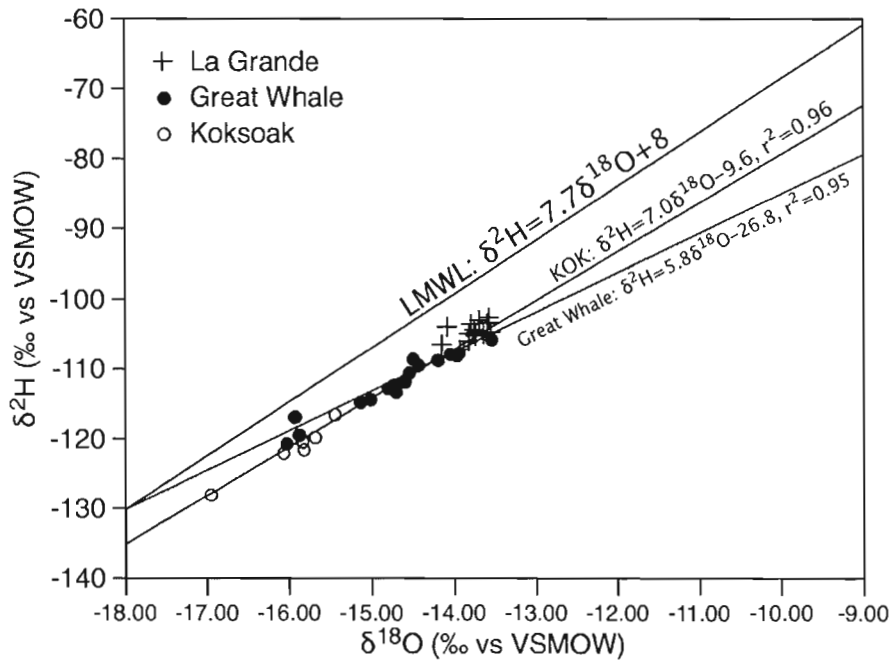
All river data plot below the LML. In the Great Whale and Koksoak, the δ^2H-$\delta^{18}O$ regressions show slopes lower than that of the LMWL and are interpreted as Local Evaporation Lines (LEL).

Figure 5. In-stream isotopic variations.
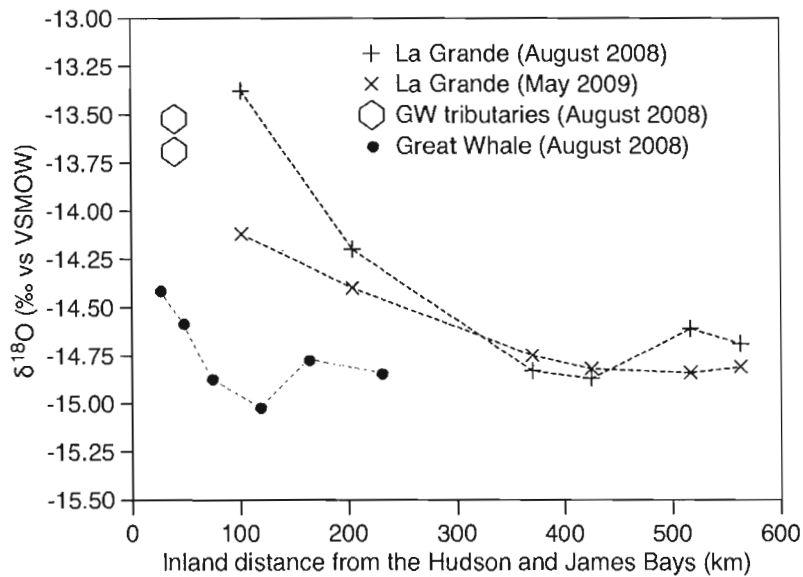
The sampling profiles conducted along the La Grande and Great Whale Rivers depict gradual heavy isotope enrichments from the rivers head lakes towards their downstream sections. This is attributed to tributary mixing and to the influence of atmospheric moisture derived from the nearby oceanic domain (Hudson and James Bays).

Figure 6. $\delta^{18}O$ latitudinal gradient.
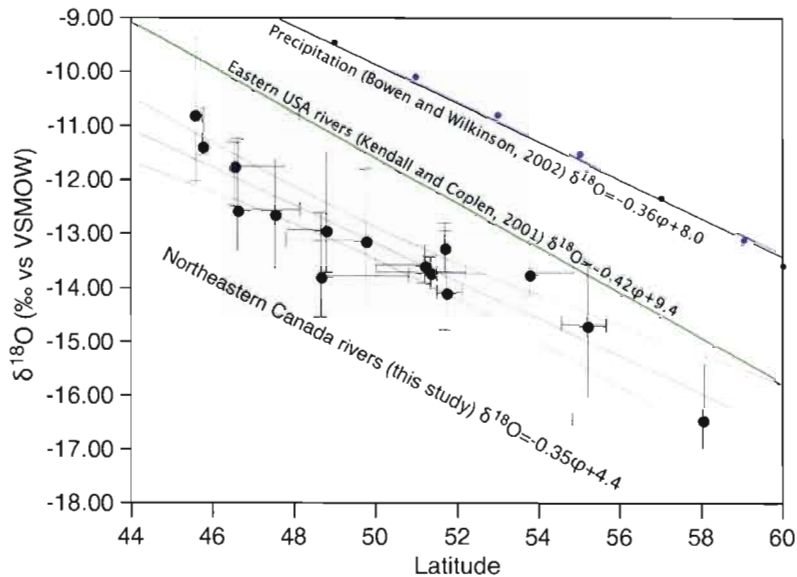
The rivers of Quebec depict a latitudinal $\delta^{18}O$ gradient that is roughly parallel to that proposed for precipitation (Bowen and Wilkinson, 2002) and for rivers of Eastern USA (Kendall and Coplen, 2001). See text for details.

Figure 7. MWL and RWL.
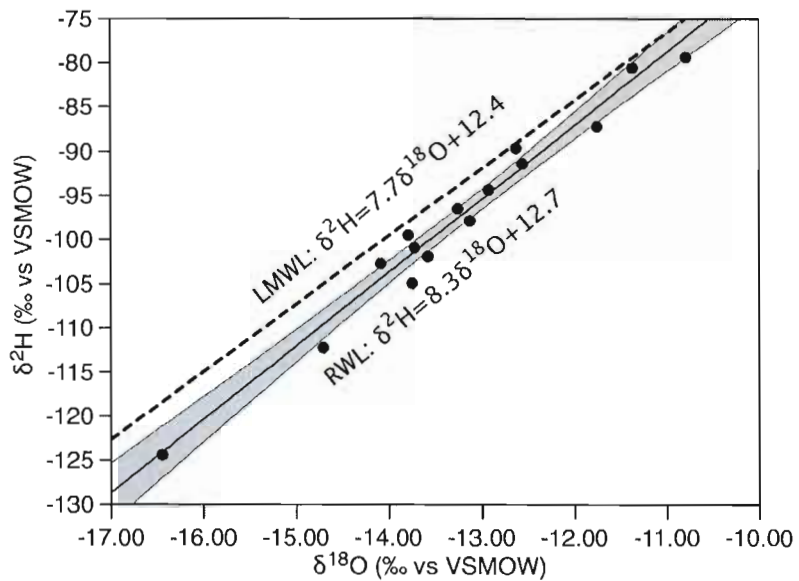
The RWL calculated from amount-weighted average riverine $\delta^{18}O$-δ^2H arises from imbricate LEL. The position of the RWL, which plots below the LMWL, is attributed to post rainfall evaporation processes. It is proposed that the distance between the lines could provide a method for estimating large-scale evaporation rates. (see text for details).

REFERENCES

Araguas-Araguas L., Froehlich K., Rozanski K. (2000). Deuterium and oxygen-18 isotope composition of precipitation and atmospheric moisture. *Hydrological Processes* **16**: 1341 – 1355.

Birks S.J., Edwards T.W.D., Gibson J.J., Drimmie R.J., Michel F.A. (2004). Canadian Network for isotopes in precipitation. http://www.science.uwaterloo.ca/~twdedwar/cnip/cniphome.html.

Bowen G.J., Wilkinson B. (2002). Spatial distribution of $\delta^{18}O$ in meteoric precipitation. *Geology* **30**, no4: 315-318.

Bowen G.J., Revenaugh J. (2003). Interpolating the isotopic composition of modern meteoric precipitation. *Water Resources Research* **39**, no 10: 1299. doi:10.1029/2003WR002086.

Boyer C., Chaumont D., Chartier I., Roy A.G. (2010). Impact of climate change on the hydrology of St. Lawrence tributaries. *Journal of Hydrology* **384**: 65–83. doi:10.1016/j.jhydrol.2010.01.011.

Clark I.D., Fritz P. (1997). Environmental Isotopes in Hydrogeology . CRC Press.

Coplen, T.B. (1996). New guidelines for reporting stable hydrogen, carbon, and oxygen isotope-ratio data. *Geochimica et Cosmochimica Acta* **60** : 3359 - 3360.

Craig H. (1961). Isotopic variations in meteoric waters. *Science* **133**: 1702 – 1703.

Craig H., Gordon L.l. (1965). Deuterium and oxygen-18 variations in the ocean and marine atmosphere. In Tongiorgi E (ed.). *Stable Isotopes in Oceanographic Studies and Paleotemperatures*, Pisa: Cons. Naz. Rich. Lab. Geol. Nucl.: 9 – 130.

Dansgaard W. (1964). Stable isotopes in precipitation. *Tellus* **16**: 436 – 468.

Déry SJ, Wood EF. 2004. Teleconnection between the Arctic Oscillation and Hudson Bay river discharge. *Geophysical Research Letters* **31**, L18205, doi:10.1029/2004GL020729.

Déry S.J., Stieglitz M., McKenna E.C., Wood E.F. (2005). Characteristics and Trends of River Discharge into Hudson, James and Ungava Bays, 1964-2000. *Journal of Climate* **18**, 2540-2557.

Environment Canada, climatic archive database: http://climate.weatheroffice.gc.ca/climateData

Fritz P., Drimmie R.J., Frape S.K., O'Shea K. (1987). The isotopic composition of precipitation and groundwater in Canada. In *Isotope techniques in water resources developments, IAEA Symposium 299*, March, Vienna; 539 – 550.

Gat J.R., Bowser C.J., Kendall C. (1994). The contribution of evaporation from the Great Lakes to the continental atmosphere: estimate based on stable isotope data. *Geophysical Research Letters* **21**: 557 – 560.

Gat J.R. (1996). Oxygen and hydrogen isotopes in the hydrological cycle. *Annual Review of Earth and Planetary Science* **24**: 225 – 262.

Gibson J.J., Edwards T.W.D., Bursey G.G., Prowse T.D. (1993). Estimating evaporation using stable isotopes: quantitative results and sensitivity analysis for two catchments in northern Canada. *Nordic Hydrology* **24**: 79 – 94.

Gibson J.J., Prowse T.D. (1999). Isotopic characteristics of ice cover in a large northern river basin. *Hydrological Processes* **13**: 2537 – 2548.

Gibson J.J. (2001). Forest – tundra water balance signals traced by isotopic enrichment in lakes. *Journal of Hydrology* **251**: 1 – 13.

Gibson J.J. (2002a). Short-term evaporation and water budget comparisons in shallow arctic lakes using non-steady isotope mass balance *Journal of Hydrology* **264**: 247 – 266. DOI: 10.1002/hyp.366.

Gibson J.J. (2002b). A new conceptual model for predicting isotope enrichment of lakes in seasonal climates. *International Geosphere Biosphere Programme IGBP PAGES News* **10**: 10 – 11.

Gibson J.J., Aggarwal P., Hogan J., Kendall C., Martinelli L.A., Stichler W., Rank D., Goni I., Choudhry M., Gat J., Bhattacharya S., Sugimoto A., Fekete B., Pietroniro A., Maurer T., Panarello H., Stone D., Seyler P., Maurice-Bourgoin L., Herczeg A. (2002). Isotope studies in large river basins: a new global research focus. *EOS* **83**(52): 613 – 617.

Gibson J.J., Edwards T.W.D. (2002). Regional surface water balance and evaporation – transpiration partitioning from a stable isotope survey of lakes in northern Canada. *Global Biogeochemical Cycles*. DOI: 10 Đ1029/2001GB001839.

Gibson J.J., Prowse T.D. (2002). Stable isotopes in river ice: identifying primary over-winter streamflow signals and their hydrological significance. *Hydrological Processes* **16**: 873 – 890.

Gibson J.J., Edwards T.W.D., Birks S.J., St Amour N.A., Buhay W.M., McEachern P., Wolfe B.B., Peters D.L. (2005). Progress in isotope tracer hydrology in Canada. *Hydrological Processes* **19**: 303-327. DOI: 10.1002/hyp.5766.

Gibson J.J., Birks S.J. and Edwards T.W.D. (2008). Global prediction of δ_A and δ^2H-δ^{18}O evaporation slopes for lakes and soil water accounting for seasonality. *Global Biogeochemical Cycles* **22**, GB2031, doi:10.1029/2007GB002997.

Gonfiantini R. (1986). Environmental isotopes in lake studies. In *Handbook of Environmental Isotope Geochemistry*, volume 3, Fritz P, Fontes JCh (eds). Elsevier: New York; 113 – 168.

Hayeur G. (2001). Synthèse des connaissances environnementales acquises en milieu nordique de 1970 à 2000. Montréal, Hydro-Québec. 110pp.

Kendall C., Coplen T.B. (2001). Distribution of oxygen-18 and deuterium in river waters across the United States. *Hydrological Processes* **15**: 1363-1393.

Laudon H., Hemon H.F., Krouse H.R., Bishop K.H. (2002). Oxygen 18 fractionation during snowmelt: implications for spring flood hydrograph separation. *Water Resources Research* **38**: 1258. DOI: 10 Đ1029/2002WR001510.

Merlivat L., Jouzel J. (1979). Global climatic interpretation of the deuterium – oxygen 18 relationship for precipitation. *Journal of Geophysical Research* **84**: 5029 – 5033.

Ministère du Développement durable, de l'Environnement et des Parcs. *www.mddep.gouv.qc.ca/ index_en.asp.*

Rozanski K., Araguàs-Araguàs L., Gonfiantini R. (1993). Isotopic patterns in global precipitation. In *Continental Isotopic Indicators of Climate*, Swart PK, McKenzie JA, Lohmann KC (eds). American Geophysical Union: Washington; 1 – 36.

Telmer K., Veizer J. (2000). Isotopic constraints on the transpiration, evaporation, energy and NPP budgets of a large boreal watershed: Ottawa River Basin, Canada. *Global Biogeochemical Cycles* **14**: 149 – 165.

Vitvar P.K., Aggarwal P.K., Herczeg A.L. (2007). Global network is launched to monitor isotopes in rivers. *EOS Transactions*, AGU 88 no 33: 325-326.

Yang C., Telmer K., Veizer J. (1996). Chemical dynamics of the "St. Lawrence" riverine system: δDH_2O, $\delta^{18}OH_2O$, $\delta^{13}CDIC$, δ^{34} Ssulfates , and dissolved $^{87}Sr/^{86}Sr$. *Geochimica et Cosmochimica Acta* **60**: 851 – 866.

Yi Y., Gibson J.J., Hélie J.F., Dick T.A. (2010). Synoptic and time-series isotope surveys of the Mackenzie River from Great Slave Lake to the Arctic Ocean, 2003 to 2006. *Journal of Hydrology* **383**: 223-232. doi:10.1016/j.jhydrol.2009.12.038.

APPENDIX 1. Analytical results.

Sample – Date (ddmmyy)	Basin (#)	daily Q (m³/s)	SC (µS/cm)	δ¹⁸O (‰ vs VSMOW)	δ²H (‰ vs VSMOW)
Koksoak 030209	1	301	53	-15.70	-119.8
Koksoak 170309	1	194	61	-15.84	-121.5
Koksoak 060409	1	181	67	-15.85	-120.4
Koksoak 290609	1	5068	41	-16.97	-127.9
Koksoak 310809	1	1792	40	-16.08	-122.0
Koksoak 051009	1	1501	38	-15.46	-116.5
Great Whale 240907	2	852	22	-13.96	-107.6
Great Whale 211007	2	874	16	-13.98	-108.0
Great Whale 120208	2	230	22	-14.51	-108.5
Great Whale 120308	2	179	39	-15.15	-114.7
Great Whale 140408	2	153	33	-14.56	-110.5
Great Whale 110508	2	602	30	-15.95	-116.8
Great Whale 160608	2	1254	17	-15.03	-114.3
Great Whale 150708	2	716	18	-14.81	-112.9
Great Whale 170808	2	581	17	-14.43	-109.4
Great Whale 151008	2	884	24	-13.56	-105.6
Great Whale 050109	2	404	24	-14.15	na
Great Whale 020209	2	285	24	-14.74	-112.3
Great Whale 020309	2	208	24	-14.21	-108.7
Great Whale 060409	2	186	36	-14.72	-113.2
Great Whale 110509	2	341	27	-16.04	-120.6
Great Whale 080609	2	1428	20	-15.89	-119.4
Great Whale 130709	2	1228	20	-14.61	-111.8
Great Whale 210909	2	714	21	-14.06	-107.8
Denys 170808	2		19	-13.69	-103.8
Coats 170808	2		24	-13.52	-104.0
GW1 170808	2		17	-14.40	-109.4
GW2 170808	2		17	-14.57	-109.0
GW3 170808	2		15	-14.87	-113.5
GW4 170808	2		16	-15.03	-113.7
GW5 170808	2		14	-14.77	-109.9
GW6 170808	2		13	-14.84	-114.1
La Grande 100907	3	n.d.i.	18	-13.74	-105.3
La Grande 021107	3	n.d.i.	15	-13.59	-103.5
La Grande 121207	3	n.d.i.	16	-13.57	-102.7
La Grande 160108	3	n.d.i.	14	-13.79	-103.7
La Grande 070408	3	n.d.i.	16	-13.82	-106.1
La Grande 220508	3	n.d.i.	15	-13.82	-105.0
La Grande 300608	3	n.d.i.	14	-13.69	-103.1
La Grande 010808	3	n.d.i.	15	-13.73	-104.9
La Grande 160808	3	n.d.i.	15	-13.55	-104.8

La Grande 280908	3	n.d.i.	15	-13.75	-104.5
La Grande 021208	3	n.d.i.	17	-13.64	-105.1
La Grande 290109	3	n.d.i.	14	-13.92	-107.3
La Grande 140509	3	n.d.i.	15	-14.15	-106.6
La Grande 250509	3	n.d.i.	15	-14.08	-104.1
LG2 160808	3	n.d.i.	15	-13.38	-104.8
LG3 160808	3	n.d.i.	15	-14.19	-106.9
LG4 1908008	3	n.d.i.	13	-14.83	-112.1
LA1 180808	3	n.d.i.	11	-14.87	-112.0
LA2 190808	3	n.d.i.	12	-14.61	-112.4
LG-Brisay 190808	3	n.d.i.	12	-14.69	-112.0
LG2 250509	3	n.d.i.	15	-14.12	-104.1
LG3 250509	3	n.d.i.	14	-14.39	-107.8
LG4 250509	3	n.d.i.	14	-14.75	-109.8
LA1 260509	3	n.d.i.	13	-14.82	-110.8
LA2 260509	3	n.d.i.	13	-14.84	-110.5
LG-Brisay 260509	3	n.d.i.	13	-14.82	-110.4
Pontax 150808	4	208	18	-12.98	-95.7
Pontax 240509	4	340	15	-14.78	-106.8
Nemiscau 220808	5		13	-12.83	-94.2
Nemiscau 270509	5		14	-13.71	-98.5
Rupert 150808	6		22	-13.43	-98.6
Rupert 240509	6		19	-14.03	-102.9
Rupert 220808	6		28	-12.97	-97.3
Rupert 270509	6		23	-13.99	-102.6
Broadback 150808	7	451	19	-13.22	-100.3
Broadback 240509	7	478	22	-13.93	-103.2
Broadback 220808	7	451	19	-12.73	-96.6
Broadback 270509	7	478	16	-14.51	-105.6
Bell 150808	8	924	25	-11.83	-90.0
Bell 240509	8	1085	23	-14.26	-104.4
Harricana 140808	9	93	67	-11.51	-86.3
Harricana 240509	9	174	70	-13.70	-98.4
Ashuapmushuan 220808	10	344	38	-12.63	-91.2
Ashuapmushuan 270509	10	539	37	-14.53	-104.6
Dozois reservoir (ottawa River) 140808	11		24	-11.67	-80.8
Dozois reservoir (ottawa River) 270509	11		18	-13.62	-98.2
Gatineau 140808	12	129	24	-11.26	-83.5
Gatineau 230509	12	230	20	-13.31	-95.7
Du Lièvre 140808	13	156	28	-11.33	-85.2
Du Lièvre 230509	13	97	32	-12.49	-90.2
Du Nord 140808	14	6	141	-10.67	-75.4
Du Nord 230509	14	28	148	-11.54	-81.5

CHAPITRE 3 : Chemical denudation rates in the James, Hudson and Ungava bays watershed: lithological and carbon cycling aspects

Rosa Eric[1,2],
Gaillardet Jérôme[2],
Hillaire-Marcel Claude[1],
Hélie Jean-François[1],
Richard Louis-Filip.[1]

[1]*GEOTOP - Université du Québec à Montréal (UQAM), C.P. 8888 Succursale Centre-ville, Montreal, Quebec, Canada H3C 3P8.*

[2]*Equipe de Géochimie et Cosmochimie, Institut de Physique du Globe de Paris, Univ. Paris 7.*

[3] *Monitoring et surveillance de la qualité de l'eau au Québec/ Quebec Water Quality Monitoring and Surveillance Direction générale des sciences et technologies/ Science and Technology Branch, Environnement Canada / Environment Canada,105 McGill, 7e étage/floor, Montréal (Québec) H2Y 2E7*

Chemical denudation rates in the James, Hudson and Ungava bays watershed: lithological and carbon cycling aspects

ABSTRACT

This study aims at documenting chemical denudation rates in the Canadian Shield and Interior Platform. It focuses on the dissolved chemistry of major rivers flowing into the Hudson, James and Ungava bays (HJUB). Dissolved major ions, strontium, neodymium and organic carbon (DOC) concentrations were monitored in four rivers (Koksoak, Great Whale, La Grande and Nelson). Six other rivers flowing into the HJUB were sampled during baseflow and snowmelt conditions, providing complementary data. The rivers of the Canadian Shield exhibit major cations concentrations ranging between 62 and 360 µM, [Nd] of 0.57 to 4.72 nM and variable [DOC] (241 – 1777 µM). In comparison, the Nelson River (Interior Platform) shows higher major cations concentrations (1200 – 2276 µM), lower [Nd] (0.14 to 0.45 nM) and intermediate [DOC] (753 – 928 µM). Altogether, the studied rivers export 8×10^6 tons/yr of dissolved major cations and 50 tons/yr of dissolved Nd towards the HJUB. Basin scale total rock cationic denudation rates (TRCDR) range from 1.0 to 5.3 tons*yr^{-1}*km^2 and are essentially controlled by lithology, as illustrated by the relationship established between rock denudation rates and the proportion of sedimentary and volcanic rocks (%S+V) within the basins: TRCDR=0.08(%S+V)+0.9. In contrast, dissolved Nd exports seem to be strongly dependent upon organic matter cycling. This is illustrated by the tight coupling between Nd and DOC fluxes. These fluxes decrease northwards, likely in response to the hydro-climatic gradient. Overall, the TRCDR evaluated within the Canadian Shield are among the lowest reported on the planet and the alkalinity generated by rock weathering remains small with respect to DOC exports.

1. INTRODUCTION

The weathering of Ca - Mg bearing silicates by carbonic acid followed by calcite precipitation in the oceans is recognized as a negative feedback mechanism regulating atmospheric pCO_2 over geological timescales (Walker et al., 1981; Berner et al., 1983). As a great proportion of the soluble ions released by the chemical weathering of surface rocks are carried through the superficial hydrographic network, the quantification of dissolved fluxes exported by rivers provides a spatiotemporally integrated response of rock denudation processes operating at the catchment scale (eg. see Gaillardet et al., 1999, and references therein). Studies focusing on riverine exports have notably shown that tectonic uplift, physical erosion, organic matter cycling, runoff, temperature and lithology influence chemical denudation rates (eg.; see Edmond et al., 1996; Huh et al., 1998; 1999; Gaillardet et al., 1999; Galy and France-Lanord, 1999; Millot et al., 2002; 2003; Dupré et al., 2003; France-Lanord et al., 2003; West et al., 2005). In addition, calculation techniques for weighting inputs from different lithological and atmospheric sources to the riverine dissolved solids (Garrels and Mackenzie, 1967; Négrel et al., 1993) and methods for evaluating the relative importance of carbonic and sulfuric acid weathering pathways (Galy and France-Lanord, 1999; Spence and Telmer, 2005; Calmels et al., 2007; Lerman et al., 2007) have been developed. A better quantification of global CO_2 consumption rates through chemical weathering therefore seems achievable, notably based on increasing data sets on chemical fluxes in large river systems (eg.; Meybeck and Ragu, 1996) and on increasingly developed global rock-weathering models (eg.: Hartmann et al., 2009). However, the documentation of chemical denudation rates in mid to high latitude Shield regions of North America is still limited. Although seasonality is a prominent feature of the hydro-climatic cycles at such latitudes, relatively few studies provide information on seasonal fluctuations in dissolved solids fluxes through catchments, adding to the uncertainty associated with the evaluation of rock denudation rates from riverine exports. Since basins set in such areas are likely to be impacted by ongoing climatic variations (Déry and Wood, 2004; Déry et al., 2005), precise information on factors controlling these rates is much needed.

Here, we document chemical denudation rates in major watersheds of the Hudson, James and Ungava bays (HJUB). The focus is on parameters governing dissolved exports through rivers, with special attention paid to seasonal variability, the role of basin lithology and the coupling between chemical weathering and organic matter (OM) cycling. Our data complement previous studies of the geochemistry of North American rivers (Yang et al., 1996; Millot et al., 2002; 2003; Gaillardet et al., 2003; Spence and Telmer, 2005) and provide new estimates of weathering rates in the Precambrian Shield and Interior Platform of Canada.

2. STUDY AREA

The physical, hydrological, climatic and geological properties of the studied watersheds are summarized in Table 1.

2.1. Hydrology and Climate

Altogether, the catchments included in this study cover more than 1.5×10^6 km^2 (Fig. 1) and account for approximately 50% of the freshwater discharge into the Hudson, James and Ungava Bays (HJUB) (Déry et al., 2005). They are set in tundra, boreal and temperate domains. The mean annual air temperature ranges from 4°C in the prairies (Southwestern region, Nelson River watershed; Déry et al., 2005) to -5.7°C in Kuujjuaq, near the outlet of the Koksoak River into Ungava Bay (Environement Canada, climatic archive database). The catchments located on the eastern shore of Hudson Bay reach maximum elevations ranging between approximately 300 m (Harricana River) and 700 m (La Grande River) whereas the Nelson River watershed reaches a maximum elevation of approximately 3000 m in its southwestern limit.

Runoff rates are lower in the southwestern portion of the study area and higher on the eastern coast of Hudson Bay. During the study period, these rates varied between 115 and 706 mm*yr^{-1}, in the Nelson River and Bell River watersheds, respectively (Table 1). Rivers of the HJUB catchments typically present hydrographs characterized by lower discharge values at the end of the freezing period followed by an increase in response to snowmelt, when the total natural freshwater discharge to the HJUB increases by a fourfold factor (Déry et al., 2005).

The Nelson and La Grande rivers present modified hydrographs in response to discharge control for hydroelectricity production. The Nelson River discharge is controlled at the outlet of Lake Winnipeg. Downstream of this point, the flow responds to water management strategies by Manitoba Hydro. Therefore, variations in dissolved solids contents and fluxes downstream of Lake Winnipeg are partly decoupled from natural hydro-climatic control. On the eastern shore of James Bay, the La Grande River and its main upstream tributary, the Laforge River, host 7 major hydroelectric reservoirs covering a total area of 13 000 km^2 (Hayeur, 2001). In its lower section, the La Grande River also receives water from the Boyd-Sakami diversion, supplying waters from southern rivers that were diverted towards the Robert-Bourassa reservoir. A review of these hydroelectric installations can be found in Hayeur (2001). At the outlet of the Robert-Bourassa reservoir, in the downstream section of

the river where one of our sampling sites was located, discharge rates are highest in winter, in response to hydroelectricity demand. Throughout the year, the river discharge responds to management strategies by Hydro-Quebec as a function of water supplies and electricity demand. In 1985, the upstream section of the Koksoak River was diverted into the Caniapiscau Reservoir, now constituting the head of the La Grande – Laforge rivers. Although the total discharge at the outlet of the Koksoak River has been reduced by approximately 30% following this diversion, the river discharge still responds to natural hydro-climatic conditions. Finally, at the Rupert River site, sampling was achieved prior to its diversion towards the La Grande hydroelectric complex.

2.2. Geological Setting

In view of the high diversity of geological units within the study area, we used the percent cover of four main lithologies based on the main rock classes of the Geological Survey of Canada Map 1860A (Wheeler et al., 1996) to characterize bedrock properties within each catchment. They include: i) sedimentary and metasedimentary rocks, ii) volcanic rocks, iii) metamorphic rocks, and iv) intrusive rocks. These values are reported in Table 1.

2.2.1. Nelson River (Interior Platform, Superior and Churchill Geological Provinces)

The Nelson River mainly drains flat-lying and undeformed Mesozoic and Paleozoic sedimentary rocks of the Interior Platform, a geological province extending from the Canadian Cordillera at its western limit to the Churchill and Superior Geological Provinces at its northern and eastern limits, respectively. Overall, fine-grained, poorly consolidated Cretaceous clastic sedimentary rocks dominate the region; mainly shales and siltstones, with narrow occurrences of Paleozoic carbonate rocks (see Stott and Aitken, 1993). In the southern area, Paleozoic clastic, carbonate and evaporite rocks lie over the Precambrian basement and are covered by Mesozoic and Tertiary clastic sedimentary rocks. Below Lake Winnipeg, the Nelson River flows along the boundary between the Archean Superior (East) and Proterozoic Churchill (West) Geological Provinces and mainly drains crystalline igneous and metamorphic rocks. Finally, in its lowermost section, near its outlet to Hudson Bay, the Nelson River flows over Paleozoic carbonate rocks of the Hudson Bay Platform.

Unconsolidated Quaternary sediments are widespread within the watershed, covering most of the Interior Platform. Clay, silt and sand mostly deposited during the last glaciation and derived from the

underlying Cretaceous and Tertiary sediments are particularly abundant (see Klassen, 1989). Clays and silts of the glacial Paleolake Agassiz are also abundant in the Lake Winnipeg area.

2.2.2. Rivers of the Eastern Hudson Bay Area (New Quebec Orogen and Superior Geological Province)

The Harricana, Bell, Rupert, Broadback, Pontax, La Grande and Great Whale rivers drain Archean (2.9-2.65 Gyr) plutonic, metamorphic and volcano-sedimentary rocks of the Superior Geological Province. Intrusive and metamorphic Archean rocks constitute the dominant lithology within these watersheds. Volcanic and metasedimentary rocks occur sporadically.

Marine sediments of the Tyrrell Sea, which replaced glacial lakes Ojibway (East) and Agassiz (West) some ~ 7 ka BP (Locat and Lefebre, 1986), are abundant in the lower altitudinal section of these watersheds, up to a maximum elevation of approximately 290 m. The fine fraction of these sediments is dominated by felsic and clay minerals. The pore waters of these sediments (35-45% by weight) have a salt content of approximately 500 mg/l (Locat and Lefebre, 1986). In the upper section of the basins, thin till deposits (generally < 2m) are widespread between glacially eroded rock surfaces. These tills are composed of material derived from igneous and metamorphic rocks of the Superior Geological Province. Carbonated tills are observed southeast of James Bay and locally at sites surrounding Proterozoic carbonates outcrops (e.g., in the Lake Mistassini area, see Vincent, 1989).

The two southernmost rivers flowing over the Superior Province, the Harricana and Bell rivers, drain extensive proportions of volcano-sedimentary rocks in the southern part of their catchments. Northward, Archean igneous and metamorphic rocks dominate, with sporadic occurrence of amphibolites and metasediments. The lower section of the Harricana and Bell rivers is also characterized by the presence of Tyrrell Sea marine deposits, often overlying sediments of paleolake Ojibway. Till is also widespread in the upstream sectors of both catchments.

The Koksoak River, which discharges into Ungava Bay, runs over plutonic and metamorphic rocks of the Superior Province in its upper section. It drains extensive areas of Paleoproterozoic (2.17 – 1.81 Gy) intrusive, volcanic and sedimentary rocks of the New Quebec Orogen within its middle and lower portions. This orogen consists in a 160 km wide geological sequence extending from Hudson Strait, in the north, to Manicouagan, in the south (See Clark, 1994 and references therein). When flowing over rocks of the New Quebec Orogen, the Koksoak River runs over an area of meta-volcanic rocks and

gabbros, flanked, east and west, by metasediments. Quaternary till deposits are widespread in the upstream section of the river whereas the lowermost section is covered with the sediments of the post-glacial Iberville Sea.

Henceforth, all rivers draining rocks of the Superior Geological Province and of the New Quebec Orogen are referred to as "Shield Rivers".

3. METHODOLOGY

3.1. Sampling Methods

Samples from the Koksoak and Great Whale rivers were collected a few kilometers upstream from their outlets, in the center of the river channel. These samples were collected in collaboration with Environment Canada. The Nelson River was sampled in the center of the main channel in proximity of the Long Spruce generating station, downstream of the Municipality of Gillam. These samples were collected in collaboration with Dr. Terry Dick (U of Manitoba). Precise sampling locations are reported Table 1. Water samples were collected approximately 30 cm below surface using a clean polypropylene container attached to a pole. During the ice-free period, samples were retrieved from a small boat. In winter, they were collected from a hole drilled in the ice, 50-100 cm below ice bottom. Samples from the La Grande River were collected at a sampling facility located within the LG2 hydroelectric dam, directly from an untreated water-supply line located ahead of the turbines, therefore directly sampling the outlet of the LG2 reservoir.

Six other rivers (Pontax, Nemiscau, Rupert, Broadback, Bell, Harricana) were sampled in August 2008 (baseflow) and may 2009 (following snowmelt) in order to provide complementary data. The samples were retrieved from bridges, rivers banks and at the outlet of hydroelectric reservoirs. Wherever samples were collected from banks (due to field constraints), sites located downstream of rapids were preferred in order to recover well-mixed waters.

Samples from the monitoring program (Koksoak, Great Whale, La Grande, Nelson) were stored in 10 liters low-density polyethylene containers and transported to the laboratory. For the rivers of the monitoring network, samples for major ions, Nd and Sr were filtered at 0.22 μM through through Millex^{TM} PES membranes within one day of collection. Samples from the field expeditions were filtered on site through 0.22 μM Millex^{TM} PES membranes. Samples for DOC were filtered through EPM-2000™ glass-fiber filters, stored in 250 ml amber-glass bottles with no head-space and kept at 4°C until analysis. Samples for major cations, Sr and Nd analyses were acidified to pH=2 with bidistilled HNO_3, stored in polypropylene bottles and kept at 4°C before analysis. A 30 ml aliquot of unacidified water was kept in HDPE bottles for water ^{2}H-^{18}O analyses. A 30 ml aliquot of unacidified filtered water was kept frozen for further anions analyses.

3.2. Analytical Methods

Whenever possible, pH and alkalinity were measured in the field. When temperature was below the freezing point or where field conditions were unfavorable, samples were brought back to the laboratory and measurements were made within a few hours of collection. Alkalinity was determined using the Gran method by adding 0.16M H_2SO_4 to 100-200 ml of sample using a Hach™ digital titrator with a precision of ±0.01 µeq/l. Major cations concentrations were measured by ionic chromatography in the *Laboratoire de Géochimie et Cosmochimie* at the *Institut de Physique du Globe de Paris (IPGP)* with a standard error of ± 5%. Anions concentrations were measured by ionic chromatography at the IPGP and at the Environment Canada laboratories in Montreal with a standard error of ± 5%. Sr and Nd concentrations were determined on a MC-ICP-MS with a standard error of 5% at the IPGP. DOC concentrations were measured at the GEOTOP laboratory (*Université du Québec à Montréal*) using a Shimadzu™ TOC-5000A and replicate measurements conducted on a natural sample (n=96) yielded a 2σ error of 10 µM.

4. RESULTS

Analytical results are presented in Table 2. Unless otherwise noted, all concentrations reported henceforth are in micromoles per liter (μM) or nanomoles per liter (nM) and represent dissolved contents ($< 0.22\ \mu M$-filtered) and all ratios are molar ratios.

4.1. Nelson River

In the Nelson River, dissolved major cations concentrations ranged between 1200 and 2277 μM. Alkalinity ranged between 1436 and 2983 $\mu eq/l$ and dissolved anions ($Cl+SO_4$) ranged between 247 and 978 μM. Dissolved Sr contents ranged between 0.64 and 1.45 μM and closely followed major cations concentrations. Nd concentrations ranged between 0.14 and 0.45 nM and followed a pattern opposite to that of major cations and Sr. DOC contents ranged between 753 and 928 μM.

4.2. Koksoak River

At this site, total dissolved cations ranged between 203 and 360 μM. Major anions ($Cl+SO_4$) ranged between 38 and 82 μM and alkalinity fluctuated between 244 and 442 $\mu eq/l$. Sr concentrations ranged between 0.21 and 0.35 μM and closely followed dissolved major cations ($r^2=0.98$). Nd concentrations varied from 0.57 to 1.12 nM without correlation with major ions. DOC ranged between 241 and 325 μM over the measurement period.

4.3. Great Whale River

Dissolved major cations at the outlet of the Great Whale River ranged between 89 and 225 μM. Alkalinity ranged between 50 and 155 $\mu eq/l$ and major anions ($Cl+SO_4$) fluctuated between 26 and 110 μM. Sr concentrations range between 0.093 and 0.225 μM and correlate positively with dissolved Ca contents ($r^2=0.88$). Nd concentrations range between 0.81 and 2.75 nM and DOC ranged between 368 and 663 μM.

4.4. La Grande River

Among the monitored sites, the La Grande River is a notable exception because of the lesser temporal variability in its dissolved cation concentrations, ranging from 73 to 88 μM. Sr concentrations ranged between 0.085 and 0.100 μM. Major anion concentrations (Cl+SO$_4$) ranged between 17 and 36 μM and alkalinity fluctuated between 27 and 62 μeq/l. Dissolved Nd contents presented small variations throughout the monitoring period, with values ranging between 0.64 and 0.87 nM. DOC ranged between 321 and 438 μM.

4.5. Other rivers of the Canadian Shield

Dissolved major cation concentrations ranged between 62 and 356 μM in the Nemiscau and Harricana rivers, respectively. In comparison with a compilation of relevant data made by Meybeck (2003), the Shield Rivers studied here are among the less concentrated rivers of the world, with $\sum$+ ranging between 94 and 579 μeq L^{-1}. These rivers presented alkalinities ranging between 14 (Pontax River) and 258 μeq L^{-1} (Harricana River). Sulfate concentrations ranged between 5 μM in the Pontax River and 84 μM in the Harricana River. Similarly, chlorine concentrations were the highest in the Harricana River (81 μM) and the lowest in the Broadback River (5 μM). Dissolved Sr concentrations ranged between 0.078 and 0.350 μM in the Pontax and Harricana rivers, respectively. Dissolved Nd concentrations varied between 0.81 and 4.72 nM in the Nemiscau and Bell rivers, respectively. DOC concentrations ranged between 421 and 1777 μM in the Rupert and Pontax rivers, respectively.

A charge imbalance was observed for most of the Shield Rivers where $(\sum+)>(\sum-)$. This is attributed to the presence of unaccounted negative charges, likely organic anions, consistent with the relatively high DOC concentrations reported here. Such excesses of positive charges have been reported elsewhere, especially in rivers characterized by very low total dissolved inorganic solids and high organic contents (Négrel et al., 1993; Edmond et al., 1995; Dupré et al., 1996; Gaillardet et al., 1997; Huh et al., 1998; Millot et al., 2002; Négrel et al., 2003; Tosiani et al., 2004).

5. DISCUSSION

5.1. Seasonal Fluctuations in Riverine Dissolved Solids

Temporal fluctuations in riverine dissolved solids depend upon a large array of variables: precipitation, atmospheric deposition, evaporation, snowmelt events, weathering and transport, tributary mixing, anthropogenic discharge control and pollution, among others. A quantitative assessment of these seasonal fluctuations is instrumental for the reduction of errors associated with estimates of geochemical fluxes exported by rivers. In addition, exploring the relationships between dissolved solids and discharge rates provides a first order evaluation of the relationships between hydro-climatic conditions and the intensity of riverine exports.

The present data provides information on temporal fluctuations in concentrations and fluxes of major ions, strontium, neodymium, DOC (Fig. 2) and their relationships with discharge rates in the four monitored rivers (Fig. 3). The use of concentrations normalized to average values (Fig. 2 and 3) allows direct comparisons between the studied catchments. The large differences in the geology and hydro-climatic properties of the watersheds (section 2), notably between those of the Canadian Shield vs that of the Interior Platform (Nelson River), prevents generalizations. Both settings will thus be discussed separately below.

5.1.1. Nelson River

Dissolved major cations, Sr and anions contents of the Nelson River follow a clear seasonal pattern, with maximum concentrations recorded during the frozen period, followed by a decrease associated with the snowmelt and a return to high values during the summer period (Fig. 2). Nd concentrations follow an opposite trend, with highest values recorded during the snowmelt period, likely in response to changes in sources and to an increased contribution from soils. In contrast, DOC contents remained fairly constant throughout the study period. This is interpreted as the result of sustained supplies from lakes and wetlands throughout the winter period when soils are frozen.

For hydroelectricity production purposes, the Nelson River discharge is controlled at the outlet of

Lake Winnipeg. The seasonal flux pattern is thus decoupled from hydro-climatic conditions, despite the clear seasonality in dissolved inorganic solids contents. For instance, during the study period, the river reached a maximum discharge rate in August in response to water management strategies by Manitoba Hydro. This strongly contrasts with natural conditions, since maximum discharge rates in this region should be observed in response to snowmelt.

5.1.2. Rivers of the Canadian Shield (Koksoak, Great Whale and La Grande)

The Koksoak and Great Whale rivers present hydrographs that respond to natural hydro-climatic conditions, with minimum discharge rates at the end of the frozen period followed by a drastic increase in response to snowmelt (see Table 2). Major cations and Sr thus display a clear seasonal pattern, with maximum concentrations during the frozen period, followed by a decrease in response to dilution during snowmelt, and a return to higher concentrations by the end of the ice-free period. Dissolved anion (SO_4+Cl) concentrations display patterns that are similar to those of major cations and Sr. Nd contents show a greater variability than major ions, likely in response to its non-conservative behavior and its association with DOC (Section 5.2). In the Koksoak River, the lowest DOC contents were measured during the frozen period, consistent with a lesser contribution from soil organic matter. However, in the Great Whale River, DOC contents remained relatively high throughout the frozen period. This seems to indicate sustained DOC supplies throughout the frozen period from the abundant lakes and wetlands present in the catchment.

Broad inverse correlations are observed between discharge rates and concentrations of major ions and Sr (Fig. 3), highlighting dilution effects resulting from changes in the hydrological regime. It is noteworthy however that at both sites, variations in discharge rates are not balanced by changes in concentrations and fluxes intensify during spring snowmelt (high flow stage). Conversely, during the frozen period, when soils and shallow pounds are frozen, water infiltration in soils is strongly reduced, discharge rates reach minimum values, and dissolved fluxes are reduced despite increases in concentrations. However, spring snowmelt occurs as a short-lived event inducing soil erosion and the export of previously weathered material. Indeed, frozen grounds and the brevity of the snowmelt event reduce any potential synchronous water-rock interactions. It is unclear whether the high dissolved solids fluxes recorded during the snowmelt event could be sustained beyond the subsequent freshwater pulse. They might simply derive from the release of water having a high total dissolved solids content formed in response to the preceding ice growth in soils.

The La Grande River differs from the Koksoak and Great Whale rivers, as its dissolved solids contents are fairly constant throughout the year. At this site, dissolved solids concentrations are completely independent of discharge rates (Fig. 3). We attribute this to a buffering effect by hydroelectric reservoirs, representing more than 100 km^3 (Hayeur, 2001), and where the residence time of water (up to six months in the Robert Bourassa reservoir; Schetagne, 1989) appears to be long enough for the smoothing of seasonal variations in dissolved solids. This could also be due to the depth of turbine intakes within the LG2 reservoir, which is within the reservoir hypolimnion, at a depth where seasonal changes in dissolved solids contents are less pronounced than at the reservoir surface. Nevertheless, any fluctuation in dissolved fluxes and concentrations measured at the La Grande River outlet will mainly depend upon water management strategies by Hydro-Quebec. One notable feature observed at this site is illustrated by maximum dissolved solids fluxes during the winter period, when turbine flows are maximized in response to the greater hydroelectricity demand. This strongly contrasts with natural conditions (as in the Great Whale and Koksoak rivers), where dissolved fluxes are usually minimized during this time period, in response to a marked decrease in discharge rates.

5.2. Dissolved Solids Exports

The elemental fluxes exported by rivers are reported in Table 3 and calculated from the product of the discharge weighted average concentration with the average discharge rate over the measurement period:

$$F = Q_{(AVG)} * [X]_{(DW-AVG)}$$
Eq. 1

F: calculated flux

$Q_{(AVG)}$: average discharge rate over the sampling period

$[X]_{(DW-AVG)}$: discharge weighted average dissolved concentration of element X

Discharge rates from the Nelson River were provided by *Manitoba Hydro* and correspond to total flow measured at the Long Spruce power station, located a few kilometers upstream of the sampling site. Discharge rates in the La Grande River were compiled by Dr. Alain Tremblay (Hydro-Québec) from non-disclosure information of Hydro-Quebec. It corresponds to the total flow measured at the outlet of the Robert-Bourassa hydroelectric reservoir. We use these data to calculate the elemental fluxes exported by the La Grande River but do not present raw discharge data. Discharge rates in the Koksoak River and in the Great Whale River (after July 2008) are based on daily measurements from the *Ministère du Développement Durable, de l'Environnement et des Parcs du Québec (MDDEP)*. For the period before July 2008, discharge rates of the Great Whale River are taken from a compilation of the *International Polar Year project* (Dr. Stephen Déry, University of Northern British Columbia). These values are averages since measurements were not performed on a daily basis by the MDDEP during this time period. In the Koksoak and Great Whale rivers, gauging stations are located upstream of the sampling sites and discharge rates have been corrected assuming that discharge along the river course is proportional to the area of the watershed drained. In the case of the Nelson and La Grande rivers, gauging stations are in proximity of sampling points and no discharge correction was required. The discharge rates presented for the Harricana, Bell, Broadback, Rupert, Nemiscau and Pontax rivers (sampled during the August 2008 and May 2009 field expeditions) are the average annual discharge rates measured at the closest MDDEP gauging stations. For consistency, the drained areas evaluated at the gauging stations were used for calculating specific fluxes (fluxes normalized to the drained area) carried by these rivers, as some were not sampled directly at their outlet (see Table 1 for exact sampling locations). The MDDEP provides discharge rates based on instantaneous flow measurements and on correlations between water level measurements and punctually measured discharge rates. Their

procedures ensure that the differences between instantaneous flow measurements and discharge rates calculations based upon water level measurements are less than 10%. Adding the analytical error and propagating it through fluxes calculations, we estimate that the error bars on calculated fluxes are of the order of 15-20% at the monitored sites. Therefore, we set 20% error bars on the calculated fluxes, which we consider realistic in view of the variability in discharge rates and dissolved solids contents. This error is likely to be higher at sites that were only sampled twice, although our data do not allow quantifying it.

The total fluxes exported by the studied rivers are reported in Table 3. The cationic fluxes range between $3,4x10^3$ and $7,1x10^6$ tons/yr in the Nemiscau and Nelson rivers, respectively. It is clear from table 3 that major cations and Sr fluxes are dominated by the inputs from the Nelson River, which alone accounts for ~ 88% of the total cationic flux exported by the studied rivers. However, dissolved Nd fluxes are dominated by rivers of the Canadian Shield and range between $2.0x10^2$ and $1.4x10^4$ kg/yr in the Nemiscau and La Grande rivers, respectively (Table 3). DOC fluxes range between $1.1x10^4$ and $1.2x10^6$ tons/yr in the Nemiscau and Nelson rivers, respectively. In terms of specific fluxes (here defined as total fluxes normalized to the watershed area), those of major cations and Sr are at a maximum in the Nelson River (Interior Platform), whereas those of Nd and DOC are at a maximum in the rivers of the Canadian Shield (Table 3). Parameters governing the intensity of these fluxes are discussed below.

5.3. Rock Denudation Rates

In the following section, we focus on evaluating rock cationic denudation rates (Na+K+Mg+Ca+Sr) based on the dissolved fluxes exported by rivers. We did not include dissolved silica in the calculations because of its non-conservative behavior (cf Viers et al., 1997; 2000; Millot et al., 2002; 2003; Spence and Telmer, 2005 and references therein).

5.3.1. Atmospheric and Marine Salts Corrections

The first step in calculating rock denudation rates on the basis of riverine dissolved fluxes involves correcting the riverine chemistry for Cl-bearing sources. Within the studied watersheds, these sources consist of atmospheric inputs (dry and wet deposition), marine salts contained in marine sediments and additionally evaporites formed under seawater evaporation within the Nelson River watershed. We assume that these sources will all present Cl-normalized elemental ratios that are similar to that of seawater. Because our data do not allow discriminating between the three categories, they are jointly labeled as "marine salts" in Table 4. We therefore correct the chemistry of all river samples for the marine salts inputs using the following approximation (eg.: see Millot et al., 2002):

$$[X]^* = [X]_{River} - [Cl]_{River} \times (X/Cl)_{Marine} \qquad \text{Eq. 2}$$

where $[X]^*$ is the concentration of element X after correction for inputs from marine salts, $[X]_{River}$ is the concentration of element X in the river before correction, $[Cl]_{River}$ is the riverine Cl content and $(X/Cl)_{Marine}$ is the Cl-normalized molar ratio of element X in seawater. In the absence of adequate measurements of average precipitation chemistry and evaporites compositions at the scale of the study area, we conclude that using the above approximation yields the most realistic estimates of contributions from Cl-bearing sources.

The riverine fluxes corrected for marine salts inputs are calculated by applying Eq. 1 to the elemental concentrations (Mg+Ca+Na+K+Sr) corrected for marine salts inputs. Calculated values are reported in Table 4. The above calculations reveal that the Canadian Shield rivers are significantly affected by supplies from marine salts, contributing as much as 23% of the dissolved cations exports carried by the Great Whale River on a yearly average basis. The importance of such atmospheric supplies to riverine dissolved loads was already highlighted in other regions of the Canadian Shield (Millot et al., 2002). In

the Nelson River 18% of the cationic dissolved load is derived from the marine salt component described above, mainly reflecting inputs from evaporites that sparsely occur within the Canadian Interior Platform.

5.3.2. Controls on Total Rock Cationic Denudations Rates in the HJUB Watershed

Once corrected for marine salts inputs, it is assumed that the dissolved loads carried by rivers are entirely inherited from rock weathering (including the weathering of unconsolidated sediments). The denudation rates are referred to as total rock cationic (Mg+Ca+Na+K+Sr) denudation rates (TRCDR), the values calculated for each basin are reported in tons km^{-2} yr^{-1} (Table 4). The calculated TRCDR range between 1.0 and 5.6 Tons km^{-2} yr^{-1} in the Nemiscau and Harricana river basins, respectively. Table 5 allows a comparison with chemical denudation rates calculated in other North American basins.

The data indicate that within the HJUB region, basin-scale TRCDR are essentially controlled by basin lithology. For instance, the calculated TRCDR systematically increase as a function of the proportion of volcanic and sedimentary rocks (% Sed.+Volc) within the catchments (Fig. 4). If such an observation could have been intuitively predicted, the interest of the data presented in Fig. 4 rests in the quantitative relationship that is established:

$$TRCDR \ (Tons \ km^{-2} \ yr^{-1}) = 0.08(\% \ Sed.+Volc) + 0.9 \qquad\qquad Eq. \ 3$$

Although tectonic uplift, physical erosion, runoff and temperature, among others, have been reported as parameters influencing TRCDR in different settings (eg.; see Edmond et al., 1996; Huh et al., 1998; Gaillardet et al., 1999; Galy et France-Lanord, 1999; Millot et al., 2002; 2003; Dupré et al., 2003; France-Lanord et al., 2003; West et al., 2005), our data do not allow highlighting the effects of these parameters. For instance, rock denudation rates do not depict any clear relationship with runoff or latitude, suggesting that within the study region, the hydro-climatic control is obscured by the effect of lithology.

Nevertheless, some observations still point towards a climatic control on weathering rates. For instance, as discussed in section 5.1, dissolved solids fluxes are reduced during the ice-on period and it seems reasonable to propose that the duration of the frozen season is likely to affect average rock denudation rates within the study region (i.e. shorter ice-on seasons would likely result in increased

average rock denudation rates). Therefore, a reduction of the ice-on period duration within the HJUB due to climatic variations, as pointed out by Déry et al (2005), could result in increased denudation rates within the HJUB.

Overall, the TRCDR calculated for the HJUB remain low in comparison to rock denudation rates reported for other regions of the planet (eg.: see Gaillardet et al., 1999). It is also clear from Table 2 that within the Canadian Shield region, the alkalinity generated by rock weathering remains small with respect to DOC contents. Therefore, organic carbon dynamics are more important than rock weathering in the role of these rivers in the global carbon budget.

5.3. The Role of Organic Matter Cycling on Denudation Rates

Within the HJUB area, TRCDR are decoupled from DOC exports, revealing that the influence of organic matter (OM) cycling on TRCDR is weak with respect to the prominent lithological control. If this is true for the conservative major cations used for establishing rock weathering budgets, it might not apply for trace elements showing affinities for colloidal OM. Notably, the affinity between lanthanides and organic substances has been reported (ex.: Dupré et al., 1999). One noticeable example is that of the Kalix River (Sweden), where ultrafiltration experiments revealed that most of lanthanide-load is carried by organic and Fe-rich colloids (Ingri et al., 2002). Similarly, Millot et al (2003) reported a close relationship between dissolved Nd and DOC concentrations in the rivers of the Mackenzie Basin. Here, we document the influence of OM cycling on riverine inorganic exports based on an assessment of dissolved (i.e. < 0.22 μm) Nd dynamics.

Among the studied rivers, overall higher Nd contents are reported in the low-pH rivers of the Canadian Shield. This is consistent with the increased mobility of lanthanides in low-pH conditions, as commonly reported (Goldstein and Jacobsen, 1988a; 1988b; Gaillardet et al., 1997; 2003; Ingri et al., 2000; Deberdt et al., 2002). Considering the hypothesis of a pH-controlled Nd-mobility, it would be reasonable to infer that Nd exports should be, at least partly, dependent upon basin lithologies through their incidence on riverine pH. However, within the HJUB catchments, Nd fluxes are decoupled from rock denudation rates and rather strongly correlated to DOC exports. This leads us to conclude that Nd exports primarily respond to OM cycling, rather than to basin lithology.

The correlation observed in Figure 5 also reveals that the parameters dictating DOC exports within the HJUB basins are likely to control (at least indirectly) the mobility of lanthanides. The data tend to indicate that hydrology and climate together modulate the exports of DOC from the watersheds of the HJUB region (Fig. 6). Overall, DOC specific fluxes are highest in the watersheds of the Canadian Shield located on the eastern shore of James and Hudson bays, where runoff rates reach higher values than those of the Nelson River. This is likely attributable to higher soil weathering rates and lower organic matter oxidation rates under the wetter conditions encountered in the Canadian Shield. The low-pH conditions encountered in the Canadian Shield region might also favor the export of DOC. In addition, DOC exports tend to decrease northwards (Fig. 6). This is attributed to the latitudinal gradient in vegetation cover and soil maturity, with more forested catchments and more developed soils in the southern portion of the study area (boreal Shield ecozone) and a gradual transition towards a sparser vegetation cover with poorly developed soils northwards (taiga Shield ecozone). If characterizations of riverine DOC contents may be required to better constrain its sources, age and mobilization pathways, the data available here still allows us to highlight the influence of hydro-climatic conditions on DOC exports, at least within the study area. In comparison, Hudon et al (1996) evaluated a general positive correlation between runoff rates and DOC exports in rivers of the Quebec Province, over a region presenting a greater gradient in runoff values.

Nevertheless, it should be kept in mind that the Nd fluxes reported in Table 3 represent continental exports, and not the fluxes truly reaching the oceanic domain. For instance, Goldstein and Jacobsen (1988) reported that as much as 70% of the light and 40% of the heavy rare earth elements are removed from solution through estuarine mixing at the outlet of the Great Whale River.

6. CONCLUSION

The aim of this paper was to document chemical denudation rates in major watersheds of the Hudson, James and Ungava bays (HJUB). The focus was set on parameters governing dissolved exports through rivers, with special attention paid to seasonal variability, basin lithology and the coupling between dissolved solids exports and organic matter cycling.

Seasonal fluctuations in dissolved major ions and Sr concentrations respond to seasonal hydroclimatic variations, with overall higher concentrations throughout the frozen period and a dilution in response to snowmelt. Contrastingly, hydroelectric impoundment and flow control structures damp the seasonal variations in the La Grande River. In rivers that are not affected by hydroelectric impoundment, dissolved major cations fluxes are reduced during the ice-on period. Therefore, a reduction in the duration of the ice-on period in response to climate change (cf.: Déry et al., 2005) would likely result in an increase in rock denudation rates in the HJUB.

Altogether, the studied rivers export 8×10^6 tons/yr of dissolved major cations and 50 tons/yr of dissolved Nd towards the HJUB. Total rock denudation rates are essentially controlled by basin lithology, as exemplified by the relationship established between rock denudation rates and the abundance of volcanic and sedimentary rocks within the basins. Contrastingly, Nd fluxes are decoupled from rock denudation rates and respond to organic matter cycling. Hydrology and climate together seem to modulate the exports of DOC from the watersheds of the HJUB region. Higher runoff rates appear to increase soil weathering rates and decrease organic matter oxidation, yielding higher riverine DOC exports in the Canadian Shield region in comparison to the Interior Platform. In addition, there is a latitudinal gradient in the intensity of riverine DOC exports within the Canadian Shield, with decreasing exports northwards. This is attributed to the latitudinal gradient in vegetation cover and soil development observed over the study region.

We stress that there is a need for river monitoring in order to reduce the error bars associated with fluxes calculations, especially in rivers set in regions undergoing strong seasonal hydro-climatic variations and at sites affected by flow control structures where discharge – concentrations relationships are modified. If the geochemical signal carried by rivers provides an integrated response to hydro-climatic forcing and anthropogenic influence within catchments, documenting the seasonal fluctuations in riverine dissolved solids might be critical for anticipating river evolution in the context of climate change.

Table 1. Watersheds characteristics.

River	Sampling Site (Lat / long) (deci. deg)	Watershed area (km2)	Mean annual discharge (m3/s)	Runoff (µM/yr)	Intrusive rocks (%)	Metamorphic rocks (%)	Sedimentary rocks (%)	Volcanic rocks (%)
Bell	49.769 / 77.627	22200	497	706	50	19	0	31
Broadback	51.185 / 77.465	17100	367	677	60	25	1	14
Great Whale	55.279 / 77.650	42700	676	499	99	0	0	1
Harricana	48.790 / 78.013	3680	70	604	23	23	3	50
Koksoak	58.029 / 68.475	94311	1600	535	68	1	20	10
La Grande	53.781 / 77.530	177678	3808	676	69	26	2	3
Nelson	56.685 / 93.790	1100000	4024	115	9	0	90	1
Nemiscau	51.688 / 75.825	3015	53	549	N/A	N/A	N/A	N/A
Pontax	51.733 / 77.383	6020	111	579	57	38	1	5
Rupert	51.353 / 77.423	40900	848	654	51	28	17	4

Rock cover (%) calculated from Geological Survey of Canada map 1860A. Runoff values calculated as mean annual discharge normalized to watershed area. See text for discharge rates and watershed area references.

Table 2. Analytical results. (continued on next page)

Site	#	Date	Q (m3/s)	pH	Alk. (μeq/l)	DOC (μM)	Na (μM)	K (μM)	Mg (μM)	Ca (μM)	Sr (μM)	Cl (μM)	SO4 (μM)	Nd (nM)
Koksoak	1	03/02/09	301	7.19	339	288	50	10	76	124	0.23	25	31	0.74
Koksoak	1	17/3/2009	194	7.15	442	258	65	14	105	151	0.33	29	38	0.60
Koksoak	1	06/04/09	181	7.12	440	241	77	14	111	158	0.35	51	31	0.57
Koksoak	1	29/6/2009	5068	7.21	262	309	32	8	67	96	0.21	14	24	0.57
Koksoak	1	31/8/2009	1792	7.33	280	271	57	9	73	102	0.22	26	21	0.60
Koksoak	1	05/10/09	1501	7.3	244	325	49	10	66	89	0.21	NA	NA	1.12
GW	2	24/9/2007	852	6.23	63	641	52	8	19	43	0.11	38	10	2.75
GW	2	21/10/2007	874	6.46	66	413	33	6	13	37	0.09	19	9	1.2
GW	2	12/02/08	230	6.13	66	485	53	9	17	47	0.12	32	13	1.45
GW	2	12/03/08	179	6.62	137	663	112	13	30	70	0.19	87	23	1.89
GW	2	14/4/2008	153	6.53	155	518	85	22	19	55	0.15	63	14	1.39
GW	2	11/05/08	602	6.65	81	586	82	12	25	49	0.12	75	12	2.67
GW	2	18/6/2008	1254	6.66	51	438	35	6	13	37	0.09	19	9	1.21
GW	2	15/7/2008	716	6.84	50	385	36	6	14	37	0.1	17	9	1.00
GW	2	17/8/2008	581	6.68	88	368	35	6	14	44	0.1	17	9	0.81
GW	2	15/10/2008	884	6.51	71	539	60	9	21	43	0.12	62	41	2.29
GW	2	05/01/09	404	6.63	84	476	43	16	16	42	0.11	38	14	1.13
GW	2	02/02/09	285	6.78	118	512	57	11	22	56	0.16	36	19	1.51
GW	2	02/03/09	208	6.87	107	402	48	9	19	47	0.14	30	17	1.01
GW	2	06/04/09	186	6.95	146	662	82	15	31	70	0.22	62	22	2.06
GW	2	11/05/09	341	6.36	88	591	72	15	22	46	0.14	56	24	2.21
GW	2	08/06/09	1428	6.59	69	508	45	7	15	36	0.11	37	22	2.04
GW	2	13/7/2009	1228	6.78	93	438	44	7	19	44	0.12	28	17	1.67
GW	2	21/9/2009	714	7.08	95	458	60	8	22	48	0.13	33	10	2.37
La Grande	3	10/09/07	n.d.i.	6.60	48	409	28	8	13	29	0.09	11	10	0.70
La Grande	3	02/11/07	n.d.i.	6.30	43	365	30	8	13	28	0.09	25	11	0.76
La Grande	3	12/12/07	n.d.i.	6.45	46	335	30	8	13	29	0.09	15	11	0.87
La Grande	3	16/1/2008	n.d.i.	6.10	43	321	28	8	13	28	0.09	11	10	0.81
La Grande	3	07/04/08	n.d.i.	5.64	27	395	29	7	13	26	0.09	14	10	0.83
La Grande	3	22/5/2008	n.d.i.	6.50	47	417	28	7	12	26	0.09	9	10	0.84
La Grande	3	30/6/2008	n.d.i.	6.64	43	411	30	8	13	27	0.09	10	9	0.69
La Grande	3	01/08/08	n.d.i.	6.46	47	401	29	8	13	29	0.09	9	9	0.78
La Grande	3	16/8/2008	n.d.i.	6.54	57	438	30	8	14	37	0.09	8	10	0.77
La Grande	3	28/9/2008	n.d.i.	6.53	53	377	26	6	11	31	0.09	9	10	0.75
La Grande	3	02/12/08	n.d.i.	6.32	49	399	27	7	12	28	0.09	9	10	0.83

Site		Date	Q (m3/s)	pH	Alk. (µeq/l)	DOC (µM)	Na (µM)	K (µM)	Mg (µM)	Ca (µM)	Sr (µM)	Cl (µM)	SO4 (µM)	Nd (nM)
La Grande	3	29/1/2009	n.d.i.	6.52	62	371	28	7	13	32	0.09	8	10	0.84
La Grande	3	14/5/2009	n.d.i.	6.23	39	352	27	7	15	32	0.09	8	10	0.64
La Grande	3	25/5/2009	n.d.i.	6.39	39	368	28	7	15	29	0.1	7	10	0.73
Pontax	4	15/8/2008	111*	5.70	14	1777	41	7	19	35	0.13	39	5	4.09
Pontax	4	24/5/2009	111*	6.10	27	971	31	7	13	22	0.08	10	7	2.04
Nemiscau	5	22/8/2008	53*	6.12	22	568	24	6	8	24	0.08	7	10	0.81
Nemiscau	5	27/5/2009	53*	6.06	30	539	26	7	9	26	0.09	7	11	0.86
Rupert	6	15/8/2008	848*	6.94	103	573	25	6	29	48	0.09	32	12	1.22
Rupert	6	24/5/2009	848*	6.84	104	521	25	6	25	41	0.09	7	11	1.1
Broadback	7	15/8/2008	367*	6.70	81	886	30	7	21	45	0.11	6	11	2.54
Broadback	7	24/5/2009	367*	6.93		855	37	9	27	52	0.13	9	12	2.34
Bell	8	15/8/2008	497*	6.40	80	1718	38	9	31	65	0.16	8	15	4.72
Bell	8	24/5/2009	497*	6.62	73	1156	37	10	29	52	0.14	9	16	3.55
Harricana	9	14/8/2008	70*	7.12	258	1366	112	21	68	154	0.35	81	84	3.52
Harricana	9	24/5/2009	70*	6.92	210	1239	111	21	71	138	0.34	63	80	3.97
Nelson	10	30/9/2007	3696	8.07	1854	864	439	44	372	679	0.94	279	160	0.36
Nelson	10	05/11/07	4421	7.86	1986	753	544	53	426	718	1.1	356	210	0.29
Nelson	10	03/12/07	3855	7.87	2146	812	655	61	489	794	1.16	729	249	0.35
Nelson	10	04/03/08	4154	7.93	2983	928	591	62	557	1066	1.45	492	211	0.27
Nelson	10	07/04/08	3961	8.06	2038	793	644	63	465	731	1.24	451	252	0.24
Nelson	10	12/05/08	3541	7.92	2186	755	567	56	421	679	1.11	387	219	0.33
Nelson	10	09/06/08	3397	7.95	1436	793	263	31	288	618	0.64	164	83	0.45
Nelson	10	08/07/08	4041	8.11	1750	780	525	52	400	680	1.03	357	197	0.17
Nelson	10	11/08/08	5229	8.16	2155	764	661	61	452	703	1.22	483	263	0.15
Nelson	10	15/9/2008	4647	8.42	2025	816	676	63	456	716	1.15	483	251	0.14

GW stands for Great Whale River. The # correspond to those reported in Fig. 1. The "*" denotes mean annual discharge rates at the closest gauging stations in some rivers. See text for details. The instantaneous (i.e. daily) discharge rates of the La Grande River are non-disclosure information (n.d.i.) provided by Hydro-Quebec.

** Complete table on two pages**

Table 3. Riverine dissolved solids exports.

Watershed	Cationic flux[1] $(T*yr^{-1})$	Cationic flux $(T*yr^{-1}*km^{-2})$	DOC flux $(T*yr^{-1})$	DOC flux $(T*yr^{-1}*km^{-2})$	Nd Flux $(kg*yr^{-1})$	Nd Flux $(kg*yr^{-1}*km^{-2})$
Koksoak	$3.5X10^5$	3.8	$1.8X10^5$	1.9	$4.9X10^3$	0.05
Great Whale	$7.7X10^4$	1.8	$1.3X10^5$	2.9	$5.4X10^3$	0.13
La Grande	$2.9X10^5$	1.7	$5.4X10^5$	3.1	$1.4X10^4$	0.08
Pontax	$9.2X10^3$	1.5	$5.8X10^4$	9.6	$1.5X10^3$	0.26
Nemiscau	$3.4X10^3$	1.1	$1.1X10^4$	3.7	$2.0X10^2$	0.07
Rupert	$8.8X10^4$	2.2	$1.8X10^5$	4.3	$4.5X10^3$	0.11
Broadback	$4.2X10^4$	2.5	$1.2X10^5$	7.1	$4.1X10^3$	0.24
Bell	$6.8X10^4$	3.1	$2.7X10^5$	12.2	$9.4X10^3$	0.42
Harricana	$2.4X10^4$	6.6	$3.5X10^4$	9.4	$1.2X10^3$	0.33
Nelson	$7.1X10^6$	6.4	$1.2X10^6$	1.1	$4.9X10^3$	0.004

[1]Cationic flux stands for (Na+K+Mg+Ca+Sr). The error bars on fluxes are of the order of 20% (see text for details).

Table 4. Marine salts contributions and total rock cationic denudation rates.

	Total cationic flux[1] $(T*yr^{-1})$	Cationic flux corrected for marine salts inputs $(T*yr^{-1})$	Marine salts contribution to dissolved cationic load (%)	TRCDR $(T*yr^{-1}*km^{-2})$
Koksoak	$3.5X10^5$	$3.3X10^5$	7	3.5
Great Whale	$7.7X10^4$	$5.9X10^4$	23	1.4
La Grande	$2.9X10^5$	$2.6X10^5$	12	1.4
Pontax	$9.2X10^3$	$7.2X10^3$	22	1.2
Nemiscau	$3.4X10^3$	$3.1X10^3$	8	1.0
Rupert	$8.8X10^4$	$7.6X10^4$	13	1.9
Broadback	$4.2X10^4$	$4.0X10^4$	5	2.3
Bell	$6.8X10^4$	$6.4X10^4$	5	2.9
Harricana	$2.4X10^4$	$2.1X10^4$	16	5.6
Nelson	$7.1X10^6$	$5.8X10^6$	18	5.3

[1]Total cationic fluxes are from Table 3.

Table 5. Comparison of North American denudation rates.

	Total rock cationic denudation rate $(T*yr^{-1}*km^{-2})$	Silicate denudation rate $(T*yr^{-1}*km^{-2})$	Carbonate denudation rate $(T*yr^{-1}*km^{-2})$
Canadian Shield (superior Province)[1]	1.0 – 5.6	N/A	N/A
Canadian Shield (New Quebec Orogen)[1]	3.5	N/A	N/A
Interior platform (Nelson Basin)[1]	5.3	1.35	3.59
Western Canadian orogenic belt[2]	8.7 – 15.9	4.1 - 5.0	4.50 - 10.90
Slave Province[3]	N/A	0.12 - 0.72	N/A
Canadian Shield (Grenville Province)[3]	N/A	0.78 - 2.88	N/A
Rocky and Mackenzie mountains[4]	5.3 – 58.6	0.13 - 1.11	4.31 - 57.97
Interior platform (Mackenzie basin)[4]	3.7 - 16.8	0.57 - 4.33	2.43 - 16.13

[1] This study
[2] Gaillardet et al., 2003; Spence and Telmer, 2005.
[3] Millot et al., 2002.
[4] Millot et al., 2003.

Figure 1: Study area.
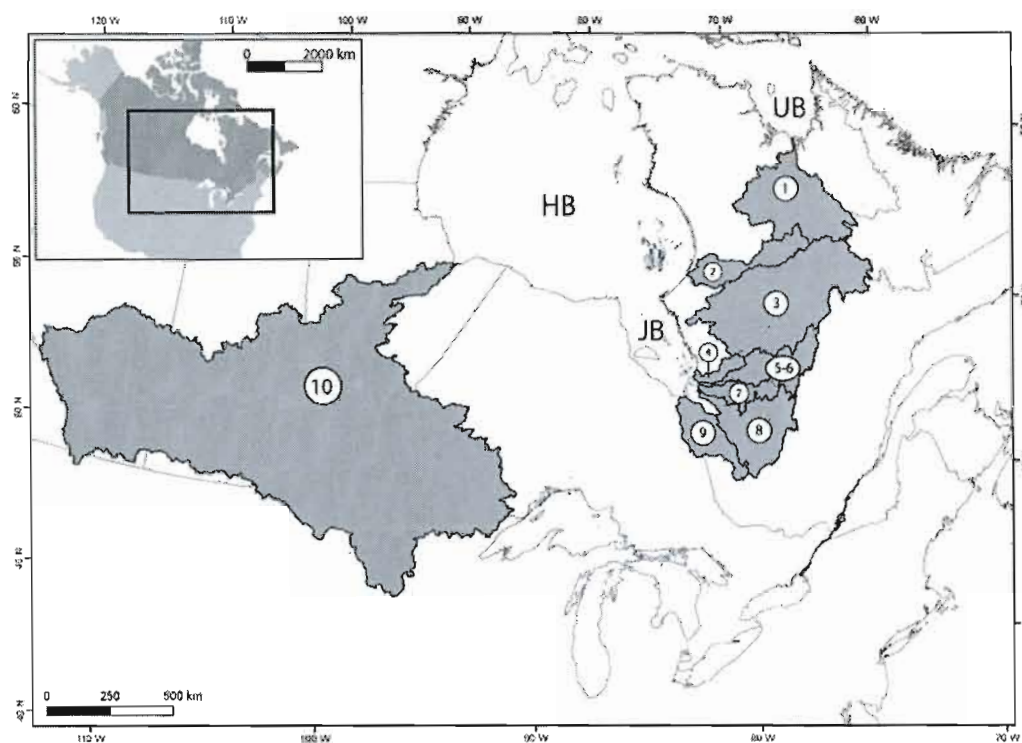
Map of the studied watersheds. HB, JB and UB stand for Hudson Bay, James Bay and Ungava Bay, respectively, together constituting the HJUB. Studied rivers are numbered as follows: 1-Koksoak, 2-Great Whale, 3-La Grande, 4-Pontax, 5-6-Rupert-Nemiscau, 7-Broadback, 8-Bell, 9-Harricana and 10-Nelson. See table 1 for watersheds characteristics and the exact location of sampling sites.

Figure 2: time series recorded at the monitored sites.
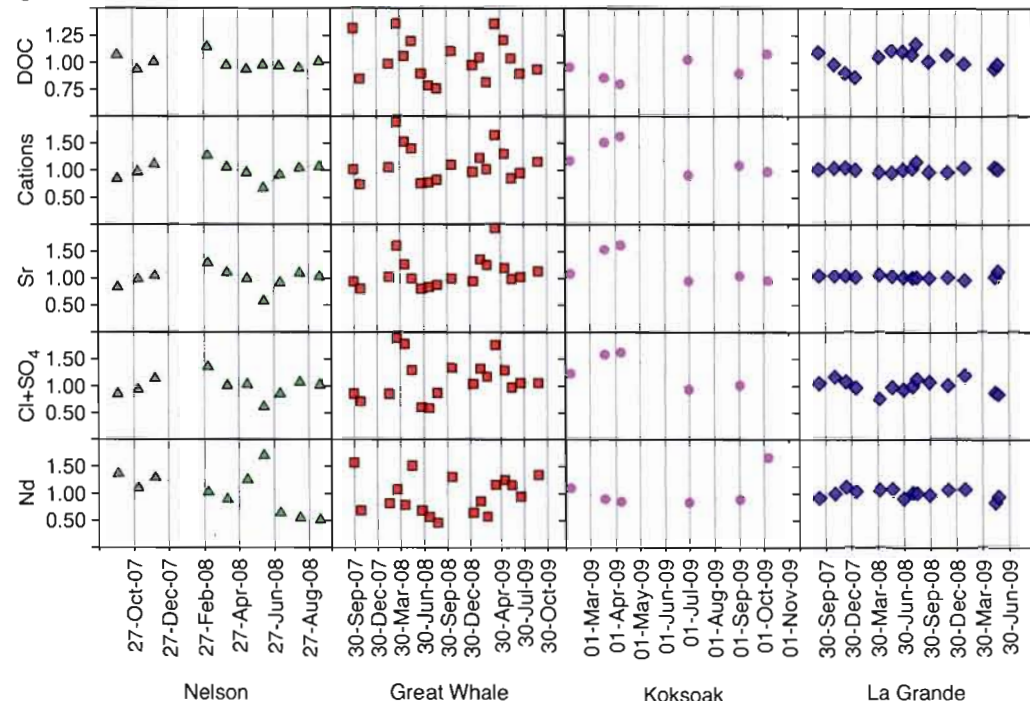
Seasonality in dissolved solids contents at the monitored sites. On the Y-axis, relative concentrations (normalized to the discharge weighted average value at each site) are reported, allowing a direct comparison between the different sites. Cations stands for Na+K+Mg+Ca. Except for the La Grande River dissolved major ions and Sr concentrations follow a predictable seasonal pattern, with highest concentration during the frozen period followed by a dilution induced by snowmelt. DOC and dissolved Nd show more variability. In the La Grande River, dissolved major ions, Sr and Nd concentrations are remarkably stable throughout the year due to the long residence time of water in hydroelectric reservoirs. At this site, DOC shows some variability in response to oxidation within reservoirs. (See text for details).

Figure 3: Relationships between dissolved solids contents and discharge.
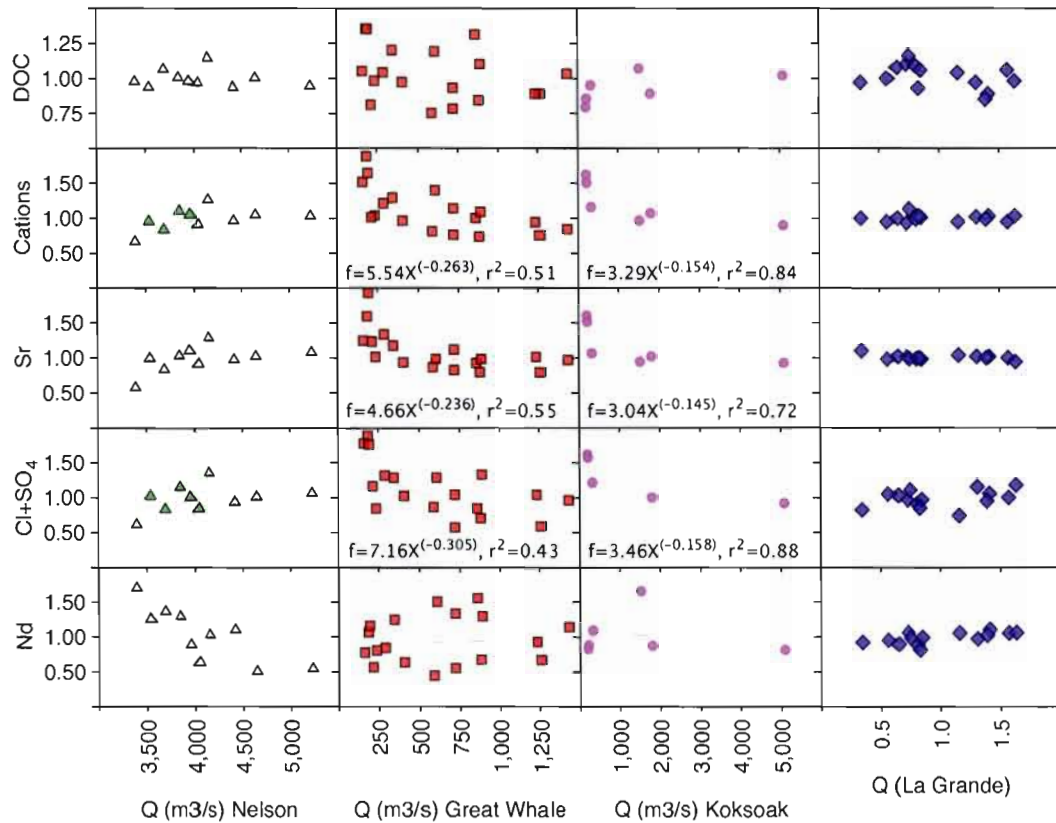
Relationships between dissolved solids concentrations and discharge at the monitored sites. Discharge rates (X axis) are in absolute values (m^3/s) whereas the concentrations (Y axis) are normalized to the discharge weighted average value for each site, allowing direct comparisons. For the La Grande River, we report average normalized discharge rates on the X-axis because discharge rates are non-disclosure information from Hydro-Quebec. Cations stands for Na+K+Mg+Ca. Regression curves (power laws) are shown in each graph but equations are only reported when $r^2>0.4$. (see text for details).

Figure 4. Total rock denudation rates reported as a function basin lithology.
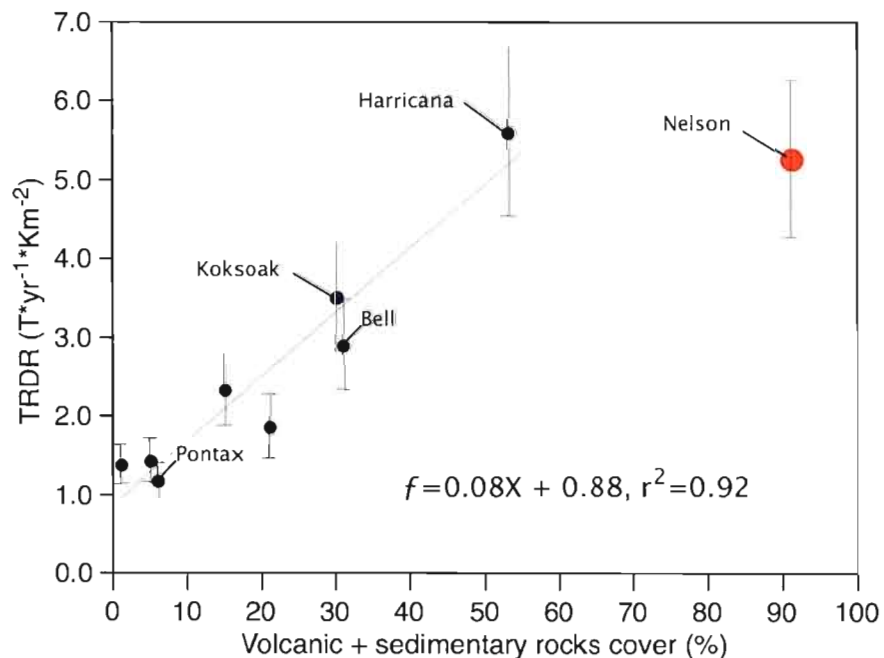
Within the Canadian Shield region, total rock denudation rates (TRDR) appear to respond to a lithological control, with increasing denudation rates as a function of the proportion of volcanic and sedimentary rocks within the basins. This lithological control buffers the potential effects of hydroclimatic conditions on rock denudation rates within the study area (see text for details).

Figure 5. DOC and dissolved Nd coupling.
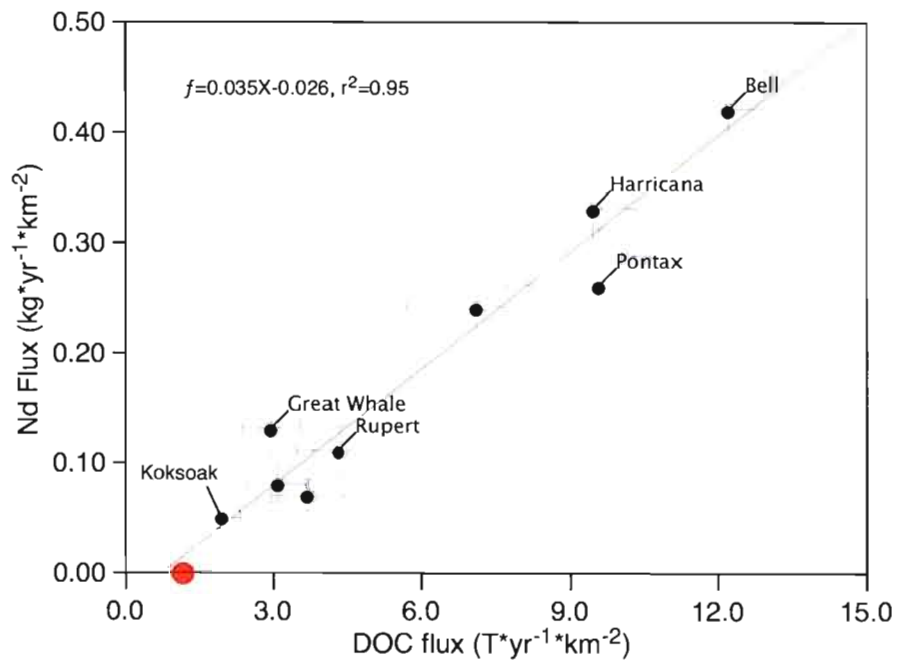
Nd vs DOC specific fluxes. The red dot represents the Nelson River; rivers of the Canadian Shield are depicted by black dots. The close correlation between Nd and DOC exports appears to reflect the influence of OM cycling on the mobility of lanthanides (see section 5.3).

Figure 6. Hydro-climatic gradient in DOC specific fluxes in the Canadian Shield.
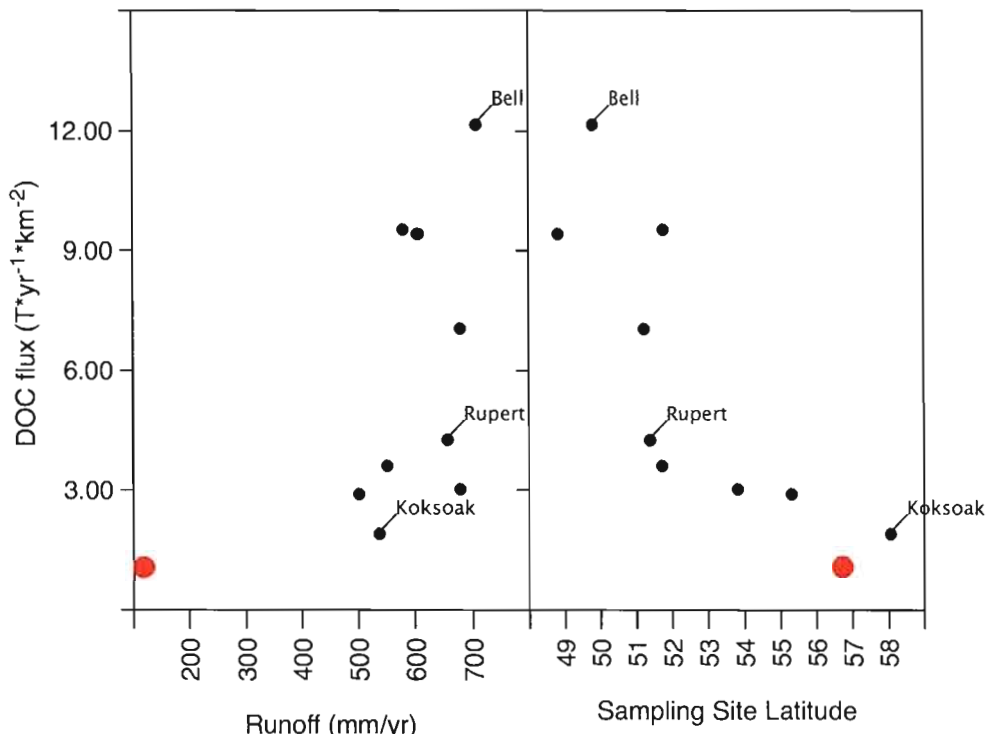
DOC specific fluxes reported against runoff and latitude (at the sampling site) for the rivers of the Canadian Shield black dots). The Nelson River is also reported (red dot). Overall higher DOC exports are reported in the rivers of the Canadian Shield that are also characterized by higher runoff values in comparison to the Interior Platform region (Nelson River). Among the rivers of the Canadian Shield, the general inverse correlation between DOC specific fluxes and latitude likely responds the latitudinal gradient in vegetation cover and soil development within the study area.

REFERENCES

Anderson S.P., Drever J.I., Frost C.D., Holden P. (2000). Chemical weathering in the foreland of a retreating glacier. *Geochimica et Cosmochimica Acta* **64**, 1173-1189.

Arctic RIMS, A Regional, Integrated Hydrological Monitoring System for the Pan-Arctic Land Mass. http://rims.unh.edu/

Berner R.A., Lasaga A.C., Garrels, R.M. (1983). The carbonate – silicate geochemical cycle and its effect on atmospheric carbon dioxide over the past 100 million years. *American Journal of Science* **284**, 1183 – 1192.

Calmels D., Gaillardet J., Brenot A., France-Lanord C. (2007). Sustained sulfide oxidation by physical erosion processes in the Mackenzie River basin: Climatic perspectives. *Chemical Geology* **35**, no 11, 1003-1006.

Clark T. (1994). Géologie et gîtes de l'Orogène du Nouveau Québec et de son arrière-pays. In *Géologie du Québec*, Les publications du Québec, pp.47-65.

Deberdt S., Viers J., Dupré B. (2002). New insights about the rare earth elements (REE) mobility in river water. *Bulletins de la Société Geologique de France* **173**, no 2, 147-160.

Déry S.J., Wood E.F. (2004). Teleconnection between the Arctic Oscillation and Hudson Bay river discharge. *Geophysical Research Letters* **31**, L18205.

Déry S.J., Stieglitz M., McKenna E.C., Wood E.F. (2005). Characteristics and Trends of River Discharge into Hudson, James and Ungava Bays, 1964-2000. *Journal of Climate* **18**, 2540-2557.

Dessert C., Dupré B., Gaillardet J., François L.M., Allègre C.J. (2003). Basalt weathering laws and the impact of basalt weathering on the global carbon cycle. *Chemical Geology* **202**, 257-273.

Dupré, B., Gaillardet, J., Rousseau D., Allègre, C.J. (1996). Major and trace element of river-borne material: the Congo Basin. *Geochimica et Cosmochimica Acta* **60**, 1301-1321.

Dupré B., Viers J., Dandurand J. L., Polve M., Bénézeth P., Vervier P., Braun J.-J. (1999). Major and trace elements associated with colloids in organic-rich river waters: Ultrafiltration of natural and spiked solutions. *Chemical Geology***160**, 63–80.

Dupré B., Dessert C., Oliva P., Goddéris Y., Viers J., François L., Millot R., Gaillardet J. (2003). Rivers, chemical weathering and Earth's climate. *Comptes Rendus de Geosciences* **335** (16), 1141-1160.

Ebelmen J.J. (1845). Sur le produit de la décomposition des espèces minérales de la famille des silicates: *Annales des Mines*, v. 7, p. 3–66.

Edmond J.M., Palmer M.R., Measures C.l., Grant B., Stallard R.F. (1995). The fluvial geochemistry and denudation rate of the Guayana Shield in Venezuela, Columbia and Brazil. *Geochimica et Cosmochimica Acta* **59**. 3301-3325.

Edmond J.M., Palmer M.R., Measures C.I., Brown E.T., Huh Y. (1996). Fluvial geochemistry of the eastern slope of the northeastern Andes and its foredeep in the drainage of the Orinoco in Columbia and Venezuela. *Geochimica et Cosmochimica Acta* **60,** 2949-2976.

Environment Canada, climatic archive database: http://climate.weatheroffice.gc.ca/climateData

France-Lanord C., Evans M., Hurtrez J.E., Riotte J. (2003). Annual dissolved fluxes from central Nepal Rivers: budget of chemical erosion in the Himalayas. *Compte Rendus Geoscience* **335,** 1131-1140.

Gaillardet J., Dupré B., Allègre C.J. (1995). A global geochemical mass budget applied to the Congo Basin rivers: erosion rates and continental crust composition. *Geochimica et Cosmochimica Acta* **59** no. 17 , 3469 – 3485.

Gaillardet J., Dupré B., Allègre C.J., Négrel P. (1997). Chemical and physical denudation in the Amazon river basin. *Chemical Geology* **142,** 141 – 173.

Gaillardet J., Dupré B., Louvat P., Allègre C.J. (1999). Global silicate weathering and CO_2 consumption rates deduced from the chemistry of large rivers. *Chemical Geology* **159,** 3–30.

Gaillardet J., Millot R., and Dupré B. (2003) Chemical denudation rates of the western Canadian orogenic belt: The Stikine terrane. *Chemical Geology* **201,** 257–259.

Gaillardet J., Viers J., Dupré B. (2003). Trace elements in river waters. In: *Treatise on Geochemistry (Eds H. D. Holland and K. K. Turekian). Vol. 5, Surface and ground water, weathering and soils (Ed J. I. Drever)*, pp. 225–272.

Galy A., France-Lanord C. (1999). Weathering processes in the Ganges-Brahmaputra basin and the riverine alkalinity budget. *Chemical Geology* **159,** 31– 60.

Garrels R.M., Mackenzie F.T. (1967). Origin of the chemical compositions of some springs and lakes. In *Equilibrium Concepts in Natural Water Systems* (ed. W. StuµM), pp. 222–242.

Goldstein S.J., Jacobsen, S.B. (1988a). REE in the Great Whale River estuary, northwest Quebec. *Earth and planetary Sciences Letters* **88**: 241-252.

Goldstein S.J., Jacobsen, S.B. (1988b). Rare earth elements in river waters. *Earth and Planetary Science Letters* **89**, 35-47.

Hartmann J., Jansen N., Dürr H.H., Kempe S., Köhler P. (2009). Global CO_2-consumption by chemical weathering: What is the contribution of highly active weathering regions? *Global and Planetary Change* **69**, 185-194.

Hayeur G. (2001). Synthèse des connaissances environnementales acquises en milieu nordique de 1970 à 2000. Montréal, Hydro-Québec. 110pp.

Hocq M. (1994). La Province du Supérieur. In *Géologie du Québec*, Les publications du Québec, pp. 7-20.

Hudon C., Morin R., Bunch J., Harland R. (1996). Carbon and nutrient output from the Great Whale River (Hudson Bay) and a comparison with other rivers around Quebec. *Canadian. J. Fish. Aquat. Sci.* **53**, 1513–1525.

Huh Y., Panteleyev G., Babich D., Zaitsev A., Edmond J. M. (1998). The fluvial geochemistry of the rivers of Eastern Siberia: II. Tributaries of the Lena, Omoloy, Yana, Indigirka, Kolyma and Anadyr draining the collisional/accretionary zone of the Verkhoyansk and Cherskiy ranges. *Geochimica et Cosmochimica Acta* **62**, 2053-2075.

Huh Y., Edmond J.M. (1999). The fluvial geochemistry of the rivers of Eastern Siberia: III. Tributaries of the Lena and Anabar draining basement terrain of the Siberian Craton and the Trans-Baikal Highlands. *Geochimica et Cosmochimica Acta* **63,** 967–987.

Ingri J., Widerlund A., Land M., Gustafsson Ö, Ardersson P., Öhlander B. (2000). Temporal variations in the fractionation of the rare earth elements in a boreal river; the role of colloidal particles. *Chemical Geology* **166**, 23-45.

Klassen K.W. (1989). Quaternary Geology of the southern Canadian Interior Plains. In Chapter 2 of *Quaternary Geology of Canada and Greenland, R. J. Fulton (ed.)* Geological Survey of Canada, Geology of Canada no. 1.

Lerman A., Wu L., Mackenzie F.T. (2007). CO_2 and H_2SO_4 consumption in weathering and material transport to the ocean, and their role in the global carbon balance. *Marine Chemistry* **106**, 326-350.

Locat J., Lefebre G. (1986). The origin of structuration of the Grande-Baleine marine sediments, Québec, Canada. *Quaterly Journal of Engineering Geology and Hydrogeology*, London 19, 365-374.

Meybeck M., Ragu A. (1996). River discharges to the oceans. An assessment of suspended solids, major ions and nutrients. *Environmental Information and Assessment Report.* UNEP, Nairobi, 250p.

Meybeck M. (2003). Global occurrence of major elements in rivers. In: *Treatise on Geochemistry (Eds H. D. Holland and K. K. Turekian). Vol. 5, Surface and ground water, weathering and soils (Ed J. I. Drever)*, pp. 207-223.

Millot R., Gaillardet J., Dupré B. and Allègre C.J. (2002). The global control of silicate weathering rates and the coupling with physical erosion: new insights from rivers of the Canadian Shield. *Earth and planetary Sciences Letters* **196**, 83-98.

Millot R., Gaillardet J., Dupré B., and Allègre C.J. (2003). Northern latitude chemical weathering rates: Clues from the Mackenzie River Basin, Canada. *Geochimica et Cosmochimica Acta* **67,** 1305–1329.

Ministère du Développement durable, de l'Environnement et des Parcs. *www.mddep.gouv.qc.ca/ index_en.asp.*

NatChem database: Canadian National Atmospheric Chemistry Precipitation Database. Environment Canada, Meteological Service of Canada, 4905 Dufferin Street, Toronto, Ontario, Canada M3H 5T4

Negrel P., Allègre C.J., Dupré B., Lewin E. (1993). Erosion sources determined by inversion of major and trace element ratios and strontium isotopic ratios in river water: The Congo Basin case. *Earth and Planetary Science Letters* **120**, 59–76.

Négrel P., Petelet-Giraud E., Barbier J., Gauthier E. (2003). Surface water-groundwater interactions in an alluvial plain: Chemical and isotopic systematics. *Journal of Hydrology* **277**, 248-267.

Shaw D.M., Reilly G.A., Muysson J.R., Pattenden G.E., Campbell F.E. (1967). An estimate of the chemical composition of the Canadian Precambrian Shield. *Canadian Journal of Earth Sciences* **4**: 827-853.

Spence J., Telmer K. (2005). The role of sulfur in chemical weathering and atmospheric CO_2 fluxes: Evidence from major ions, $\delta^{13}C_{DIC}$ and $\delta^{34}S_{SO4}$ in rivers of the Canadian Cordillera. *Geochimica et Cosmochimica Acta* **69**, no 23, 5441-5458.

Stott D.F., Aitken J.D. (1993). Introduction to the Interior Platform, Western Basins and Eastern Cordillera. Chapter 2 in *Sedimentary Cover of the Craton in Canada, Stott D.F. and Aitken J.D. (ed.)*, Geological Survey of Canada, Geology of Canada no. 5, pp. 11-54.

Tosiani T., Loubet M., Viers J., Valladon M., Tapia J., Marrero S., Yanes C., Ramirez A., Dupre B. (2004). Major and trace elements in river-borne materials from the Cuyuni basin (southern Venezuela): evidence for organo-colloidal control on the dissolved load and element redistribution between the suspended and dissolved load. *Chemical Geology* **211**, 305-334.

Vincent J.S. (1989). Quaternary geology of the Southeastern Canadian Shield. In chap. 3 of *Quaternary Geology of Canada and Greenland, R. J. Fulton (ed.)*, Geological Survey of Canada, Geology of Canada no. 1.

Walker J.C.G., Hays P.B., Kasting J.F. (1981). A negative feedback mechanism for the long-term stabilization of Earth's surface temperature. *Journal of Geophysical Research* **86** (C10), 9776 –9782.

West A.J., Galy A., Bickle M. (2005). Tectonic and climatic controls on silicate weathering. *Earth and Planetary Science Letters* **235**, 211-228.

Wheeler J.O., Hoffman P.F., Card K.D., Davidson A., Sanford B.V., Okulich A.V., Roest W. R. (1996). Geological Map of Canada, Geological Survey of Canada, map 1860A, scale 1:5 000 000.

Yang C., Telmer K., Veizer J. (1996). Chemical dynamics of the "St. Lawrence" riverine system: δD_{H2O}, $\delta^{18}O_{H2O}$, $\delta^{13}C_{DIC}$, $\delta^{34}S_{sulphate}$ and dissolved $^{87}Sr/^{86}Sr$. *Geochimica et Cosmochimica Acta* **60**, 851– 866.

CHAPITRE 4 : Environmental controls on riverine dissolved uranium contents in the Hudson, James and Ungava Bays region, Canada

Rosa Eric[1,2],
Hillaire-Marcel Claude[1],
Ghaleb Bassam[1]
Dick Terry A[3]

.

[1]GEOTOP - Université du Québec à Montréal (UQAM), C.P. 8888 Succursale Centre-ville, Montreal, Quebec, Canada H3C 3P8.

[2]Equipe de Géochimie et Cosmochimie, Institut de Physique du Globe de Paris, Univ. Paris 7.

[3] University of Manitoba, Dept. of Biological Sciences, Winnipeg, Manitoba Canada R3T 2N2

Environmental controls on riverine dissolved uranium contents in the Hudson, James and Ungava Bays region, Canada

ABSTRACT

This study documents U sources, mobilization pathways and seasonal fluxes in rivers discharging into the Hudson, James and Ungava bays (HJUB). Samples retrieved during a monitoring program of the Koksoak, Great Whale, La Grande and Nelson Rivers were analyzed for dissolved uranium concentration and isotopic composition ([U] - $^{234}U/^{238}U$) as well as $^{87}Sr/^{86}Sr$. Field surveys conducted during baseflow and snowmelt in 6 other rivers provided complementary data. Altogether, the studied rivers export 3.4×10^5 moles.yr^{-1} of U towards the HJUB, with an amount-weighted average ($^{234}U/^{238}U$) of 1.27. A large-amplitude temporal variability is observed among the monitored rivers, notably due to dissolved-U dilution following snowmelt. ($^{234}U/^{238}U$) also show some temporal variability but without clear seasonal patterns. The monitored rivers define distinct [U] vs ($^{234}U/^{238}U$) clusters and the data suggest the influence of lithlogy on riverine U contents. In the Nelson River, draining the Interior sedimentary platform, U concentrations are highest (1.05 - 2.45 nM) whereas ($^{234}U/^{238}U$) show little variability (1.21 – 1.25). U concentrations are comparatively lower in the rivers of the Canadian Shield (0.04 – 1.24 nM) whereas ($^{234}U/^{238}U$) span from 1.11 to 1.99. Comparisons of ($^{234}U/^{238}U$) with $^{87}Sr/^{86}Sr$ and Ca/U ratios support the hypothesis of a prominent lithological control on riverine U contents. At the scale of the study area, U and major cations exports are decoupled, suggesting that rock weathering processes do not solely control U budgets. First-order calculations reveal that U accumulation in peatlands could significantly influence basin-scale U budgets.

1. INTRODUCTION

Disequilibria among U-series isotopes in the hydrosphere are increasingly documented (e.g.; see reviews by Osmond and Ivanovitch, 1992; Chabaux et al., 2003; 2008). Notably, the preferential mobility of ^{234}U during water-rock interactions has been highlighted. This feature is attributed to the recoil effect (Cherdyntsev, 1955; Kigoshi, 1971) associated with the alpha decay of ^{238}U, a process that seems critical in governing surface and ground waters ^{234}U/^{238}U activity ratios (eg.: see Osmond and Ivanovich, 1992; Osmond and Kowart, 1992; Sun and Semkow, 1998). In riverine systems, U-series isotopes in the dissolved and particulate phases can be used to document chemical weathering and to quantify the timescale of sediments transfer (Moreira-Nordemann, 1980; Vigier et al., 2001; 2005; DePaolo et al., 2006; Dosseto et al., 2006 a; b; c; Chabaux et al., 2006; Granet et al., 2007). The lithological control on the riverine U-content seems significant in some settings (Sarin et al., 1990; Pande et al., 1994). Other parameters influencing riverine-U properties include physical weathering rates and the production of fresh mineral surfaces (Kronfeld and Vogel, 1991; Robinson et al., 2004), exchange with particles and colloids (Dupré et al., 1996; 1999; Porcelli et al., 1997; Andersson et al., 1998; 2001; Riotte et al., 2003) and groundwater - surface water mixing (Riotte and Chabaux, 1999; Riotte et al., 2003; Durand et al., 2005). Nevertheless, despite the recent advances, it appears that further insights on large river systems are still needed to better constrain the U environmental cycle. Notably, the temporal variability in riverine U contents in regions with prominent seasonality needs to be further addressed. In addition, continental U exports (Palmer and Edmond, 1993) are based on fragmentary data on riverine supplies and the residence time of U in the oceans is still loosely constrained (Dunk et al., 2002). Moreover, few studies have addressed the seasonal variations in U fluxes and isotopic properties in freshwaters (Blacke et al., 1998; Grzymko et al., 2007; Ryu et al., 2009), adding uncertainties in the evaluation of U fluxes exported from continents. Improving the understanding of U cycling at the global scale therefore requires further information on riverine-U fluxes, seasonal variability as well as the related isotopic fractionation.

Here, we document the spatiotemporal variability in the dissolved-U fluxes exported from basins of the Canadian Shield and Platform regions and emphasize linkages to bedrock geology. It provides information on U cycling in watersheds covering more than 1.5×10^6 km^2 of the North American tundra and boreal domain within the Hudson, James and Ungava bays basins (HJUB), a region that is of particular interest as it may be highly sensitive to short-term (yearly to decennial) hydro-climatic variations (Déry et al., 2005). The studied rivers allow accounting for ~50% of the total freshwater discharge into the HJUB.

2. STUDY AREA

The studied catchments are illustrated in Fig. 1. Watershed characteristics and sampling site locations are presented in Table 1. The samples analyzed here were collected as part of a project aimed at documenting chemical denudation rates and fluxes in the HJUB catchment (Chapter 3). A description of the hydro-climatic and geological setting of the basins can be found there.

2.1. Hydrology and Climate

The watersheds included in this study cover more than 15° of latitude and the mean annual temperatures range between approximately 4°C in the Canadian prairies (Déry et al., 2005) and -5.7°C at Kuujjuaq (Environement Canada, climatic archive database), in the north of the Koksoak River watershed. Runoff rates (calculated as mean annual discharge divided by watershed area) are lowest in the Nelson (115 mm/yr) watershed and highest in the Canadian Shield region (499-706 mm/yr) (Table 1). The study area is characterized by a prominent seasonality and natural hydrographs present patterns with increased discharge rates during the spring snowmelt (and to a lesser extent during the wetter fall season). Some of the studied rivers are affected by hydroelectric installations and flow control structures. Notably, the Nelson River discharge is controlled for hydroelectricity production. Similarly, the La Grande River and its upstream tributary (the Laforge River) host 7 hydroelectric reservoirs. The La Grande River also draws waters from southern sub-basins through the Boyd-Sakami diversion, feeding the Robert-Bourassa reservoir (note that the outflow from this reservoir was selected as a sampling site). The reader is referred to Hayeur (2001) for details on the hydroelectric installations of the La Grande River complex. The La Grande River discharge is controlled and typically highest during the winter period due to increased energy demands. Following 1985, the outflow of the Caniapiscau Reservoir towards the Koksoak River was diverted and the reservoir now constitutes the head of the La Grande – Laforge Rivers. This reduced the Koksoak River discharge by ~30% but the river discharge still responds to natural hydro-climatic conditions. Sampling in the Rupert River occurred prior to its diversion into the La Grande hydroelectric complex.

2.2. Geological Setting

The geological characteristics are reported in Table 1 and briefly summarized below. Rocks of the Superior province host the rivers of the Canadian Shield. This region mainly consists of Archean metamorphic and igneous rocks with occurrences of volcanosedimentary rocks and Proterozoic continental and platform sequences. The Koksoak River also drains extensive areas of Paleoproterozoic intrusive, volcanic and sedimentary rocks of the New Quebec Orogen. These formations appear to strongly influence the Koksoak River dissolved chemistry (Chapter 3).

On the western side of the Hudson Bay, the Nelson River mainly drains Mesozoic and Paleozoic sedimentary rocks of the Interior Platform, a region is dominated by fine-grained poorly consolidated Cretaceous clastic sedimentary rocks, with narrow occurrences of Paleozoic carbonate rocks (see Stott and Aitken, 1993). In its downstream section, the Nelson River flows at the juncture of the Archean Superior (East) and Proterozoic Churchill (West) geological provinces. In this region, the river mainly drains crystalline igneous and metamorphic rocks. Finally, in its lowermost section and in proximity to its outlet in the Hudson Bay, the Nelson River flows over Paleozoic carbonate rocks of the Hudson Bay Platform.

3. METHODOLOGY

3.1 Sampling Methods

As stated above, the samples analyzed for dissolved U were retrieved as part of a project aimed at documenting chemical denudation rates in the Hudson, James and Ungava bays (HJUB) (Chapter 3). Field sampling procedures are detailed there.

Samples from the monitoring program (Koksoak, Great Whale, La Grande, Nelson) were stored in 10 l polypropylene containers, transported to the laboratory and filtered within 1 day of collection. Samples from the field expeditions were filtered on site. Samples for Sr contents were filtered through 0.22 μm PES membranes fixed to a syringe. Because a large volume of water was required for U isotopic analyses, these samples were filtered at 0.45 μm using 142 mm-diameter nylon membranes. Filtered samples were acidified to pH = 2 with distilled HNO₃, stored in clean polypropylene bottles and kept at 4°C before analysis. All of the sampling material and filtration equipment was cleaned with diluted distilled nitric acid and rinsed 3 times with river water prior to sampling. Similarly, polypropylene containers and bottles were washed with distilled nitric acid and rinsed 3 times with filtered water before sample storage.

3.2 Analytical Methods

Sr concentrations were determined on a MC-ICP-MS in the *Laboratoire de Géochimie et Cosmochimie* at the *Institut de Physique du Globe de Paris* with a standard error of 5%. Sr isotopic ratios were measured at the same laboratory by MC-ICP-MS. Prior to isotopic analyses, Sr extraction was performed by ionic chromatography following the method described in Meynadier et al. (2007). Repeated measurements (n=30) of the NIST standard during the period of analysis yielded an average value of 0.71027 ± 0.00006. Uranium concentrations and $^{234}U/^{238}U$ ratios were determined at the GEOTOP laboratory using a VG-Sector™ thermal ionization mass spectrometer (TIMS) equipped with a Daly detector. U concentrations and isotopic composition were carried on the same sample using 10 to 500 ng of U and a double spike ($^{233}U - {^{236}U}$). The isotopic composition of the least concentrated samples was duplicated without spike. The analytical uncertainty on activity ratios ($^{234}U/^{238}U$) is ≈ ±1% at the 2σ level. Total blanks for the whole procedure ranged between 10 and 30

pg U and are negligible with respect to analytical uncertainties. Measurements (n=16) of the HU-1 standard during the period of analysis yielded an average $(^{234}U/^{238}U)$ value of 1.003 ± 0.006. All concentrations measured by TIMS at GEOTOP were duplicated using the MC-ICP-MS of the *Laboratoire de Géochimie et Cosmochimie* at the *Institut de Physique du Globe de Paris* and were concordant within quoted uncertainties. Otherwise notified, all elemental ratios reported henceforth are molar ratios, whereas $(^{234}U/^{238}U)$ represents activity ratios.

3.3 Fluxes calculation

Among the monitored sites, uranium fluxes were calculated using a product of the mean weighted concentration with discharge on the sampling interval (Meybeck et al., 1992):

$$F = Q_T \left(\frac{\sum_{i=1}^{n} C_i Q_i}{\sum_{i=1}^{n} Q_i} \right) \qquad \text{Eq. 1}$$

F: calculated U flux (in moles/yr)

Q_T: Total river flow over the measurement period (m^3/year)

C_i: instantaneous U concentrations (in moles/m^3)

Q_i: daily discharge rates on the days of sampling (in m^3/day).

Accordingly, standard error estimations are calculated as (Rondeau et al., 2005):

$$SE(CQ) = \frac{Q_T}{\sum_i Q_i} \sqrt{\sum_i Q_i^2 \, \text{var}(C)} \qquad \text{Eq.2}$$

Equation 1 provides discharge weighted estimates of fluxes and is adequate when weak or inexistent correlations between instantaneous concentrations and discharge rates are observed (e.g.: Hélie et al., 2002; Rondeau et al., 2005). We set the minimum error on fluxes estimates at 20%, which we assume to be conservative based on the estimate that discharge rates have a 5-15% error (criteria for MDDEP

discharge rates measurement, see text below) whereas analytical measurements have a ~5% error. If the standard error calculated using Eq.2 exceeds 20%, we use this value, if not, we use the 20% minimum error bar.

Discharge rates from the Nelson River are provided by *Manitoba Hydro* and correspond to total flow measured at the Long Spruce power station located a few kilometers upstream of the sampling site. Discharge rates in the La Grande River are non-disclosure information provided by *Hydro-Quebec*. The discharge values used to evaluate the fluxes correspond to the total flow measured at the LG2 and LG2A power stations, representing the outflow of the Robert-Bourassa hydroelectric reservoir. Discharge rates in the Koksoak River and in the Great Whale River (after July 2008) are based on daily measurements, the data are provided by the *Ministère du Développement durable, de l'environnement et des Parcs du Québec (MDDEP)*. For the period before July 2008, discharge rates of the Great Whale River are taken from a compilation of the *International Polar Year project* (Dr. Stephen Déry, University of Northern British Columbia). These values represent averages since measurements were not performed on a daily basis by the MDDEP during this time period. In the case of the Koksoak and Great Whale Rivers, gauging stations are located upstream of the sampling sites and discharges rates were corrected, assuming that discharge along the river course is proportional to the area of the watershed drained. In the case of the Nelson and La Grande rivers, gauging stations are in proximity of sampling points and no discharge correction was required.

The U fluxes presented for the rivers sampled during the August 2008 and May 2009 field expedition represent first order assessments of mean annual fluxes, as these sites were not monitored over time. At these sites, fluxes were calculated using average annual discharge rates measured at the nearest gauging station.

4. RESULTS

Analytical results are reported in Table 2. Major ions, Sr, Nd and DOC fluxes along with chemical denudation rates in the HJUB watershed are documented in Chapter 3. Therefore, here, we focus on U geochemistry. Unless specified, all concentrations reported henceforth are for the dissolved phase (<0.45 µm) and all ratios are molar ratios.

4.1. Dissolved Uranium Contents

Uranium concentrations and activity ratios are reported in Table 2. As for major ions, [U] are highest in the Nelson River (Interior Platform). All of the studied rivers show ^{234}U enrichments with respect to secular equilibrium. However, in view of the differences between rivers draining the Canadian Shield vs the Interior Platform (Nelson River), both are presented separately below.

4.1.1. Rivers of the Canadian Shield

Among the rivers of the Canadian Shield, uranium concentrations range between 0.041 nM in the Laforge River (a tributary of the La Grande River) and a maximum of 1.236 nM in the Pontax River, which is also characterized by the highest DOC content (1777 µM). (^{234}U/^{238}U) range between 1.11 in the Harricana River and 1.99 in the middle section of the Great Whale River and are not correlated to U concentrations.

Sampling profiles were carried out along the Great Whale and La Grande river courses in August 2008 in order to address the downstream variability of uranium concentrations and isotopic properties (Table 2).

In the La Grande – Laforge River system, samples were collected at the outlets of the hydroelectric reservoirs, including those set on the course of the major upstream tributary, the Laforge River. Among these sites, [U] range between 0.041 and 0.211 nM and follow a general increasing trend from headwaters towards the downstream reservoirs (Table 2). (^{234}U/^{238}U) activity ratios vary between 1.24 and 1.34 and are also higher in the downstream section of the river.

Similarily, the Great Whale River shows increasing U-concentrations from its headwaters to its estuary, except for a significant anomaly about 175 km inland (Table 2). At this site, a rise in [U] from 0.149 to 0.300 nM is associated with a drastic increase in $(^{234}U/^{238}U)$ activity ratio from 1.50 to 1.99. This divergence does not seem to be linked to any major change in the catchment lithology, as the river flows over Archean granites and gneisses on its entire length and it is not associated with a major confluence.

Overall, most of the U contents reported here are high in comparison to values reported by Palmer and Edmond (1993) for other rivers draining Precambrian shields (Guyana and Brazilian shields). The $(^{234}U/^{238}U)$ values fall within the range of values typically reported for rivers, which vary greatly (~ 0.9 – 4) (ex.: see compilation by Chabaux et al (2008) and references therein). Overall, the rivers flowing directly into the Arctic Ocean present higher $(^{234}U/^{238}U)$ (Mackenzie ≈ 1.38; Ob ≈ 1.66, Lena ≈ 2.26, Yenisey ≈ 2.59) (Vigier et al., 2001; Andersen et al., 2007) in comparison to the rivers of the Canadian Shield.

4.2.2. Interior Platform: Nelson River

In the Nelson River, U contents range between 1.05 and 2.43 nM. Uranium isotopic disequilibria are less variable than for the monitored rivers of the Canadian Shield and range between 1.21 and 1.25.

When compared to other North American rivers draining watersheds containing extensive areas of platform rocks, the Nelson River presents lower U contents than the Mississippi (3.319 nM) (Grzynko et al., 2007) and Mackenzie (2.681 nM) (Vigier et al., 2001; Andersen et al., 2007) Rivers, but higher U contents than the St. Lawrence River (1.22 nM) (Durand, 2000). Overall, these dissolved U contents remain high with respect to the world average riverine [U] as evaluated by Palmer and Edmond (1993) (1.30 nM, with a significantly lower value of 0.78 nM when the Ganges-Brahmaputra and Yellow rivers are excluded) and fall within the middle to high range of [U] values commonly reported (Chabaux et al., 2008). The range of $(^{234}U/^{238}U)$ reported for the Nelson River is slightly lower than that of the Mackenzie (~ 1.38) (Vigier et al., 2001; Andersen et al., 2007) and Mississippi (1.24 – 1.47) (Grzymko et al., 2007) rivers but compares well to that of the St. Lawrence River (1.15-1.24) (Durand, 2000).

5. DISCUSSION

5.1. Temporal variability in Riverine Dissolved U

The temporal variability in riverine dissolved U responds to hydroclimatic conditions, dam effects, tributary water mixing, weathering of soils, wetland contributions and groundwater supplies, among others (eg. See Grzymko et al., 2007; Ryu et al., 2009 and references therein). Seasonal [U] and $(^{234}U/^{238}U)$ records are illustrated on Fig. 2 where [U] values are normalized to the discharge-weighted average concentration in each river, allowing a direct comparison of [U] variability between sites, independently of absolute concentrations.

Apart from the La Grande River exception, the monitored rivers display important seasonal fluctuations in [U] (Fig. 2 a-b-d), reaching more than a twofold factor in the Nelson River. The temporal variations in dissolved [U] match the observed seasonality: overall higher concentrations are measured during the ice-on period whereas a dilution is recorded following snowmelt. Gradual increases in concentrations are recorded throughout the ice-free season, similar to what is observed for major cations and Sr (Table 2). The La Grande River (Fig. 2c) is an exception due to the lesser temporal variability in its dissolved [U]. This is attributed to the buffering effect of the large hydroelectric reservoirs found along its course (n=6). These reservoirs comprise more than 100 km³ of water (Hayeur, 2001) and appear to smooth out the variations in dissolved [U] due to an increased residence time of water (up to 6 months in the Robert Bourassa (LG2) reservoir, upstream of the La Grande River sampling site, Hayeur (2001)). A similar situation is observed for dissolved major ions and Nd in this river (Chapter 3).

Among the monitored sites, the Great Whale and Koksoak rivers are the only presenting hydrographs directly responding to hydroclimatic conditions. At these sites, the highest U concentrations are associated with the lowest discharge rates occurring during the frozen period (Table 2). However, dilution does not compensate for the increase in discharge during snowmelt and U fluxes are intensified during this time period. By contrast, in the La Grande and Nelson rivers, discharge rates respond to flow control at hydroelectric installations and are decoupled from natural hydro-climatic conditions. At these sites, flow rates and dissolved U contents are completely decoupled. In the La Grande River, U fluxes are intensified during the winter period, as turbine flows are increased in response to electricity demand, yielding a seasonality in U fluxes that is contrary to what is observed under natural conditions within this region. In the Nelson River, discharge rates are controlled at the

outlet of Lake Winnipeg. Over the study period, flow rates were highest during the month of August in response to water management strategies by Manitoba Hydro, resulting in "artificially" increased U fluxes during this time period.

Some temporal variability in $(^{234}U/^{238}U)$ is also observed at all sites, but without clear seasonal patterns (Fig. 2 a-b-c-d). The lack of imprint of the snowmelt event suggests that the corresponding drop in [U] concentrations is mostly due to dilution with little mineralized snowmelt waters. Similarly, the $(^{234}U/^{238}U)$ variability recorded during the frozen period reveals that the relative contribution from ^{234}U-enriched groundwaters during this period cannot be highlighted. If groundwater supplies to rivers have been successfully documented on the basis of dissolved U disequilibria in given settings (eg.: see Riotte and Chabaux, 1999; Durand et al., 2005), the absence of systematic seasonal patterns in $(^{234}U/^{238}U)$ indicates that within the studied basins, disequilibria among dissolved-U isotopes need further assessments before it can be used for delineating hydrological flowpaths

Nevertheless, apart from the La Grande River exception, the recorded temporal variability highlights the importance of a multi-season sampling program to reduce errors associated with estimates of riverine U fluxes, at least for regions characterized by a prominent seasonality. Within the study region, calculations based on a single [U] measurement could yield over/under estimations of up to a twofold factor (Fig. 2). Similarly, the temporal variability in U activity ratios highlights the need for documenting the amount-weighted average $(^{234}U/^{238}U)$ of rivers. We agree with Palmer and Edmond (1993) and Grzymko et al (2007) that the global riverine U exports need to be further constrained on the basis of riverine fluxes monitoring, an issue that needs to be addressed for better constraining U oceanic residence time (see Dunk et al., 2002).

5.2. Spatial Variability in Riverine Dissolved U: Shield and Platform Environments

5.2.1. Controls on riverine U contents: Shield vs Platform Environments

As illustrated in Fig. 3, the studied rivers show distinct clusters in a $(^{234}U/^{238}U)$ vs [U] plot. The Nelson River, draining Phanerozoic sedimentary rocks of the Interior Platform, shows an overall greater [U] and a smaller variability in $(^{234}U/^{238}U)$. By comparison, rivers draining catchments of the Canadian Shield present overall lower [U] and a greater variability in $(^{234}U/^{238}U)$.

Sarin et al. (1990) proposed that the slow and incongruent dissolution of silicates should yield higher U isotopic disequilibria than the faster congruent dissolution of carbonates. Similarly, based on a compilation of data, Vigier et al. (2005) highlighted that ^{234}U excesses are generally lower in watersheds undergoing high carbonate dissolution rates and more variable in rivers draining silicate-rich areas. A potential lithological influence on riverine dissolved U contents was also highlighted in the rivers of the Himalaya on the basis of $(^{234}U/^{238}U) - {}^{87}Sr/^{86}Sr$ systematic (Chabaux et al., 2001), although these authors suggested that the lithological control might be indirect.

Here, the distinct $(^{234}U/^{238}U)$ vs Ca/U and $^{87}Sr/^{86}Sr$ clusters (Fig. 4) seem consistent with U supplies originating from silicate weathering within the Canadian Shield (higher $^{87}Sr/^{86}Sr$, lower Ca/U, variable $^{234}U/^{238}U$) and a greater influence of carbonate dissolution within the Interior Platforms (lower $^{87}Sr/^{86}Sr$, higher Ca/U, lower $^{234}U/^{238}U$), supporting the hypothesis of a lithological control on riverine dissolved U contents. The average Ca/U and $^{87}Sr/^{86}Sr$ ratios of the Canadian Precambrian Shield (data from McCulloch and Wasserburg, 1978 and Shaw et al., 1986) and of typical carbonate rocks containing between 2 and 5 ppm of U (e.g. see Palmer and Edmond, 1993) are also reported in Fig. 4, where both lithologies are assumed to be at secular equilibrium. All of the rivers present Ca/U ratios that fall between that of the silicate and carbonate endmembers described above, except for one sample from the Pontax River displaying an exceptionally high U content. The La Grande and Great Whale rivers present Ca/U and $^{87}Sr/^{86}Sr$ ratios that are close to that of the silicate endmember, and relatively high U disequilibria, consistent with the predominance of silicate rocks within these watersheds (Table 1). The Koksoak River appears to stand out in Fig. 4, with relatively high $(^{234}U/^{238}U)$ despite overall higher Ca/U ratios in comparison to the other rivers of the Canadian Shield. This likely reflects Ca-rich supplies from silicates found in volcano-sedimentary sequences within its catchment, as this lithology

represents a dominant source of dissolved solids in the Koksoak watershed (Chapter 3). The Ca/U ratios measured in the Nelson River are slightly higher, $^{87}Sr/^{86}Sr$ are lower and $(^{234}U/^{238}U)$ are overall lower in comparison to most of the rivers of the Canadian Shield, consistent with the hypothesis that carbonate dissolution significantly influences the U budgets within the Interior Platform (Nelson River). Among rivers of the Canadian Shield, $^{87}Sr/^{86}Sr$ are higher than that of the parent bedrock (Fig. 4). This could indicate a preferential leaching of minerals enriched in ^{87}Sr. The reader is referred to Wadleigh et al (1985) for thorough documentation of dissolved $^{87}Sr/^{86}Sr$ in Canadian rivers.

Part of the scatter observed in Fig. 4 might also result from U supplies from localized U-rich lithological sources. Indeed, pegmatites, veins, unconformity-related mineralization, U-rich trace minerals, clastic sedimentary rocks, banded iron formations, black shales, impurities and/or clayey interlayers in carbonates, among others, may all significantly contribute to riverine dissolved U budgets even if they only sporadically occur within watersheds. Notably, U-Cu mineralizations in clastic rocks are found within the Nelson River watershed (Bell, 1996) and might influence riverine U contents. Similarly, the U mineralization associated with veins, unconformities and pegmatites along with stratabound U-Cu mineralization that occur sporadically in the James Bay region (see Gauthier, 2000 and references therein) are likely to influence riverine U budgets. Yet, other tracers of weathering that are known to respond to basin lithology (major ions and Sr) might not be strongly influenced by these localized U sources.

Nevertheless, we argue that the distinct signature of riverine $(^{234}U/^{238}U)$ within the monitored basins should allow the use of U-isotope to document U sources in the nearby oceanic domain in a fashion similar to that employed in the Arctic by Anderson et al (2007). This seems especially useful for documenting inputs from the Canadian Shield, a region where the dissolved $^{87}Sr/^{86}Sr$ of major rivers overlap (Fig. 4). Under such conditions, it appears that $(^{234}U/^{238}U)$ could stand as a useful complementary tracer for identifying the sources of continental inputs in the HJUB.

5.3. Towards the establishment of basin scale U budgets

The calculated dissolved U exports and area specific fluxes are reported in Table 3. Altogether, the rivers included in this study annually export 3.4×10^5 moles of U towards the HJUB. The Nelson River clearly dominates these U exports, with an annual flux reaching 2.7×10^5 moles. The amount-weighted ($^{234}U/^{238}U$) of the U flux exported by the studied rivers yields a value of 1.27, which is significantly higher that the average seawater activity ratio (1.144, Chen et al., 1986). As a whole, the rivers sampled here account for approximately 1% of the global riverine U flux as evaluated by Palmer and Edmond (1993) and Dunk (2002). However, since the behavior of dissolved U in estuaries varies and is not conservative (Andersson et al., 1995; Porcelli et al., 1997; Windom et al., 2000; Andersson et al., 2001; Swarzensky et al., 2004; Andersen et al., 2007; Moore et al., 2008), these fluxes represent continental exports and are therefore an upper limit for the actual U flux truly reaching the oceans.

At the scale of the study area, basin scale area specific U fluxes range between 0.13 and 0.56 moles yr^{-1} km^{-2} in the La Grande and Pontax rivers, respectively. These area-specific U fluxes by rivers are decoupled from cations-area-specific fluxes (also reported in Table 3), suggesting that rock-weathering processes do not solely control U exports. U-removal processes related to the redox-sensitive nature of dissolved U could intervene and a key process might be U accumulation in the abundant organic soils and peatlands found within the studied basins (Table 1). Such environments are known to concentrate U through removal from solution under reducing conditions (and to a lesser extent ion exchange processes) (e.g., Porcelli et al., 1997; Shotyk et al., 1988; 1992). Indeed, based on 35 peat cores collected in Canada, Shotyk et al (1992) evaluated that on average, peat ashes are enriched in U by a factor of 4 with respect to the mineral substrate. A first order estimate of the incidence of U accumulation in peatlands is obtained from the calculated areal extent of peatlands within each of the studied basins (Table 1). Based on Shotyk (1992), we assume that average peat ashes contain ~11ppm U (yielding approximate U contents of 1.1 ppm in dry peat and 0.11 ppm in bulk peat). We assume an average peat depth of 2m, consistent with measurements conducted in the James Bay region (Van Bellen et al., 2010). Under these assumptions, we estimate the total amount of U accumulated within peatlands in each basin (Table 4). Although, peat accumulation started at around 7.5 kyrs BP in the James Bay region (Van Bellen et al., 2010) we consider that U accumulation mainly occurred during the last 5 kyrs (i.e. U accumulation only begun at a time when peatlands had reached a sufficient thickness for allowing the establishment of the reducing conditions required for U accumulation). We then propose a first-order estimate of the long-term average U-accumulation rate within each basin

(Table 4). These calculations reveal that basin-scale average U accumulation rates in peatlands range between approximately 0.0005 and 0.14 moles yr^{-1} km^{-2} (Table 4). Such U-accumulation rates represent an equivalent of up to approximately 24% of the present-day riverine dissolved U exports (Table 4). Although this remains a first-order estimate, it highlights the need to further constrain the role of peatlands on basin-scale U budgets, an issue that seems critical for better understanding the continental part of the U cycle.

6. CONCLUSION

This study aimed at documenting the fluxes and sources of U exported by rivers discharging into the Hudson, James and Ungava Bays (HJUB). The studied rivers account for approximately 50% of the total freshwater discharge into the HJUB.

The studied rivers export an annual U flux of 3.4×10^5 moles of U towards the HJUB, with an amount-weighted $(^{234}U/^{238}U)$ of 1.27. This accounts for approximately 1% of the global riverine-U flux (Palmer and Edmond, 1993; Dunk et al., 2002). The rivers define distinct $(^{234}U/^{238}U)$ vs [U] clusters and the data support the hypothesis of a prominent lithological control on riverine U contents. In addition, the distinct $(^{234}U/^{238}U)$ observed for each monitored river should allow the use of U-isotopes for tracing the sources of continental inputs in the HJUB, in a fashion similar to that employed in the Arctic by Anderson et al (2007). The amplitude of seasonal variations in U contents (up to a twofold factor) recorded in rivers highlights the interest of seasonal river monitoring to reduce the error associated with the evaluation riverine U exports, a critical issue for better constraining oceanic-U residence time. Finally, first-order calculations suggest that U accumulation in peatlands significantly influences basin-scale U budgets. This issue needs to be further addressed in order to document the continental U cycle within the study region.

Acknowledgements.

Table 1. Watersheds Characteristics.

River	#	Lat/long	Q (m3/s)	A (Km2)	Runoff (mm/yr)	Geol. Prov.	Int. rocks (%)	Met. rocks (%)	Sed. rocks (%)	Volc. rocks (%)	Peatlands (%)
Bell[1]	8	49.769 / -77.627	497	22200	706	S	50	19	0	31	14
Broadback[3]	7	51.185 / -77.465	367	17100	677	S	60	25	1	14	29
Great Whale[1]	2	55.279 / -77.650	676	42700	499	S	99	0	0	1	0
Harricana[1]	9	48.790 / -78.013	70	3680	604	S	23	23	3	50	26
Koksoak[1]	1	58.029 / -68.475	1600	94311	535	S,C	68	1	20	10	6
La Grande[3]	3	53.781 / -77.530	3808	177678	676	S	69	26	2	3	8
Nelson[2]	10	56.685 / -93.790	4024	1100000	115	HBP, C, S, IP, CO	9	0	90	1	20
Nemiscau[3]	5	51.688 / -75.825	53	3015	549	S	N.A	N.A	N.A	N.A	N.A
Pontax[1]	4	51.733 / -77.383	111	6020	579	S	57	38	1	5	80
Rupert[3]	6	51.353 / -77.423	848	40900	654	S	51	28	17	4	13

The basin numbers corresponds to those reported in Fig. 1. The percent cover of each lithology is based on geological map 1860A from the Geological Survey of Canada (Wheeler et al., 1996). Values are calculated by normalizing the areal extent of each lithology to the watershed area. Geological Provinces are: C = Churchill, S = Superior, HBP = Hudson Bay Platform, IP = Interior Platform, CO = Cordilleran Orogen. Discharge and watershed area are from: [1]Ministère du développement durable, de l'environnement et des parcs (MDDEP), [2]Water Survey of Canada, [3]Hydro-Quebec Data. The peatlands covers are evaluated from Tarnocai et al (2000). Modified from Chapter 3.

Table 2. Analytical results (continued on 3 pages).

	Date	daily Q (m³/s)	pH	Alk. (µeq/l)	DOC (µM)	Na (µM)	K (µM)	Mg (µM)	Ca (µM)	Sr QUAD (µM)	Nd (nM)	Cl (µM)	SO4 (µM)	^{87}Sr/^{86}Sr	Ba (µM)	U (nM)	(^{234}U/^{238}U) activity	(^{234}U/^{238}U) +
La Grande	10-Sep-07		6.6	48	409	28	8	13	29	0.092	0.70	11	10	0.7308	0.019	0.174	1.29	0.018
La Grande	02-Nov-07		6.3	43	365	30	8	13	28	0.092	0.76	25	11	0.7300	0.017	0.180	1.25	0.012
La Grande	12-Dec-07		6.5	46	335	30	8	13	29	0.092	0.87	15	11	0.7304	0.017	0.193	1.25	0.015
La Grande	16-Jan-08		6.1	43	321	28	8	13	28	0.091	0.81	11	10	0.7304	0.018	0.174	1.23	0.016
La Grande	07-Apr-08		5.6	27	395	28	7	12	26	0.094	0.83	14	10	0.7261	0.021	0.184	1.29	0.011
La Grande	22-May-08		6.5	47	417	28	7	12	25	0.092	0.84	9	10	0.7299	0.020	0.186	1.23	0.018
La Grande	30-Jun-08		6.6	43	411	30	8	13	27	0.090	0.69	10	9	0.7274	0.018	0.176	1.29	0.016
La Grande	01-Aug-08		6.5	47	401	29	8	13	29	0.089	0.78	9	9	0.7307	0.019	0.201	1.31	0.021
La Grande	16-Aug-08		6.5	57	438	30	8	13	36	0.090	0.77	8	10	0.7300	0.019	0.211	1.30	0.015
La Grande	28-Sep-08		6.5	53	377	26	6	11	31	0.089	0.75	9	10	0.7310	0.019	0.189	1.30	0.013
La Grande	02-Dec-08		6.3	49	399	27	7	12	28	0.090	0.83	9	10	0.7283	0.018	0.205	1.29	0.014
La Grande	29-Jan-09		6.5	62	371	28	7	13	31	0.085	0.84	8	10	0.7311	0.019	0.194	1.27	0.022
La Grande	14-May-09		6.2	39	352	27	7	15	32	0.091	0.64	8	10	0.7259	0.021	0.155	1.29	0.018
LG2	16-Aug-08		6.5	57	439	30	8	13	36	0.089	0.77	8	10	0.7300	0.020	0.211	1.33	0.026
LG3	16-Aug-08		6.4	48	319	23	6	12	32	0.074	0.35	5	9	0.7330	0.022	0.095	1.34	0.010
LG4	19-Aug-08		6.5	47	303	22	6	11	22	0.076	0.49	4	9	0.7357	0.025	0.089	1.25	0.012
LA1	18-Aug-08		6.3	36	314	19	5	11	26	0.058	0.15	6	7	0.7356	0.020	0.041	1.27	0.016
LA2	19-Aug-08		6.4	43	301	20	5	13	18	0.064	0.17	4	7	0.7371	0.020	0.045	1.29	0.025
LG-Brisay	19-Aug-08		6.4	46	313	21	5	13	20	0.070	0.15	4	8	0.7357	0.022	0.052	1.24	0.019
Great Whale	24-Sep-07	852	6.2	63	641	52	7	19	43	0.108	2.75	38	10	0.7318	0.026	0.405	1.40	0.012
Great Whale	21-Oct-07	874	6.5	66	413	33	6	13	37	0.093	1.20	19	9	0.7337	0.025	0.302	1.49	0.036
Great Whale	12-Feb-08	230	6.1	66	485	53	9	17	47	0.119	1.45	32	13	0.7339	0.035	0.407	1.51	0.014
Great Whale	12-Mar-08	179	6.6	137	663	112	13	30	70	0.187	1.89	87	23	0.7319	0.052	0.568	1.50	0.007
Great Whale	14-Apr-08	153	6.5	155	518	85	22	19	55	0.146	1.39	63	14		0.039	0.421	1.52	0.019
Great Whale	11-May-08	602	6.7	81	586	82	11	25	49	0.116	2.67	75	12	0.7301	0.022	0.483	1.38	0.013
Great Whale	18-Jun-08	1254	6.7	51	438	35	6	13	37	0.094	1.21	19	9	0.7339	0.027	0.296	1.48	0.013
Great Whale	15-Jul-08	716	6.8	50	385	36	6	14	37	0.097	1.00	17	9	0.7341	0.027	0.292	1.47	0.016
Great	17-	581	6.7	88	368	35	6	14	44	0.102	0.81	17	9	0.7338	0.028	0.303	1.46	0.022

Site	Date																	
Whale	Aug-08																	
Great Whale	14-Oct-08	884	6.5	71	539	60	9	21	43	0.116	2.29	62	41	0.7314	0.027	0.383	1.43	0.016
Great Whale	05-Jan-09	404	6.6	84	476	43	16	16	42	0.110	1.13	38	14	0.7334	0.038	0.324	1.43	0.015
Great Whale	02-Feb-09	285	6.8	118	512	57	11	22	56	0.156	1.51	36	19	0.7337	0.044	0.457	1.48	0.014
Great Whale	02-Mar-09	208	6.9	107	402	47	9	19	47	0.144	1.01	30	17	0.7340	0.037	0.340	1.51	0.010
Great Whale	04-Apr-09	186	7.0	146	662	82	15	31	70	0.225	2.06	62	22	0.7332	0.057	0.525	1.43	0.017
Great Whale	11-May-09	341	6.4	88	591	72	15	22	46	0.137	2.21	56	24	0.7320	0.036	0.415	1.48	0.017
Great Whale	08-Jun-09	1428	6.6	69	508	45	7	15	36	0.114	2.04	37	22	0.7312	0.026	0.373	1.42	0.012
Great Whale	13-Jul-09	1228	6.8	93	438	44	7	19	44	0.119	1.67	28	17	0.7339	0.025	0.295	1.44	0.015
Great Whale	21-Sep-09	714	7.1	95	458	60	8	21	48	0.131	2.37	33	10	0.7333	0.031	0.353	1.44	0.014
Denys	17-Aug-08		7.0	78	433	42	6	15	37	0.102	1.28	26	12	0.7319	0.019	0.411	1.35	0.014
Coats	17-Aug-08		6.9	106	483	54	6	17	50	0.158	1.51	37	13	0.7284	0.034	0.621	1.56	0.016
GW1 (30)	17-Aug-08		6.7	88	369	35	6	14	44	0.107	0.81	16	9	0.7338	0.029	0.303	1.46	0.020
GW2 (80)	17-Aug-08		6.7	69	348	29	5	12	34	0.101	0.65	14	9	0.7342	0.030	0.266	1.51	0.038
GW3 (107)	17-Aug-08		6.6	66	323	24	5	11	31	0.091	0.51	9	8	0.7357	0.031	0.208	1.51	0.027
GW4 (170)	17-Aug-08		6.6	70	328	23	5	10	32	0.090	0.37	9	8	0.7351	0.030	0.300	1.99	0.025
GW5 (223)	17-Aug-08		6.7	62	317	21	5	10	28	0.077	0.34	7	7	0.7379	0.029	0.149	1.49	0.020
GW6 (292)	17-Aug-08		6.6	66	322	20	5	10	26	0.073	0.29	6	7	0.7380	0.027	0.132	1.47	0.030
Koksoak	03-Feb-09	301	7.2	339	288	50	10	76	124	0.234	0.74	25	31	0.7280	0.059	0.393	1.58	0.015
Koksoak	17-Mar-09	194	7.2	442	258	65	14	105	151	0.329	0.60	29	38	0.7269	0.074	0.397	1.57	0.015
Koksoak	06-Apr-09	181	7.1	440	241	77	14	111	158	0.349	0.57	51	31	0.7304	0.075	0.392	1.59	0.017
Koksoak	29-Jun-09	5068	7.2	262	309	32	8	67	96	0.205	0.57	14	24	0.7320	0.049	0.254	1.62	0.014
Koksoak	31-Aug-09	1792	7.3	280	271	57	9	73	102	0.224	0.60	26	21	0.7287	0.049	0.323	1.59	0.016
Koksoak	05-Oct-09	1501	7.3	244	325	49	10	66	89	0.206	1.12			0.7283	0.043	0.384	1.55	0.016
Nelson	30-Sep-07	3696	8.1	1854	864	439	44	371	679	0.937	0.36	279	160	0.7135	0.154	1.678	1.21	0.010
Nelson	05-Nov-07	4421	7.9	1986	753	544	53	426	718	1.097	0.29	356	210	0.7135	0.193	2.085	1.23	0.012
Nelson	03-Dec-07	3855	7.9	2146	812	655	61	489	794	1.160	0.35	729	249	0.7126	0.221	2.427	1.24	0.012
Nelson	04-Mar-08	4154	7.9	2983	928	591	62	557	1066	1.446	0.27	492	211	0.7128	0.219	2.381	1.22	0.009
Nelson	07-Apr-08	3961	8.1	2038	793	644	63	465	731	1.244	0.24	451	252	0.7127	0.222	2.384	1.22	0.012
Nelson	12-May-08	3541	7.9	2186	755	566	56	421	679	1.113	0.33	387	219	0.7130	0.198	2.175	1.23	0.012
Nelson	09-Jun-08	3397	8.0	1436	793	263	31	288	618	0.643	0.45	164	83	0.7136	0.102	1.047	1.22	0.012

Sample	Date																
Nelson	08-Jul-08	4041	8.1	1750	780	524	52	400	680	1.025	0.17	357	197	0.7128	0.174	1.966	1.25	0.018
Nelson	11-Aug-08	5229	8.2	2155	764	661	61	452	702	1.217	0.15	483	263	0.7123	0.207	2.367	1.25	0.005
Nelson	15-Sep-08	4647	8.4	2025	816	676	63	456	716	1.154	0.14	483	251	0.7126	0.192	2.426	1.22	0.014
Harricana	14-Aug-08		7.1	258	1366	112	21	68	154	0.350	3.52	81	84		0.057	0.322	1.11	0.012
Harricana	24-May-09		6.9	210	1239	111	21	71	138	0.341	3.97	63	80		0.059	0.306		
Bell	15-Aug-08		6.4	80	1718	38	9	31	65	0.158	4.72	8	15		0.050	0.219		
Bell	24-May-09		6.6	73	1156	37	10	29	52	0.140	3.55	9	16		0.041	0.218		
Broadback	15-Aug-08		6.7	81	886	30	7	21	45	0.110	2.54	6	11		0.027	0.411	1.62	0.016
Broadback	24-May-09		6.9		855	37	9	27	52	0.135	2.34	9	12		0.029	0.478		
Broadback	22-Aug-08		6.6	82	751	27	5	11	50	0.105	1.29	14	12			0.688		
Broadback	27-May-09		6.3	37	678	24	6	11	43	0.088	1.07	5	11		0.021	0.588		
Rupert	15-Aug-08		6.9	103	573	25	6	29	48	0.089	1.22	32	12		0.035	0.497	1.50	0.015
Rupert	24-May-09		6.8	104	521	25	6	25	41	0.087	1.10	7	11		0.029	0.601		
Rupert	22-Aug-08		7.2	179	421	22	7	41	60	0.092	0.87	5	14		0.041	0.384		
Rupert	27-May-09		6.9	109	434	24	7	31	48	0.091	0.94	5	13		0.032	0.430		
Nemiscau	22-Aug-08		6.1	22	568	24	6	8	24	0.078	0.81	7	10		0.023	0.263	1.24	0.016
Nemiscau	27-May-09		6.1	30	539	26	7	9	26	0.089	0.86	7	11		0.025	0.223		
Pontax	15-Aug-08		5.7	14	1777	41	7	19	35	0.127	4.09	39	5		0.032	1.236	1.44	0.015
Pontax	24-May-09		6.1	27	971	31	7	13	22	0.078	2.04	10	7		0.017	0.710		

Samples labeled LG2-LG3-LG4-LA1-LA2-Brisay are those retrieved at the outlets of the main hydroelectric reservoirs found along the La Grande River and its main upstream tributary, the Laforge River (Brisay is upstream, LG2 is downstream). See Hayeur (2001) for details on these reservoirs. Samples labeled GW1 to GW6 are those retrieved along the Great Whale River, the numbers in parentheses indicate the distance from the river outlet. The Denys and Coats rivers are the two main tributaries of the Great Whale River in its downstream section. Major ions, Sr, Nd and DOC concentrations are from Chapter 3.

Table 3. Exported fluxes.

	DOC (moles*yr⁻¹*km⁻²)	Cations sum (moles*yr⁻¹*km⁻²)	Nd (moles*yr⁻¹*km⁻²)	Ba (moles*yr⁻¹*km⁻²)	U (moles*yr⁻¹)	U (moles*yr⁻¹*km⁻²)
Bell	1.0×10^6	9.6×10^4	2.9	32	3.4×10^3	0.15
Broadback	5.9×10^5	7.8×10^4	1.6	19	5.1×10^3	0.30
Great Whale	2.4×10^5	5.9×10^4	0.9	14	7.6×10^3	0.18
Harricana	7.9×10^5	2.1×10^5	2.3	35	7.0×10^2	0.19
Koksoak	1.6×10^5	1.2×10^5	0.4	26	1.5×10^4	0.16
La Grande	2.6×10^5	5.3×10^4	0.5	13	2.2×10^4	0.13
Nelson	9.3×10^4	2.1×10^5	0.03	22	2.7×10^5	0.25
Nemiscau	3.0×10^5	3.6×10^4	0.5	13	4.0×10^2	0.13
Pontax	8×10^5	5.1×10^4	1.8	14	3.4×10^3	0.56
Rupert	3.6×10^5	6.8×10^4	0.8	21	1.5×10^4	0.36

Major ions, and DOC fluxes are from Chapter 3.

Table 4. U accumulation in peatlands.

|	Riverine U export $(moles*yr^{-1}*km^{-2})$	First order estimates		
		U accumulated in peat (moles)	Rate of U accumulation in peat $(moles*yr^{-1}*km^{-2})$	Rate of U accumulation in peat / riverine U export
Bell	0.15	$2.6x10^6$	$2.4x10^{-2}$	0.15
Broadback	0.30	$4.2x10^6$	$4.9x10^{-2}$	0.16
Great Whale	0.18	$1.0x10^5$	$4.9x10^{-4}$	0
Harricana	0.19	$8.2x10^5$	$4.5x10^{-2}$	0.24
Koksoak	0.16	$5.0x10^6$	$1.1x10^{-2}$	0.07
La Grande	0.13	$1.3x10^7$	$1.4x10^{-2}$	0.11
Nelson	0.25	$1.8x10^8$	$3.3x10^{-2}$	0.14
Nemiscau	0.13	N.A.	N.A.	N.A.
Pontax	0.56	$4.1x10^6$	$1.4x10^{-1}$	0.24
Rupert	0.36	$4.5x10^6$	$2.2x10^{-2}$	0.06

Fig. 1. Study area.
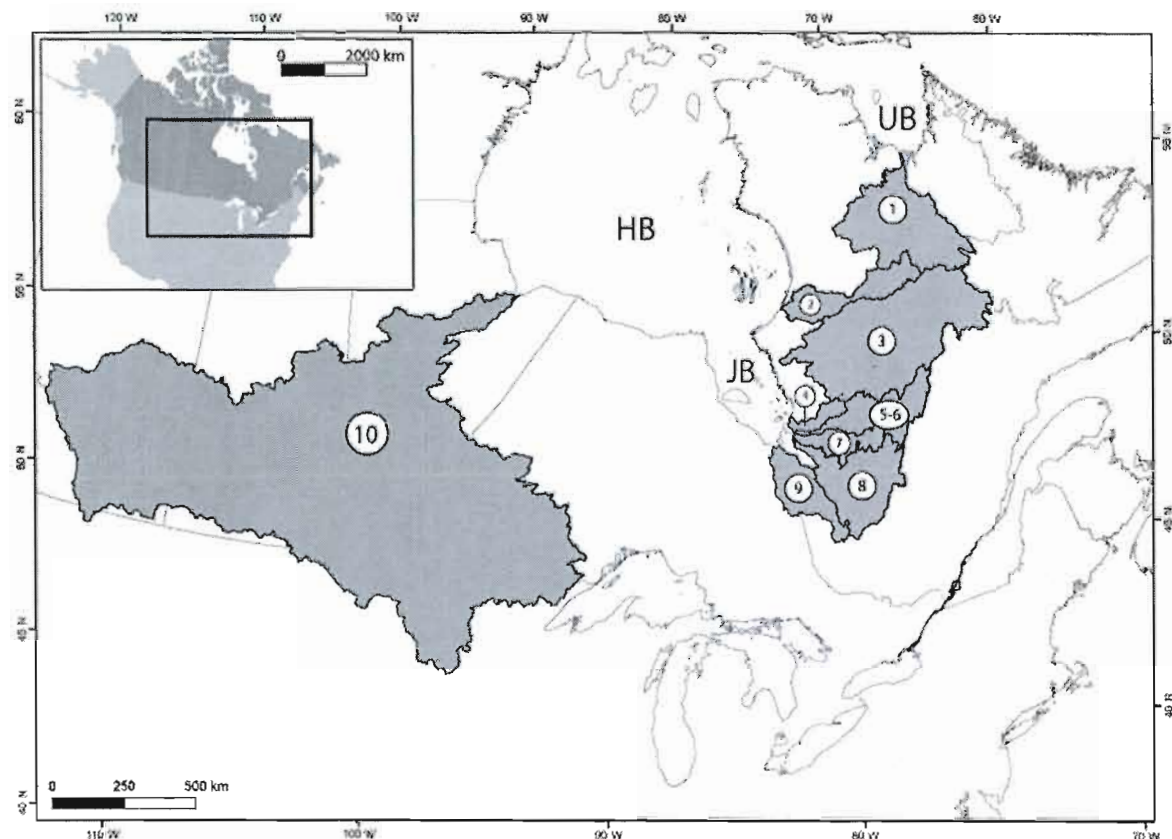
Map of the studied watersheds. Numbers refer to Table 1. See Table 1 for sampling sites exact locations. HB, JB and UB stand for Hudson Bay, James Bay and Ungava Bay, respectively. Modified from Chapter 1

Fig. 2 a. Temporal variations in U and (^{234}U/^{238}U) concentrations among the monitored rivers.
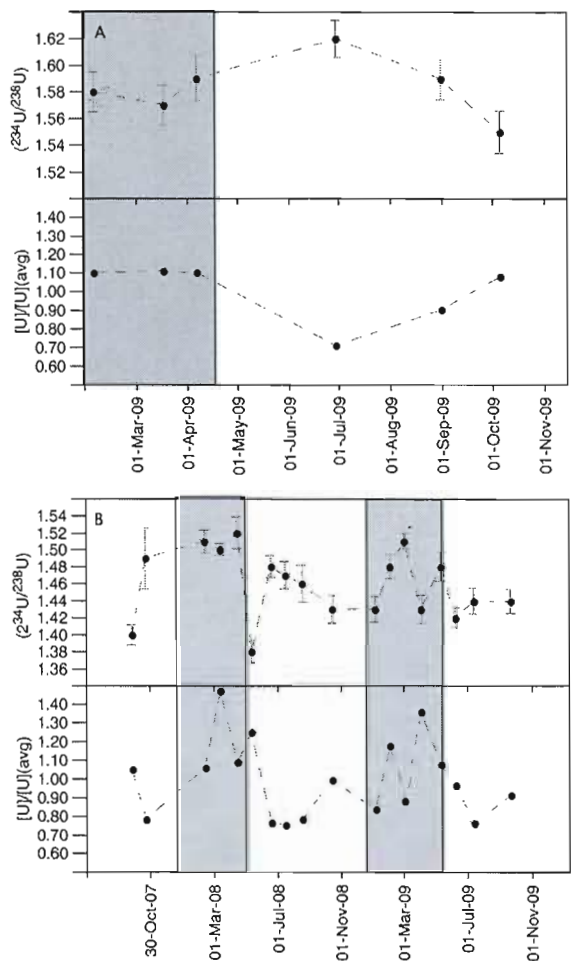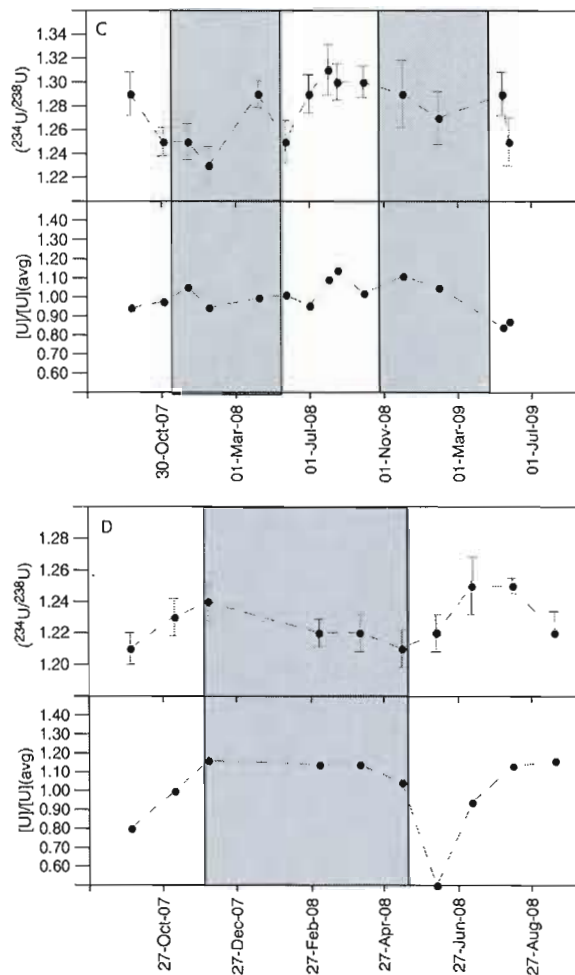
In the Koksoak (a), Great Whale (b) and Nelson (d) Rivers, the temporal variations in [U] match the seasonality, the main event being U dilution following snowmelt (the ice-on period is colored in light grey). The La Grande River (c) shows lesser variations in [U] in response to the increased water residence time within the large hydroelectric reservoirs built along its course, smoothing the seasonal variations. Some temporal variability in (^{234}U/^{238}U) is also observed (see differences in scales), but without clear seasonal pattern. The lack of imprint of the snowmelt event on (^{234}U/^{238}U) suggests that the corresponding drop in [U] concentrations is mostly due to dilution with dilute snowmelt waters.

Fig. 3. Dissolved U contents and isotopic properties in shield and platform regions
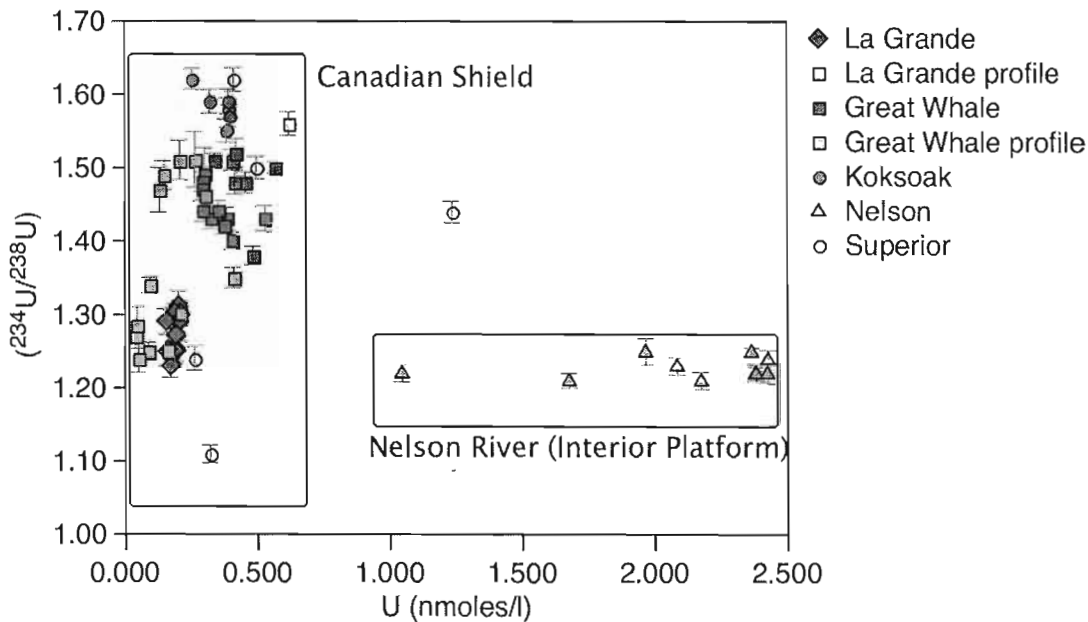
The distinct $(^{234}U/^{238}U)$ vs |U| clusters defined by the studied rivers are consistent with the hypothesis of a prominent lithological control on riverine U contents. The Nelson River (draining the Interior sedimentary Platform) shows an overall greater |U| and a smaller variability in $(^{234}U/^{238}U)$. In comparison, rivers draining shield catchments of the Canadian Shield present overall lower |U| and a greater variability in $(^{234}U/^{238}U)$. The Pontax River is an exception because of its comparatively high U content, which is attributed to the high DOC content of this river.

Fig. 4. $(^{234}U/^{238}U)$ vs Ca/U vs $^{87}Sr/^{86}Sr$.
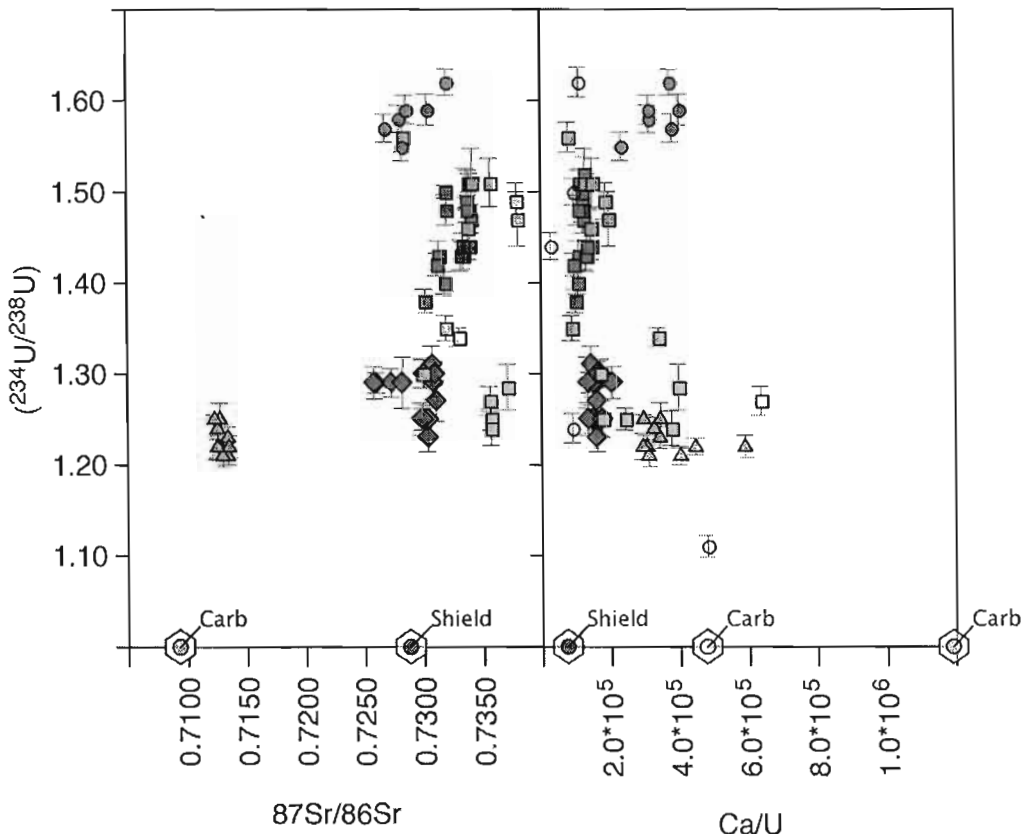
The distribution of $(^{234}U/^{238}U)$ reported against $^{87}Sr/^{86}Sr$ and Ca/U is consistent with the hypothesis of a lithological control on riverine U contents. The Canadian Shield silicate source (red symbol on the X axis), characterized by higher $^{87}Sr/^{86}Sr$ and lower Ca/U, presents overall higher and more variable $(^{234}U/^{238}U)$. See Fig.3 for legend.

REFERENCES

Andersen M.B., Stirling C.H., Porcelli D., Halliday A.N., Andersson P.S., Baskaran M. (2007). The tracing of riverine U in arctic seawater with very precise $^{234}U/^{238}U$ measurements. *Earth and Planetary Science Letters* **259**, 171-185.

Andersson P.S., Wasserburg G.J., Chen J.H., Papanastassiou D.A., Ingri J. (1995). ^{238}U-^{234}U and ^{232}Th-^{230}Th in the Baltic Sea and in river water. *Earth and Planetary Science Letters* **130**, 217–234.

Andersson P.S., Porcelli D., Wasserburg G.J., Ingri J. (1998). Particle transport of ^{234}U-^{238}U in the Kalix r iver and in the Baltic Sea. *Geochimica et Cosmochimica Acta* **62**, No 1, 385–392.

Andersson P.S., Porcelli D., Gustafsson Ö, Ingri J., Wasserburg G.J. (2001). The importance of colloids for the behavior of uranium isotopes in the low-salinity zone of a stable estuary. *Geochimica et Cosmochimica Acta* **65**, 13-25.

Bell R.T. (1996). Evaporites. In Géologie des types de gîtes minéraux du Canada. Revised by Eckstrand O.R., Sinclair W.D. and Thorpe R.I. Canada Geological Survey, pp 133-140.

Blacke W.H., Plater A.J., Boyle J. F. (1998). Seasonal trends in the uranium series isotopic signatures of lake waters and sediments: Hawes Water, Northwest England. *Journal of Paleolimnology* **20**, 1–14.

Chabaux F., Riotte J., Clauer N., France-Lanord C. (2001). Isotopic tracing of the dissolved U fluxes of Himalayan rivers: Implications for present and past U budgets of the Ganges-Brahmaputra system. *Geochimica et Cosmochimica Acta* **65**, 3201-3217.

Chabaux F., Riotte J., Dequincey O. (2003). U-Th-Ra fractionation during weathering and river transport. *Reviews in Mineralogy and Geochemistry* **52**, 533–576

Chabaux F., Granet M., Pelt E., France-Lanord C., Galy V. (2006). ^{238}U-^{234}U-^{230}Th disequilibria and timescale of sedimentary transfers in rivers: Clues from the Gangetic plain rivers. *Journal of Geochemical Exploration* **88**, 373-375.

Chabaux F, Bourdon B., Riotte J. (2008). U-Series Geochemistry in Weathering Profiles, River Waters and Lakes. In *Radioactivity in the Environment*, Volume 13, Chap. 3. Elsevier. pp. 49-104.

Chen J.H., Edwards R.L., Wasserburg G.J. (1986). ^{238}U, ^{234}U and ^{232}Th in seawater. *Earth and Planetary Science Letters* **80**, 241 – 251.

Cherdyntsev V.V., Chalov P.I., Khaidarov G.Z. (1955). Uranium series disequilibrium dating. *In:* Trans. 3rd Sess. Commission for determining the absolute age of geological formations, pp. 175-182

DePaolo D.J., Maher K., Christensen J.N., McManus J. (2006). Sediment transport time measured with U-series isotopes: Results from ODP North Atlantic dr ift site 984. *Earth and Planetary Science Letters* **248**, 394–410.

Déry S.J., Stieglitz M., McKenna E.C., Wood E.F. (2005). Characteristics and trends of river discharge into Hudson, James and Ungava Bays, 1964-2000. *Journal of Climate* **18**, 2540-2557.

Dosseto A., Bourdon B., Gaillardet J., Allègre C.J. and Filizola N. (2006a). Time scale and conditions of weathering under tropical climate : Study the Amazon basin with U-series. *Geochimica et Cosmochimica Acta* **70**, 71–89.

Dosseto A., Turner S. P. and Douglas G. B. (2006b). Uranium-series isotopes in colloids and suspended sediments: Timescale for sediment production and transport in the Murray-Darling river system. *Earth and Planetary Science Letters* **246**, 418–431.

Dosseto A.B., Bourdon B., Gaillardet J., Allègre C.J., Maurice-Bourgoin L. (2006c). Weathering and transport of sediments in the Bolivian Andes: Time constraints from uranium-series isotopes. *Earth and Planetary Science Letters* **248**, 759–771.

Dunk R.M., Mills R.A., Jenkins W.J. (2002). A reevaluation of the oceanic uranium budget for the Holocene. *Chemical Geology*. **190**, 45-67.

Dupré B., Gaillardet J., Rousseau D., Allègre, C.J. (1996). Major and trace element of river-borne material: the Congo Basin. *Geochimica et Cosmochimica Acta* **60**, 1301-1321.

Dupré B., Viers J., Dandurand L.J., Polve M., Bénézeth P., Vervier P., Braun J.J. (1999). Major and trace elements associated with colloids in organic-rich river waters: Ultrafiltration of natural and spiked solutions. *Chemical Geology* **160**, 63–80.

Durand S. (2000). Suivi saisonnier des teneurs en ^{238}U-^{234}U et en ^{226}Ra du fleuve St-Laurent un regard sur les conditions hydroclimatiques dans le bassin de drainage. Master thesis, Université du Québec à Montréal, 33 p.

Durand S., Chabaux F., Rihs S., Duringer P., Elsass P. (2005). U isotope ratios as tracers of groundwater inputs into surface waters: Example of the Upper Rhine hydrosystem. *Chemical Geology* **220**, 1–19.

Environment Canada, climatic archive database, http://climate.weatheroffice.gc.ca/climateData

Gauthier M. (2000). Mineral deposit characteristics and distribution in the James Bay region of Quebec. *Chroniques de la Recherche Minière* **539**, 17-61.

Granet M., Chabaux F., Stille P., France-Lanord C., Pelt E. (2007). Time-scales of sedimentary transfer and weathering processes from U-series nuclides: Clues from the Himalayan rivers. *Earth and Planetary Science Letters* **261**, 389–406.

Grzymko T.J., Marcantonio F., McKee B.A., Stewart C. M. (2007). Temporal variability of uranium concentrations and ^{234}U/^{238}U activity ratios in the Mississippi river and its tributaries. *Chemical Geology* **243**, 344-356.

Hayeur G. (2001). Synthèse des connaissances environnementales acquises en milieu nordique de 1970 à 2000. Montréal, Hydro-Québec. 110pp.

Hélie J.F., Hillaire-Marcel C., Rondeau B. (2002). Seasonal changes in the sources and fluxes of dissolved inorganic carbon through the St. Lawrence River – isotopic and chemical constraint. *Chemical Geology* **186**, 117-138.

Kigoshi K. (1971). Alpha-recoil thorium-234: disequilibrium in nature. *Science* **173**, 47-48.

Kronfeld J., Vogel J. C. (1991). Uranium isotopes in surface waters from southern Africa. *Earth and Planetary Science Letters* **105**, 191–195.

McCulloch M.T., Wasserburg G.J. (1978). Sm-Nd and Rb-Sr Chronology of Continental Crust Formation. *Science* **200**, No 4345, 1003-1011.

Meybeck M., Pasco A., Ragu A. (1992). Établissement des flux polluants dans les rivières. Étude Inter-agences No 28. Agence de l'Eau / Ministère de l'Environnement, Paris.

Meybeck M., Ragu A. (1996). River discharges to the oceans. An assessment of suspended solids, major ions and nutrients. Environmental Information and Assessment Report. UNEP, Nairobi, 250p.

Meynadier L., Gorge C., Birck J.L., Allègre C.J. (2006). Automated separation of Sr from natural water samples or carbonate rocks by high performance ion chromatography. *Chemical Geology* **227**, 26-36.

Ministère du Développement durable, de l'Environnement et des Parcs. www.mddep.gouv.qc.ca

Moore W.S. and Shaw T.J. (2008). Fluxes and behavior of radium isotopes, barium and uranium in seven Southeastern US rivers and estuaries. *Marine Chemistry* **108**, issue 3-4, 236-254.

Moreira-Nordemann L.M. (1980). Use of $^{234}U/^{238}U$ disequilibrium in measuring chemical weathering rate of rocks. *Geochimica et Cosmochimica Acta* **44**, 103–108.

Osmond J.K., Ivanovitch M. (1992). Uranium-series mobilization and surface hydrology. *In:* Uranium series disequilibrium: Application to Earth, Marine, and Environmental Sciences. Ivanovich M, Harmon RS (eds), Oxford Sciences Publications, Oxford, pp. 259-289.

Osmond J.K., Kowart J.B. (1992). Ground Water. *In:* Uranium series disequilibrium: Application to Earth, Marine, and Environmental Sciences. Ivanovich M, Harmon RS (eds), Oxford Sciences Publications, Oxford, pp. 290-333.

Palmer M.R., Edmond J.M. (1993). Uranium in river water. *Geochimica et Cosmochimica Acta* **57**, 4947-4955.

Pande K., Sarin M. M., Trivedi J. R., Krishnaswami S., and Sharma K. K. (1994). The Indus River system (India–Pakistan): Major-ion chemistry, uranium and strontium isotopes. *Chemical Geology* **116**, 245–259.

Porcelli D., Andersson P.S., Wasserburg G.J., Ingri J., Baskaran M. (1997). The importance of colloids and mires for the transport of U isotopes through the Kalix River watershed and Baltic Sea. *Geochimica et Cosmochimica Acta* **61**, 4095-4113.

Riotte J. and Chabaux F. (1999) $(^{234}U/^{238}U)$ activity ratios in freshwaters as tracers of hydrological processes: The Strengbach watershed (Vosges, France). *Geochimica et Cosmochimica Acta* **63**, 1263-1275.

Riotte J., Chabaux F., Benedetti M., Dia A., Boulègue J., Gérard M., Etamé J. (2003). Uranium colloidal transport and the origin of the ^{234}U-^{238}U fractionation in surface waters: New insights from

Mount Cameroun. *Chemical Geology* **202**, 365–381.

Robinson L.F., Henderson G.M., Hall L., Matthews I. (2004). Climatic control of riverine and seawater uranium-isotope ratios. *Science* **305**, 851–854.

Rondeau B., Cossa D., Gagnon P., Pham T.T., and Surette C. (2005). Hydrological and biogeochemical dynamics of the minor and trace elements in the St. Lawrence River. *Applied Geochemistry* **20**, 1391-1408.

Ryu J.S., Lee K.S., Chang H.W., Cheong C.S. (2009). Uranium isotopes as a tracer of sources of dissolved solutes in the Han River, South Korea. *Chemical Geology* **258**, 354-361.

Sarin M.M., Krishnaswami S., Somayajulu B.L.K. and Moore W.S. (1990). Chemistry of uranium, Thorium, and Radium isotopes in the Ganga–Brahmaputra river system: Weathering processes and fluxes to the Bay of Bengal. *Geochimica et Cosmochimica Acta* **54**, 1387–1396.

Shaw D.M., Cramer J.J., Higgins M.D. and Truscott M.G. (1986). Composition of the Canadian Precambrian Shield and the continental crust of the Earth. Geological Society, London, Special Publications 24, 275-282.

Shotyk W. (1988). Review of the Inorganic Geochemistry of Peats and Peatland Waters. *Earth-Science Reviews* **25**, 95-176.

Shotyk W., Nesbitt H.W. and Fyfe W.S. (1992). Natural and anthropogenic enrichments of tracemetals in peat profiles. *International Journal of Coal Geology* **20**, 49-84

Stott D.F., Aitken J.D. (1993). Introduction to the Interior Platform, Western Basins and Eastern Cordillera. Chapter 2 in Sedimentary cover of the Craton in Canada, Stott D.F. and Aitken J.D. (ed.), Geological Survey of Canada, Geology of Canada no. 5, pp. 11-54.

Sun H., Semkow T.M. (1998). Mobilization of thorium, radium and radon nuclides in ground water by successive alpha-recoils. *Journal of Hydrology* **205**,126-136.

Swarzensky P., Campbell P., Porcelli D. McKee B. (2004). The estuarine chemistry and isotope systematics of $^{234, 238}$U in the Amazon and Fly Rivers. *Continental Shelf Research* **24**, 2357-2372.

Tarnocai C., Kettles I.M., Lacelle B. (2000). Peatlands of Canada Database. Geological Survey of Canada Open File 3834.

Van Bellen S., Dallaire P.L., Garneau M., Bergeron Y. (in press). Quantifying spatial and temporal Holocene carbon accumulation in ombrotrophic peatlands of the Eastmain region, Quebec, Canada. *Global Biogeochemical Cycles*, in press.

Vigier N., Bourdon B., Turner S., Allègre C.J. (2001). Erosion timescales derived from U-decay series measurements in rivers. *Earth and Planetary Science Letters* **193**, 485–499.

Vigier N., Bourdon B., Lewin E., Dupré B., Turner S., Chakrapani G.J., Van Calsteren P., Allègre C.J. (2005). Mobility of U-series nuclides during Basalt Weathering: An example from the Deccan Traps (India). *Chemical Geology* **219**, 69–91.

Wadleigh M.A., Veizer J., Brooks C. (1985). Strontium and its isotopes in Canadian rivers: fluxes and

global implications. *Geochimica et Cosmochimica Acta* **49**, 1727 – 1736.

Wheeler J.O., Hoffman P.F., Card K.D., Davidson A., Sanford B.V., Okulich A.V., Roest W.R. (1996). Geological Map of Canada, Geological Survey of Canada, map 1860A, scale 1:5 000 000.

Windom H., Smith R., Niencheski F., Alexander C. (2000). Uranium in rivers and estuaries of globally diverse, smaller watersheds. *Marine Chemistry* **68**, 307-321.

CONCLUSION GÉNÉRALE

L'objectif général de la présente thèse était d'évaluer les incidences de l'environnement géologique et du climat sur le cycle de l'eau et l'altération chimique au sein de bassins hydrographiques du nord-est du Canada. Afin de répondre à cet objectif, une approche fondée sur la documentation de la variabilité spatiotemporelle des signaux géochimiques (δ^{18}O-δ^{2}H, ions majeurs, Sr, U, Nd, DOC) transportés par les rivières a été privilégiée. D'un point de vue scientifique, l'étude s'insère dans le cadre des démarches visant à améliorer la compréhension de deux processus qui dictent l'évolution de la surface terrestre : le cycle de l'eau et l'altération chimique. D'un point de vue pratique, elle s'insère dans le cadre des démarches visant améliorer la prévisibilité des changements dans la qualité et la quantité des ressources hydriques renouvelables, en lien avec les changements climatiques et les pressions anthropiques sur ces ressources.

L'originalité de cette étude réside (i) en l'utilisation couplée de traceurs géochimiques permettant de documenter quantitativement le cycle de l'eau et l'altération chimique, (ii) en l'établissement d'un réseau de monitoring temporel des flux exportés par les rivières, (iii) en la comparaison directe de rivière drainant des bassins contigus couvrant plus de 2.8×10^6 km^2 sur plus de 15 degrés de latitude et (iv) en l'établissement de règles quantitatives permettant d'illustrer les contrôles géologiques et climatiques sur la géochimie des rivières.

Les conclusions qui émergent de la présente étude peuvent être regroupées en deux grands ensembles : les conclusions relatives au traçage géochimique du cycle de l'eau (i) et les conclusions relatives à la dynamique de l'altération chimique (ii). Dans les deux cas, la variabilité spatiotemporelle est explorée.

Conclusions relatives au traçage isotopique du cycle de l'eau

En ce qui a trait à au traçage isotopique du cycle de l'eau, la présente étude permet de documenter le bassin hydrographique du Saint-Laurent et les bassins du Bouclier Canadien alimentant les baies d'Hudson, de James et d'Ungava (HJUB). Les principales conclusions sont rapportées ci-dessous.

1- L'étude a permis d'illustrer que les signaux $\delta^{18}O$-δ^2H mesurés dans les rivières de la région d'étude présentent des variations saisonnières systématiques qui sont atténuées et déphasées par rapport à celles observées dans les précipitations. L'amplitude de ces variations saisonnières est de l'ordre 1 à 5‰ ($\delta^{18}O$), selon les bassins. Deux principaux mécanismes dictent ces variations saisonnières : (i) la fonte des neiges induit un appauvrissement en isotopes lourds marquant l'apport de précipitations (appauvries en isotopes lourds) accumulées dans les bassins au cours de la saison hivernale, (ii) L'évaporation entraine un enrichissement graduel en isotopes lourds au cours de la période libre de glace. La rivière La Grande est une exception à cette règle en raison de l'effet tampon causé par les réservoirs hydroélectriques qui la ponctuent. Ainsi, l'amplitude des variations saisonnières en δ^2H-$\delta^{18}O$ est indépendante de la taille des bassins et semble plutôt fonction de l'effet tampon des réservoirs hydroélectriques.

2- Les résultats de la présente étude permettent l'estimation des taux d'évaporation dans les bassins hydrographiques à l'étude. Les données tendent à indiquer que les rivières définissent des droites évaporatoires locales. Notamment, lorsque rapportées dans un graphique δ^2H vs $\delta^{18}O$, les rivières définissent des droites situées sous la droite des eaux météoriques et ayant une pente plus faible que cette dernière. Ainsi, il est possible d'estimer les taux d'évaporation dans les bassins hydrographiques à partir des enrichissements isotopiques mesurés le long des droites évaporatoires. Par exemple, à partir de bilans de masses isotopiques, il a été estimé que 40% de l'eau atteignant le bassin des Grands Lacs est retournée vers l'atmosphère par évaporation avant de rejoindre le tronçon sud du Fleuve Saint Laurent via l'exutoire du Lac Ontario. De façon similaire, il a été possible d'estimer à 5-15% les taux d'évaporation dans les bassins hydrographiques du nord-est du Canada.

3- Dans le cas de l'estuaire fluvial du Saint-Laurent, un bilan de masse isotopique a pu être établi afin de départager les contributions relatives des masses d'eau provenant des Grands Lacs vs de la rivière des Outaouais.

4- Les résultats présentés dans le cadre de cette étude ont permis d'illustrer les variations spatiales systématiques dans les teneurs en ^2H-^{18}O au sein de rivières drainant des bassins hydrographiques contigus sur plus de 12 degrés de latitude. Les rivières du nord-est du Canada définissent un gradient isotopique latitudinal ($\delta^{18}O_{(‰\ vs\ VSMOW)} = -0.36 * Latitude + 4.4‰$) parallèle à celui rapporté pour les précipitations au niveau de la même région. Cette observation tend à indiquer que le gradient isotopique hérité des précipitations est conservé dans les rivières, malgré les processus

hydrologiques subséquents à la recharge des bassins. Ainsi, les données isotopiques recueillies au sein du programme GNIR (*Global Network for Isotopes in Rivers*) de l'agence internationale de l'Énergie Atomique (IAEA) pourraient constituer un complément aux données du programme GNIP (*Global Network for Isotopes in Precipitation*). Notamment, tel que suggéré par les résultats de la présente étude, les rivières offrent l'avantage d'intégrer les signaux isotopiques à l'échelle des bassins qu'elles drainent, contrairement aux stations GNIP qui sont ponctuelles et distribuées de façon hétérogène.

Conclusions relatives à la dynamique de l'altération chimique:

En ce qui a trait à la documentation de la dynamique de l'altération chimique, la présente étude se concentre sur les rivières drainant des bassins hydrographiques alimentant les baies d'Hudson, James et d'Ungava (HJUB). Les rivières étudiées transportent environ 50% des flux d'eau douce atteignant l'HJUB. Les principales conclusions sont rapportées ci-dessous.

1- Les résultats de cette thèse ont permis de quantifier l'amplitude et de discuter des causes des variations saisonnières dans les concentrations en éléments dissous des rivières. Comme pour les teneurs en ^{2}H-^{18}O, les concentrations dissoutes en cations majeurs, en strontium et en uranium mesurées au sein des rivières de la région d'étude présentent des variations saisonnières qui transcrivent l'effet des conditions hydro-climatiques. La dilution causée par la fonte des neiges constitue le trait caractéristique des chroniques saisonnières de concentrations d'éléments dissous. L'amplitude des variations saisonnières de concentrations en éléments dissous (jusqu'à un facteur 2 pour les ions majeurs et 4 pour le Nd) illustre l'importance du monitoring saisonnier pour la quantification des flux exportés par les rivières. Ici encore, la rivière La Grande constitue une exception, ses concentrations en éléments dissous étant stables en raison de l'effet tampon des réservoirs hydroélectriques.

2- Les résultats présentés pour les rivières alimentant l'HJUB ont permis d'évaluer les compositions chimiques moyennes des rivières drainant le Bouclier canadien et de les comparer à celles du fleuve Nelson, ce dernier drainant principalement les roches sédimentaires de la Plate-Forme Intérieure. Les rivières du Bouclier présentent des concentrations dissoutes en cations majeurs variant entre 62 et 360 µM, des concentrations en Nd de 0.57 à 4.72 nM et des teneurs en carbone organique dissous (COD) de 241 et 1777 µM. En comparaison, le fleuve Nelson présente des

concentrations en cations majeurs plus élevées (1200-2276 µM), des concentrations en Nd dissous plus faibles (0.14-0.45 nM) et des teneurs intermédiaires en COD (753-928 µM).

3- L'étude a permis de quantifier les flux cationiques exportés par les rivières et de les transcrire en taux d'altération des roches au sein des bassins. Les rivières étudiées exportent vers l'HJUB un flux cationique dissous (Na-K-Mg-Ca-Sr) atteignant 8×10^6 tonnes an^{-1}. De ce flux total, 88% est attribuable au fleuve Nelson. Les taux d'altération chimique des roches calculés à partir de ces flux varient entre 1.0 et 5.6 tonnes km^{-2} an^{-1} au sein des bassins hydrographiques du Bouclier Canadien et ont une valeur moyenne de 5.3 tonnes km^{-2} an^{-1} au sein de la Plate-forme Intérieure (Fleuve Nelson).

4- Les résultats présentés dans le cadre de l'étude ont permis d'identifier le mécanisme de contrôle principal sur les taux d'altération chimique des roches dans la région de l'HJUB. Ces taux d'altération sont essentiellement contrôlés par la composition lithologique des bassins, tel que démontré par la relation établie entre l'abondance de roches volcaniques et sédimentaires (V+S%) dans les bassins et les taux d'altération cationiques des roches (en tonnes km^{-2} an^{-1}) (ACR): ACR=0.8(V+S%)+0.9. Au sien des rivières de l'HJUB, l'alcalinité produite par l'altération de roches demeure faible en comparaison aux exports de COD. Ainsi, la dynamique du carbone organique est plus importante que l'altération chimique des roches en ce qui a trait au rôle de ces rivières sur le cycle global du carbone.

5- Les données permettent d'illustrer le rôle du cycle de la matière organique sur les flux dissous inorganiques exportés par les rivières. Au sein des bassins hydrographiques de l'HJUB, les flux de DOC sont découplés des taux d'altération cationique des roches. Or, le rôle de la matière organique sur les processus d'altération chimique des roches est illustré par la corrélation évaluée entre les flux de COD et de lanthanides (r^2=0.95). Ainsi, les données suggèrent que le cycle de la matière organique contrôle la mobilité de certains éléments traces ayant une affinité pour les colloïdes organiques. L'intensité des les flux de COD exportés par les rivières de l'HJUB semble tributaire des conditions hydro-climatiques. Par exemple, au sein du Bouclier canadien, l'intensité de ces flux diminue vers le nord, une observation attribuée aux taux de ruissellement plus faibles et aux sols moins développés vers le nord de la région d'étude.

6- L'étude des isotopes de l'U en phase dissoute dans les rivières a permis d'identifier un traceur isotopique qui pourrait permettre de tracer les apports fluviaux d'U dans le domaine océanique, tel

qu'illustré par les signatures $(^{234}U/^{238}U)$ distinctes mesurées au niveau des grandes rivières de l'HJUB (Koksoak, Great Whale, La Grande et Nelson). Ce traceur serait spécialement utile pour départager les flux provenant des rivières du bouclier, où les signatures dissoutes en $(^{87}Sr/^{86}Sr)$ se chevauchent. Notons aussi que l'étude a permis d'évaluer que les rivières étudiées exportent 3.4×10^5 moles/an d'U vers l'HJUB, avec un ratio $(^{234}U/^{238}U)$ moyen de 1.27.

Retombées et applications

En ce qui a trait au traçage géochimique du cycle de l'eau, les principales applications de cette thèse concernent l'évaluation des taux d'évaporation à l'échelle des bassins versants. Ainsi, les isotopes de la molécule d'eau pourraient s'avérer un outil pertinent afin de calibrer les modèles hydrologiques prédictifs. Une telle validation semble essentielle dans une région comme le nord-est canadien, où les changements climatiques anticipés pourraient fortement impacter la quantité des eaux de surface (Déry et al., 2004; 2005; 2009; Boyer et al., 2010). En ce qui a trait à la documentation de la dynamique de l'altération chimique, les principales retombées de cette thèse concernent la quantification de la variabilité saisonnière des concentrations dissoutes dans les rivières et l'établissement de règles quantitatives permettant d'illustrer les paramètres qui dictent l'intensité des flux dissous exportés par les rivières.

Ouvertures

La présente étude s'est concentrée sur les flux dissous exportés par les rivières, permettant d'estimer les taux d'altération chimique des roches. Dans le future, la documentation des flux particulaires s'avèrera fondamentale à l'évaluation des taux d'érosion mécanique. La documentation des processus de mélange au sein des estuaires sera fondamentale à l'établissement des flux dissous exportés par les rivières atteignant réellement le domaine océanique de l'HJUB. La prise en charge du réseau de monitoring des rivières du nord du Québec exploité lors de cette thèse par Environnement Canada devrait permettre, à terme, d'évaluer les changements interannuels dans les flux exportés par les rivières, en lien avec les synoptiques climatiques (AO, NAO, ENSO). L'établissement de bilans de carbone, en traçant les sources et l'âge du carbone organique exporté par les rivières de même que son taux d'enfouissement dans les estuaires, s'avèrera cruciale à l'évaluation du rôle des bassins de l'HJUB dans le cycle global du carbone.

RÉFÉRENCES

Andersen M.B., Stirling C.H., Porcelli D., Halliday A.N., Andersson P.S., Baskaran M. (2007). The tracing of riverine U in arctic seawater with very precise $^{234}U/^{238}U$ measurements. *Earth and Planetary Sciences Letters* **259**, 171-185.

Anderson S.P., Drever J.I., Frost C.D., Holden P. (2000). Chemical weathering in the foreland of a retreating glacier. *Geochimica et Cosmochimica Acta* **64**, 1173-1189.

Andersson P.S., Wasserburg G.J., Chen J.H., Papanastassiou D.A., Ingri J. (1995). ^{238}U-^{234}U and ^{232}Th-^{230}Th in the Baltic Sea and in river water. *Earth and Planetary Science Letters* **130**, 217–234.

Andersson P.S., Porcelli D., Wasserburg G.J., Ingri J. (1998). Particle transport of ^{234}U-^{238}U in the Kalix r iver and in the Baltic Sea. *Geochimica et Cosmochimica Acta* **62**, No 1, 385–392.

Andersson P.S., Porcelli D., Gustafsson Ö, Ingri J., Wasserburg G.J. (2001). The Importance of colloids for the behavior of uranium isotopes in the low-salinity zone of a sTable estuary. *Geochimica et Cosmochimica Acta* **65**, 13-25.

Araguas-Araguas L., Froehlich K., Rozanski K. (2000). Deuterium and oxygen-18 isotope composition of precipitation and atmospheric moisture. *Hydrological Processes* **16**: 1341 – 1355.

Arctic RIMS, A Regional, Integrated Hydrological Monitoring System for the Pan-Arctic Land Mass. http://rims.unh.edu/

Bell R.T. (1996). Evaporites. In Géologie des types de gîtes minéraux du Canada. Revised by Eckstrand O.R., Sinclair W.D. and Thorpe R.I. Canada Geological Survey, pp 133-140.

Berner R.A., Lasaga A.C., Garrels, R.M. (1983). The carbonate – silicate geochemical cycle and its effect on atmospheric carbon dioxide over the past 100 million years. *American Journal of Science* **284**, 1183 – 1192.

Birks S.J., Edwards T.W.D., Gibson J.J., Drimmie R.J., Michel F.A. (2004). Canadian Network for isotopes in precipitation. http://www.science.uwaterloo.ca/~twdedwar/cnip/cniphome.html.

Blacke W.H., Plater A.J., Boyle J. F. (1998). Seasonal trends in the uranium series isotopic signatures of lake waters and sediments: Hawes Water, Northwest England. *Journal of Paleolimnology* **20**, 1–14.

Bowen G.J., Wilkinson B. (2002). Spatial distribution of $\delta^{18}O$ in meteoric precipitation. *Geology* **30**, no4: 315-318.

Bowen G.J., Revenaugh J. (2003). Interpolating the isotopic composition of modern meteoric precipitation. *Water Resources Research* **39**, no 10: 1299. doi:10.1029/2003WR002086.

Boyce F.M., Donelan M.A., Hamblin P.F., Murthy C.R., Simons T.J. (1989). Thermal Structure and Circulation in the Great Lakes. *Aymosphere-Ocean* **27** (4): 607-642. doi: 0705-5900/89/0000-0607$01.25/0

Boyer C., Chaumont D., Chartier I., Roy A.G. (2010). Impact of climate change on the hydrology of St. Lawrence tributaries. *Journal of Hydrology* **384**: 65–83. doi:10.1016/j.jhydrol.2010.01.011.

Calmels D., Gaillardet J., Brenot A., France-Lanord C. (2007). Sustained sulfide oxidation by physical erosion processes in the Mackenzie River basin: Climatic perspectives. *Chemical Geology* **35**, no 11, 1003-1006.

Card K.D., Poulsen K.H. (1998). Géologie des gîtes minéraux de la province du la Supérieur, Bouclier canadien; dans Géologie des provinces précambriennes du lac Supérieur et de Grenville et fossiles du Précambrien en Amérique du Nord, chap. 2, coord. S.B. Lucas et M.R. St-Onge, Commission Géologique du Canada no. 7.

Chabaux F., Riotte J., Clauer N., France-Lanord C. (2001). Isotopic tracing of the dissolved U fluxes of Himalayan rivers: Implications for present and past U budgets of the Ganges-Brahmaputra system. *Geochimica et Cosmochimica Acta* **65**, 3201-3217.

Chabaux F., Riotte J., Dequincey O. (2003). U-Th-Ra fractionation during weathering and river transport. *Reviews in Mineralogy and Geochemistry* **52**, 533–576

Chabaux F., Granet M., Pelt E., France-Lanord C., Galy V. (2006). ^{238}U-^{234}U-^{230}Th disequilibria and timescale of sedimentary transfers in rivers: Clues from the Gangetic plain rivers. *Journal of Geochemical Exploration* **88**, 373–375.

Chabaux F, Bourdon B., Riotte J. (2008). U-Series Geochemistry in Weathering Profiles, River Waters and Lakes. In *Radioactivity in the Environment*, Volume 13, Chap. 3. Elsevier. pp. 49-104.

Chen J.H., Edwards R.L., Wasserburg G.J. (1986). ^{238}U, ^{234}U and ^{232}Th in seawater. *Earth and Planetary Science Letters* **80**, 241 – 251.

Cherdyntsev V.V., Chalov P.I., Khaidarov G.Z. (1955). Uranium series disequilibrium dating. *In:* Trans. 3rd Sess. Commission for determining the absolute age of geological formations, pp. 175-182.

Clark I.D., Fritz P. (1997). Environmental Isotopes in Hydrogeology . CRC Press.

Coplen, T.B. (1996). New guidelines for reporting stable hydrogen, carbon, and oxygen isotope-ratio data. *Geochimica et Cosmochimica Acta* **60** : 3359 - 3360.

Craig H. (1961). Isotopic variations in meteoric waters. *Science* **133**: 1702 – 1703.

Craig H., Gordon L.I. (1965). Deuterium and oxygen-18 variations in the ocean and marine atmosphere. In Tongiorgi E (ed.). *Stable Isotopes in Oceanographic Studies and Paleotemperatures*, Pisa: Cons. Naz. Rich. Lab. Geol. Nucl.: 9 – 130.

Dansgaard W. (1964). Stable isotopes in precipitation. *Tellus* **16**: 436 – 468.

Davidson A. (1998). Survol de la géologie de la province de Grenville, Bouclier canadien; dans Géologie des provinces précambriennes du lac Supérieur et de Grenville et fossiles du Précambrien en Amérique du Nord, chap. 3, coord. S.B. Lucas et M.R. St-Onge, Commission Géologique du Canada no. 7.

Deberdt S., Viers J., Dupré B. (2002). New insights about the rare earth elements (REE) mobility in river water. *Bulletins de la Société Geologique de France* **173**, no 2, 147-160.

DePaolo D.J., Maher K., Christensen J.N., McManus J. (2006). Sediment transport time measured with U-series isotopes: Results from ODP North Atlantic dr ift site 984. *Earth and Planetary Science Letters* **248**, 394–410.

Déry SJ, Wood EF. 2004. Teleconnection between the Arctic Oscillation and Hudson Bay river discharge. *Geophysical Research Letters* **31**, L18205, doi:10.1029/2004GL020729.

Déry S.J., Stieglitz M., McKenna E.C., Wood E.F. (2005). Characteristics and Trends of River Discharge into Hudson, James and Ungava Bays, 1964-2000. *Journal of Climate* **18**, 2540-2557.

Déry S.J., Hernandez-Henriquez M.A., Burford J.E., Wood E.F. (2009). Observational evidence of an intensifying hydrological cycle in northern Canada. *Geophysical Research Letters* 36, 13, L13402.

Dessert C., Dupré B., Gaillardet J., François L.M., Allègre C.J. (2003). Basalt weathering laws and the impact of basalt weathering on the global carbon cycle. *Chemical Geology* **202**, 257-273.

Dosseto A., Bourdon B., Gaillardet J., Allègre C.J. and Filizola N. (2006a). Time scale and conditions of weathering under tropical climate : Study the Amazon basin with U-series. *Geochimica et Cosmochimica Acta* **70**, 71–89.

Dosseto A., Turner S. P. and Douglas G. B. (2006b). Uranium-series isotopes in colloids and suspended sediments: Timescale for sediment production and transport in the Murray-Darling river system. *Earth and Planetary Science Letters* **246**, 418–431.

Dosseto A.B., Bourdon B., Gaillardet J., Allègre C.J., Maurice-Bourgoin L. (2006c). Weathering and transport of sediments in the Bolivian Andes: Time constraints from uranium-series isotopes. *Earth and Planetary Science Letters* **248**, 759–771.

Dunk R.M., Mills R.A., Jenkins W.J. (2002). A reevaluation of the oceanic uranium budget for the Holocene. *Chemical Geology.* **190**, 45-67.

Dupré, B., Gaillardet, J., Rousseau D., Allègre, C.J. (1996). Major and trace element of river-borne material: the Congo Basin. *Geochimica et Cosmochimica Acta* **60**, 1301-1321.

Dupré B., Viers J., Dandurand J. L., Polve M., Bénézeth P., Vervier P., Braun J.-J. (1999). Major and trace elements associated with colloids in organic-rich river waters: Ultrafiltration of natural and spiked solutions. *Chemical Geology* **160**, 63–80.

Dupré B., Dessert C., Oliva P., Goddéris Y., Viers J., François L., Millot R., Gaillardet J. (2003). Rivers, chemical weathering and Earth's climate. *Comptes Rendus de Geosciences* **335** (16), 1141-1160.

Durand S., Chabaux F., Rihs S., Duringer P., Elsass P. (2005). U isotope ratios as tracers of

groundwater inputs into surface waters: Example of the Upper Rhine hydrosystem. *Chemical Geology* **220**, 1–19.

Durand S., Chabaux F., Rihs S., Duringer P., Elsass P. (2005). U isotope ratios as tracers of groundwater inputs into surface waters: Example of the Upper Rhine hydrosystem. *Chemical Geology* **220**, 1–19.

Ebelmen J.J. (1845). Sur le produit de la décomposition des espèces minérales de la famille des silicates: *Annales des Mines*, v. 7, p. 3–66.

Edmond J.M., Palmer M.R., Measures C.I., Grant B., Stallard R.F. (1995). The fluvial geochemistry and denudation rate of the Guayana Shield in Venezuela, Columbia and Brazil. *Geochimica et Cosmochimica Acta* **59**. 3301-3325.

Edmond J.M., Palmer M.R., Measures C.I., Brown E.T., Huh Y. (1996). Fluvial geochemistry of the eastern slope of the northeastern Andes and its foredeep in the drainage of the Orinoco in Columbia and Venezuela. *Geochimica et Cosmochimica Acta* **60**, 2949-2976.

Energy, mines and resources Canada. 1991. Canada Precipitation. The Atlas of Canada, 5th Edition, MCR 4097.

Energy, mines and resources Canada. 1991. Canada Precipitation. The Atlas of Canada, 5th Edition, MCR 4145.

Environment Canada, climatic archive database: http://climate.weatheroffice.gc.ca/climateData

France-Lanord C., Evans M., Hurtrez J.E., Riotte J. (2003). Annual dissolved fluxes from central Nepal Rivers: budget of chemical erosion in the Himalayas. *Compte Rendus Geoscience* **335**, 1131-1140.

Frenette M., Barbeau C., Verrette J.L. (1989). Aspects quantitatifs, dynamiques et qualitatifs des sédiments du Saint-Laurent, Projet de mise en valeur du Saint-Laurent. Hydrotech Inc., Consultants for Environment Canada and the Government of Quebec.

Fritz P., Drimmie R.J., Frape S.K., O'Shea K. (1987). The isotopic composition of precipitation and groundwater in Canada. In *Isotope techniques in water resources developments, IAEA Symposium 299*, March, Vienna; 539 – 550.

Fulton R.J. (Compiler). (1995). Surficial Materials of Canada. Geological Survey of Canada Map. 1880A, scale 1 :5 000 000.

Gaillardet J., Dupré B., Allègre C.J. (1995). A global geochemical mass budget applied to the Congo Basin rivers: erosion rates and continental crust composition. *Geochimica et Cosmochimica Acta* **59** no. 17 , 3469 – 3485.

Gaillardet J., Dupré B., Allègre C.J., Négrel P. (1997). Chemical and physical denudation in the Amazon river basin. *Chemical Geology* **142**, 141 – 173.

Gaillardet J., Dupré B., Louvat P., Allègre C.J. (1999). Global silicate weathering and CO_2 consumption rates deduced from the chemistry of large rivers. *Chemical Geology* **159**, 3–30.

Gaillardet J., Millot R., and Dupré B. (2003) Chemical denudation rates of the western Canadian orogenic belt: The Stikine terrane. *Chemical Geology* **201**, 257–259.

Gaillardet J., Viers J., Dupré B. (2003). Trace elements in river waters. In: *Treatise on Geochemistry (Eds H. D. Holland and K. K. Turekian). Vol. 5, Surface and ground water, weathering and soils (Ed J. I. Drever)*, pp. 225–272.

Galy A., France-Lanord C. (1999). Weathering processes in the Ganges-Brahmaputra basin and the riverine alkalinity budget. *Chemical Geology* **159**, 31– 60.

Gariepy C., Ghaleb B., Hillaire-Marcel C., Mucci A. Vallieres S. (1994). Early Diagenetic Processes in Labrador Sea Sediments - Uranium-Isotope Geochemistry. *Canadian Journal of Earth Sciences* **31**, 28-37.

Garrels R.M., Mackenzie F.T. (1967). Origin of the chemical compositions of some springs and lakes. In *Equilibrium Concepts in Natural Water Systems* (ed. W. StuµM), pp. 222–242.

Gat J.R., Bowser C.J., Kendall C. (1994). The contribution of evaporation from the Great Lakes to the continental atmosphere: estimate based on stable isotope data. *Geophysical Research Letters* **21**: 557 – 560.

Gat J.R. (1996). Oxygen and hydrogen isotopes in the hydrological cycle. *Annual Review of Earth and Planetary Science* **24**: 225 – 262.

Gauthier M. (2000). Mineral deposit characteristics and distribution in the James Bay region of Quebec. *Chroniques de la Recherche Minière* **539**, 17-61.

Gibson J.J., Edwards T.W.D., Bursey G.G., Prowse T.D. (1993). Estimating evaporation using stable isotopes: quantitative results and sensitivity analysis for two catchments in northern Canada. *Nordic Hydrology* **24**: 79 – 94.

Gibson J.J., Prowse T.D. (1999). Isotopic characteristics of ice cover in a large northern river basin. *Hydrological Processes* **13**: 2537 – 2548.

Gibson J.J. (2001). Forest – tundra water balance signals traced by isotopic enrichment in lakes. *Journal of Hydrology* **251**: 1 – 13.

Gibson J.J. (2002a). Short-term evaporation and water budget comparisons in shallow arctic lakes using non-steady isotope mass balance *Journal of Hydrology* **264**: 247 – 266.

Gibson J.J. (2002b). A new conceptual model for predicting isotope enrichment of lakes in seasonal climates. *International Geosphere Biosphere Programme IGBP PAGES News* **10**: 10 – 11.

Gibson J.J., Aggarwal P., Hogan J., Kendall C., Martinelli L.A., Stichler W., Rank D., Goni I., Choudhry M., Gat J., Bhattacharya S., Sugimoto A., Fekete B., Pietroniro A., Maurer T., Panarello H., Stone D., Seyler P., Maurice-Bourgoin L., Herczeg A. (2002). Isotope studies in large river basins: a new global research focus. *EOS* **83**(52): 613 – 617.

Gibson J.J., Edwards T.W.D. (2002). Regional surface water balance and evaporation – transpiration partitioning from a stable isotope survey of lakes in northern Canada. *Global Biogeochemical Cycles*. DOI: 10 Ð1029/2001GB001839.

Gibson J.J., Prowse T.D. (2002). Stable isotopes in river ice: identifying primary over-winter streamflow signals and their hydrological significance. *Hydrological Processes* **16**: 873 – 890.

Gibson J.J., Edwards T.W.D., Birks S.J., St Amour N.A., Buhay W.M., McEachern P., Wolfe B.B., Peters D.L. (2005). Progress in isotope tracer hydrology in Canada. *Hydrological Processes* **19**: 303-327. DOI: 10.1002/hyp.5766.

Gibson J.J., Birks S.J. and Edwards T.W.D. (2008). Global prediction of δ_A and δ^2H-δ^{18}O evaporation slopes for lakes and soil water accounting for seasonality. *Global Biogeochemical Cycles* **22**, GB2031, doi:10.1029/2007GB002997.

Goldstein S.J., Jacobsen, S.B. (1988a). REE in the Great Whale River estuary, northwest Quebec. *Earth and planetary Sciences Letters* **88**: 241-252.

Goldstein S.J., Jacobsen, S.B. (1988b). Rare earth elements in river waters. *Earth and planetary Sciences Letters* **89**, 35-47.

Gonfiantini R. (1986). Environmental isotopes in lake studies. In *Handbook of Environmental Isotope Geochemistry* , volume 3, Fritz P, Fontes JCh (eds). Elsevier: New York; 113 – 168.

Granet M., Chabaux F., Stille P., France-Lanord C., Pelt E. (2007). Time-scales of sedimentary transfer and weathering processes from U-series nuclides: Clues from the Himalayan rivers. *Earth and Planetary Science Letters* **261**, 389–406.

Grzymko T.J., Marcantonio F., McKee B.A., Stewart C. M. (2007). Temporal variability of uranium concentrations and ^{234}U/^{238}U activity ratios in the Mississippi river and its tributaries. *Chemical Geology* **243**, 344-356.

Hartmann J., Jansen N., Dürr H.H., Kempe S., Köhler P. (2009). Global CO_2-consumption by chemical weathering: What is the contribution of highly active weathering regions? *Global and Planetary Change* **69**, 185-194.

Hayeur G. (2001). Synthèse des connaissances environnementales acquises en milieu nordique de 1970 à 2000. Montréal, Hydro-Québec. 110pp.

Hélie J.F., Hillaire-Marcel C., Rondeau B. (2002). Seasonal changes in the sources and fluxes of dissolved inorganic carbon through the St. Lawrence River – isotopic and chemical constraints. *Chemical Geology* **186**: 117 – 138.

Hélie J.F., Hillaire-Marcel C. (2006). Sources of particulate and dissolved organic carbon in the St. Laurence River : isotopic approach. *Hydrological Processes* **20** : 1945 – 1959.

Hocq M. (1994). La Province du Supérieur. In *Géologie du Québec*, Les publications du Québec, pp. 7-20.

Huddart P.A., Longstaffe F.J., Crowe A.S. (1999). δD and δ18 O evidence for inputs to groundwater at a wetland coastal boundary in the southern Great Lakes region of Canada. *Journal of Hydrology* **214**: 18 – 31.

Hudon C., Morin R., Bunch J., Harland R. (1996). Carbon and nutrient output from the Great Whale River (Hudson Bay) and a comparison with other rivers around Quebec. *Canadian. J. Fish. Aquat. Sci.* **53**, 1513 –1525.

Huh Y., Panteleyev G., Babich D., Zaitsev A., Edmond J. M. (1998). The Fluvial geochemistry of the rivers of Eastern Siberia: II. Tributaries of the Lena, Omoloy, Yana, Indigirka, Kolyma and Anadyr draining the collisional/accretionary zone of the Verkhoyansk and Cherskiy ranges. *Geochimica et Cosmochimica Acta* **62**, 2053-2075.

Huh Y., Edmond J.M. (1999). The fluvial geochemistry of the rivers of Eastern Siberia: III. Tributaries of the Lena and Anabar draining basement terrain of the Siberian Craton and the Trans-Baikal Highlands. *Geochimica et Cosmochimica Acta* **63,** 967–987.

IFYGL the International Field Year for the Great Lakes (1981). Aubert E. and Richards T.L., eds, Great Lakes Environmental Research Laboratory.

Ingri J., Widerlund A., Land M., Gustafsson Ö, Ardersson P., Öhlander B. (2000). Temporal variations in the fractionation of the rare earth elements in a boreal river; the role of colloidal particles. *Chemical Geology* **166**, 23-45.

Kendall C., Coplen T.B. (2001). Distribution of oxygen-18 and deuterium in river waters across the United States. *Hydrological Processes* **15**: 1363-1393.

Kigoshi K. (1971). Alpha-recoil thorium-234: disequilibrium in nature. *Science* **173**, 47-48.

Klassen K.W. (1989). Quaternary Geology of the southern Canadian Interior Plains. In Chapter 2 of *Quaternary Geology of Canada and Greenland, R. J. Fulton (ed.)* Geological Survey of Canada, Geology of Canada no. 1.

Kronfeld J., Vogel J. C. (1991). Uranium isotopes in surface waters from southern Africa. *Earth and Planetary Science Letters* **105**, 191–195.

Laudon H., Hemon H.F., Krouse H.R., Bishop K.H. (2002). Oxygen 18 fractionation during snowmelt: implications for spring flood hydrograph separation. *Water Resources Research* **38**: 1258. DOI: 10 Ð1029/2002WR001510.

Lerman A., Wu L., Mackenzie F.T. (2007). CO_2 and H_2SO_4 consumption in weathering and material transport to the ocean, and their role in the global carbon balance. *Marine Chemistry* **106**, 326-350.

Locat J., Lefebre G. (1986). The origin of structuration of the Grande-Baleine marine sediments, Québec, Canada. *Quaterly Journal of Engineering Geology and Hydrogeology*, London 19, 365-374.

McCulloch M.T., Wasserburg G.J. (1978). Sm-Nd and Rb-Sr Chronology of Continental Crust Formation. *Science* **200**, No 4345, 1003-1011.

Merlivat L., Jouzel J. (1979). Global climatic interpretation of the deuterium – oxygen 18 relationship for precipitation. *Journal of Geophysical Research* **84**: 5029 – 5033.

Meybeck M., Pasco A., Ragu A. (1992). Établissement des flux polluants dans les rivières. Étude Inter-agences No 28. Agence de l'Eau / Ministère de l'Environnement, Paris.

Meybeck M., Ragu A. (1996). River discharges to the oceans. An assessment of suspended solids, major ions and nutrients. *Environmental Information and Assessment Report*. UNEP, Nairobi, 250p.

Meybeck M. (2003). Global occurrence of major elements in rivers. In: *Treatise on Geochemistry (Eds H. D. Holland and K. K. Turekian). Vol. 5, Surface and ground water, weathering and soils (Ed J. I. Drever)*, pp. 207-223.

Meynadier L., Gorge C., Birck J.L., Allègre C.J. (2006). Automated separation of Sr from natural water samples or carbonate rocks by high performance ion chromatography. *Chemical Geology* **227**, 26-36.

Millot R., Gaillardet J., Dupré B. and Allègre C.J. (2002). The global control of silicate weathering rates and the coupling with physical erosion: new insights from rivers of the Canadian Shield. *Earth and planetary Sciences Letters* **196**, 83-98.

Millot R., Gaillardet J., Dupré B., and Allègre C.J. (2003). Northern latitude chemical weathering rates: Clues from the Mackenzie River Basin, Canada. *Geochimica et Cosmochimica Acta* **67**, 1305–1329.

Ministère du Développement durable, de l'Environnement et des Parcs. *www.mddep.gouv.qc.ca/index_en.asp*.

Moore W.S. and Shaw T.J. (2008). Fluxes and behavior of radium isotopes, barium and uranium in seven Southeastern US rivers and estuaries. *Marine Chemistry* **108**, issue 3-4, 236-254.

Moreira-Nordemann L.M. (1980). Use of $^{234}U/^{238}U$ disequilibrium in measuring chemical weathering rate of rocks. *Geochimica et Cosmochimica Acta* **44**, 103–108.

NatChem database: Canadian National Atmospheric Chemistry Precipitation Database. Environment Canada, Meteological Service of Canada, 4905 Dufferin Street, Toronto, Ontario, Canada M3H 5T4

Négrel P., Allègre C.J., Dupré B., Lewin E. (1993). Erosion sources determined by inversion of major and trace element ratios and strontium isotopic ratios in river water: The Congo Basin case. *Earth and planetary Sciences Letters* **120**, 59 –76.

Négrel P., Petelet-Giraud E., Barbier J., Gauthier E. (2003). Surface water-groundwater interactions in an alluvial plain: Chemical and isotopic systematics. *Journal of Hydrology* **277**, 248-267.

Osmond J.K., Ivanovitch M. (1992). Uranium-series mobilization and surface hydrology. *In:* Uranium series disequilibrium: Application to Earth, Marine, and Environmental Sciences. Ivanovich M, Harmon RS (eds), Oxford Sciences Publications, Oxford, pp. 259-289.

Osmond J.K., Kowart J.B. (1992). Ground Water. *In:* Uranium series disequilibrium: Application to Earth, Marine, and Environmental Sciences. Ivanovich M, Harmon RS (eds), Oxford Sciences Publications, Oxford, pp. 290-333.

Palmer M.R., Edmond J.M. (1993). Uranium in river water. *Geochimica et Cosmochimica Acta* **57**, 4947-4955.

Pande K., Sarin M. M., Trivedi J. R., Krishnaswami S., and Sharma K. K. (1994). The Indus River system (India–Pakistan): Major-ion chemistry, uranium and strontium isotopes. *Chemical Geology* **116**, 245–259.

Porcelli D., Andersson P.S., Wasserburg G.J., Ingri J., Baskaran M. (1997). The importance of colloids and mires for the transport of U isotopes through the Kalix River watershed and Baltic Sea. *Geochimica et Cosmochimica Acta* **61**, 4095-4113.

Quinn F.H. (1992). Hydraulic residence times for the Laurentian Great Lakes. *Journal of Great Lakes Research* **18**: 22-28.

Riotte J. and Chabaux F. (1999) ($^{234}U/^{238}U$) activity ratios in freshwaters as tracers of hydrological processes: The Strengbach watershed (Vosges, France). *Geochimica et Cosmochimica Acta* **63**, 1263-1275.

Riotte J., Chabaux F., Benedetti M., Dia A., Boulègue J., Gérard M., Etamé J. (2003). Uranium colloidal transport and the origin of the ^{234}U-^{238}U fractionation in surface waters: New insights from Mount Cameroun. *Chemical Geology* **202**, 365–381.

Robinson L.F., Henderson G.M., Hall L., Matthews I. (2004). Climatic control of riverine and seawater uranium-isotope ratios. *Science* **305**, 851–854.

Rondeau B., Cossa D., Gagnon P., Pham T.T., Surette C. (2005). Hydrological and biogeochemical dynamics of the minor and trace elements in the St. Lawrence River. *Applied Geochemistry* **20** (7) : 1391-1408.

Rozanski K., Araguàs-Araguàs L., Gonfiantini R. (1993). Isotopic patterns in global precipitation. In *Continental Isotopic Indicators of Climate*, Swart PK, McKenzie JA, Lohmann KC (eds). American Geophysical Union: Washington; 1 – 36.

Ryu J.S., Lee K.S., Chang H.W., Cheong C.S. (2009). Uranium isotopes as a tracer of sources of dissolved solutes in the Han River, South Korea. *Chemical Geology* **258**, 354-361.

Sarin M.M., Krishnaswami S., Somayajulu B.L.K. and Moore W.S. (1990). Chemistry of uranium, Thorium, and Radium isotopes in the Ganga–Brahmaputra river system: Weathering processes and fluxes to the Bay of Bengal. *Geochimica et Cosmochimica Acta* **54**, 1387–1396.

Shaw D.M., Reilly G.A., Muysson J.R., Pattenden G.E., Campbell F.E. (1967). An estimate of the chemical composition of the Canadian Precambrian shield. *Canadian Journal of Earth Sciences* **4**: 827-853.

Shaw D.M., Cramer J.J., Higgins M.D. and Truscott M.G. (1986). Composition of the Canadian Precambrian Shield and the continental crust of the Earth. Geological Society, London, Special Publications 24, 275-282.

Shotyk W. (1988). Review of the Inorganic Geochemistry of Peats and Peatland Waters. *Earth-Science Reviews* **25**, 95-176.

Shotyk W., Nesbitt H.W. and Fyfe W.S. (1992). Natural and anthropogenic enrichments of tracemetals in peat profiles. *International Journal of Coal Geology* **20**, 49-84.

Spence J., Telmer K. (2005). The role of sulfur in chemical weathering and atmospheric CO_2 fluxes: Evidence from major ions, $\delta^{13}C_{DIC}$ and $\delta^{34}S_{SO4}$ in rivers of the Canadian Cordillera. *Geochimica et Cosmochimica Acta* **69**, no 23, 5441-5458.

St Lawrence Centre. (1996). State of the Environment Report on the St. Lawrence River, The St. Lawrence Ecosystem, Vol. 1. Eds MultiMondes, Montreal.

Stott D.F., Aitken J.D. (1993). Introduction to the Interior Platform, Western Basins and Eastern Cordillera. Chapter 2 in *Sedimentary cover of the Craton in Canada, Stott D.F. and Aitken J.D. (ed.)*, Geological Survey of Canada, Geology of Canada no. 5, pp. 11-54.

Sun H., Semkow T.M. (1998). Mobilization of thorium, radium and radon nuclides in ground water by successive alpha-recoils. *Journal of Hydrology* **205**,126-136.

Swarzensky P., Campbell P., Porcelli D. McKee B. (2004). The estuarine chemistry and isotope systematics of $^{234, 238}U$ in the Amazon and Fly Rivers. *Continental Shelf Research* **24**, 2357-2372.

Tarnocai C., Kettles I.M., Lacelle B. (2000). Peatlands of Canada Database. Geological Survey of Canada Open File 3834.

Telmer K.H., Veizer J. (1999). Carbon fluxes, pCO_2 and substrate weathering in a large northern river basin, Canada: carbon isotope perspective. *Chemical Geology* **159**: 61 – 86.

Telmer K., Veizer J. (2000). Isotopic constraints on the transpiration, evaporation, energy and NPP budgets of a large boreal watershed: Ottawa River Basin, Canada. *Global Biogeochemical Cycles* **14**: 149 – 165.

Tosiani T., Loubet M., Viers J., Valladon M., Tapia J., Marrero S., Yanes C., Ramirez A., Dupre B. (2004). Major and trace elements in river-borne materials from the Cuyuni basin (southern Venezuela): evidence for organo-colloidal control on the dissolved load and clement redistribution between the suspended and dissolved load. *Chemical Geology* **211**, 305-334.

UNESCO. World Water Assessment Programme. (2009). The United Nations World Water Development Report 3: Water in a Changing World. Paris: UNESCO, and London: Earthscan.

Van Bellen S., Dallaire P.L., Garneau M., Bergeron Y. (in press). Quantifying spatial and temporal Holocene carbon accumulation in ombrotrophic peatlands of the Eastmain region, Quebec, Canada. *Global Biogeochemical Cycles*, in press.

Vigier N., Bourdon B., Turner S., Allègre C.J. (2001). Erosion timescales derived from U-decay series measurements in rivers. *Earth and Planetary Science Letters* **193**, 485–499.

Vigier N., Bourdon B., Lewin E., Dupré B., Turner S., Chakrapani G.J., Van Calsteren P., Allègre C.J. (2005). Mobility of U-series nuclides during Basalt Weathering: An example from the Deccan Traps (India). *Chemical Geology* **219**, 69–91.

Vincent J.S. (1989). Quaternary geology of the Southeastern Canadian Shield. In chap. 3 of *Quaternary Geology of Canada and Greenland, R. J. Fulton (ed.)*, Geological Survey of Canada, Geology of Canada no. 1.

Vitvar P.K., Aggarwal P.K., Herczeg A.L. (2007). Global network is launched to monitor isotopes in rivers. *EOS Transactions*, AGU 88 no 33: 325-326.

Wadleigh M.A., Veizer J., Brooks C. (1985). Strontium and its isotopes in Canadian rivers: fluxes and global implications. *Geochimica et Cosmochimica Acta* **49**, 1727 – 1736.

Walker J.C.G., Hays P.B., Kasting J.F. (1981). A negative feedback mechanism for the long-term stabilization of Earth's surface temperature. *Journal of Geophysical Research* **86** (C10), 9776 – 9782.

Water Survey of Canada, Archived Hydrometric Data Online, http://www.wsc.ec.gc.ca/hydat.

West A.J., Galy A., Bickle M. (2005). Tectonic and climatic controls on silicate weathering. *Earth and planetary Sciences Letters* **235**, 211-228.

Wheeler J.O., Hoffman P.F., Card K.D., Davidson A., Sanford B.V., Okulich A.V., Roest W. R. (1996). Geological Map of Canada, Geological Survey of Canada, map 1860A, scale 1:5 000 000.

Windom H., Smith R., Niencheski F., Alexander C. (2000). Uranium in rivers and estuaries of globally diverse, smaller watersheds. *Marine Chemistry* **68**, 307-321.

Yang C., Telmer K., Veizer J. (1996). Chemical dynamics of the "St. Lawrence" riverine system: δDH_2O, $\delta^{18}OH_2O$, $\delta^{13}CDIC$, δ^{34} Ssulfates, and dissolved $^{87}Sr/^{86}Sr$. *Geochimica et Cosmochimica Acta* **60**: 851 – 866.

Yi Y., Gibson J.J., Hélie J.F., Dick T.A. (2010). Synoptic and time-series isotope surveys of the Mackenzie River from Great Slave Lake to the Arctic Ocean, 2003 to 2006. *Journal of Hydrology* **383**: 223-232. doi:10.1016/j.jhydrol.2009.12.038.